Utrecht University

Institute for Theoretical Physics

Master's Thesis

Holographic Entanglement Entropy using Bit Threads

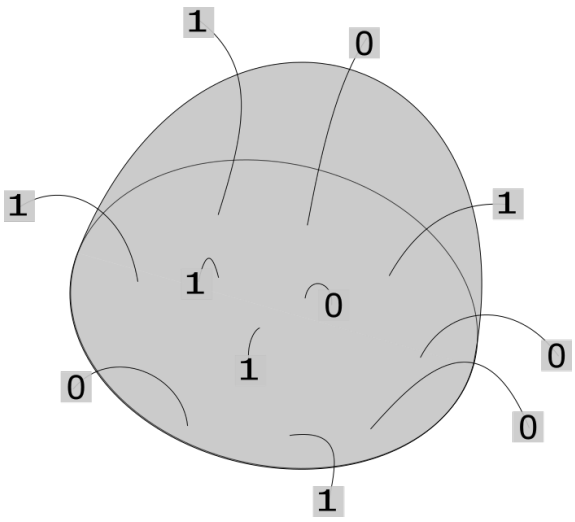

Author:
Aylon Pinto

Supervisor:
Dr. Umüt Gursoy

Co-supervisor:
Dr. Juan F. Pedraza

January 2022

Abstract

It is known that the entanglement entropy of a region in a CFT can be holographically mapped to the Ryu-Takayanagi(RT) surface. This is the minimal surface in AdS homologous to the entangling region. In this project, we use the bit thread interpretation of the RT formula. We investigate if it can be used to find a more concrete algorithm for calculating the entanglement entropy of a given entangling region. Our first results are promising, recovering the right bit thread configurations for specific cases in time slices of two and three-dimensional CFT's. However, a careful analysis reveals that a generalization to arbitrary entangling regions should be shape-dependent. For the case of a three-dimensional CFT, the bit thread prescription suggests a generalized Biot-Savart law that depends on the local curvature of the entangling surface.

Contents

1 Introduction

In 1975 Steven Hawking discovered that black holes radiate particles [1]. He was able to associate a black-body temperature to the spectrum of radiation. He concluded that, if left alone, black holes would eventually evaporate and lose all their mass. This was a big problem. Quantum mechanics tells us that quantum information can never be lost.[1] But what would happen if one would write something on a piece of paper and throw it into a black hole? The black hole would evaporate and the information on that piece of paper would be lost forever. Or would it? In 1993 Gerard 't Hooft proposed the holographic principle [2, 3]. In 1973, Bekenstein had already published that the entropy of a black hole should be proportional to its area [4]. As it is understood, black holes form an upper bound to the amount of information that can be stored in a volume of their size. 't Hooft concluded that the maximum amount of information in a certain volume scaled with the area of its boundary, not its volume. This realization led to the holographic principle, which offered a solution to the information paradox described above. It states that the information thrown into a black hole is stored on its boundary. This would then allow Hawking radiation to carry it back into the universe.

The holographic principle laid the foundation for holography, a new field in theoretical physics that finds and uses dualities between bulk and boundary. But what do we actually mean by 'dualities between bulk and boundary'? First, we need to understand what we mean by 'bulk' and 'boundary'. In Figure 1, we see examples of shapes that have a boundary. In general, we refer to the interior of a shape as the bulk, and to its lower-dimensional sub-shape at the edge, as the boundary. A duality between bulk and boundary means that there is a physical theory (or quantity) that has a dual description in the bulk and in the boundary. This means that there might be a difference in the mathematical description of the two theories, but that they are inherently 'two sides of the same coin'. Finding such a duality can be a great advantage since it would be able to move freely from one theory to the other. This can be beneficial because one could choose the theory that requires the least computational work, to calculate certain quantities. Another advantage of holography is that the bulk theory is a theory of quantum gravity, and the boundary theory is an ordinary quantum theory. Because of the duality, the boundary quantum theory can teach us about the emergence of quantum gravity in the bulk.

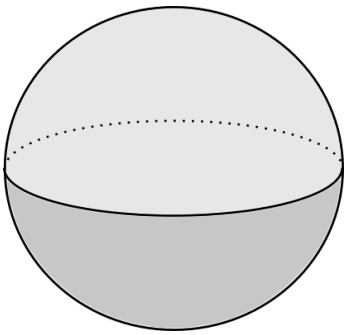

(a) The three-dimensional 'ball' is a solid symmetrical shape. Its boundary is the two-dimensional sphere pictured here. Think of the sphere as the peel of the ball that is left after we remove its inside.

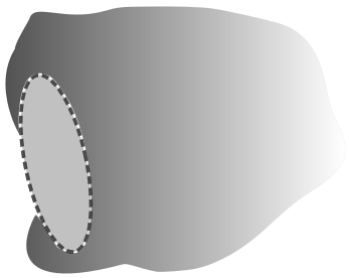

(b) Here we see a two-dimensional balloon-like shape. Its boundary is the one-dimensional circle indicated with the dotted line.

Figure 1: Shapes and their boundaries.

One of the first examples of a holographic duality is the AdS/CFT correspondence. Conjectured by Juan Maldacena in 1999 [5]. This is a duality between a theory of gravity living in the bulk of an AdS space[2] and a quantum theory living on its boundary. By a theory 'living' on a shape

[1] Quantum information is the information encoded in a quantum state. It can be measured using Von Neumann entropy. This will be discussed in chapter 3.

[2] This AdS space is just like a sphere but with negative curvature. For now, this is all we need to know, we will go a bit more into the details later.

or space, we mean that this space is the domain of the theory. So all quantities of the theory, i.e. the fields or operators, depend on which point in the space one considers. One can note that the gravity theory lives in one dimension higher than the quantum theory. This is always the case with bulk/boundary duality, since the boundary is always of one dimension lower than the bulk. We will go more into detail on the AdS/CFT correspondence in the next chapter, as we will be using this duality to find alternative descriptions of entanglement entropy in this project.

Another example of holography can be found in tensor networks. Let us explain these tensor networks briefly. Say we consider a quantum system of several particles. We know the system is described by a state vector in its combined Hilbert space. However, this Hilbert space can be huge, especially if the number of particles increases. A solution for dealing with this is to consider only parts of the Hilbert space. For instance, only the part that is needed to find the ground state of the system. But, how does one only consider a part of a Hilbert space? This is done using tensor networks. We know such a state vector is described as

$$|\psi\rangle = \sum_{k_1,k_2,\cdots,k_N} T_{k_1,k_2,\cdots,k_N} |k_1, k_2, \cdots, k_N\rangle \tag{1.1}$$

where we consider N different particles and the indices k_i run over the basis states of the i^{th} particle. Now $T_{k_1,k_2,\cdots,k_N}$ can be seen as a tensor without any co- or contravariant way of transforming. The ansatz is now that $T_{k_1,k_2,\cdots,k_N}$ can be written as a contraction over different tensors. For instance, there are tensors T^1, T^2 and T^3 such that

$$T_{k_1,k_2,k_3} = \sum_{j_1,j_2,j_3} T^1_{j_3,k_1,j_1} T^2_{j_1,k_2,j_2} T^3_{j_2,k_3,j_3} \tag{1.2}$$

in the case $N = 3$. One can now visualize the tensor T as a network of different tensors. By graphically indicating a tensor as a vertex and a contraction as an edge. One obtains a graph-like structure for the tensor network shown below in Figure 2a. Imagine now that there are more tensors used to describe T. They could be contracted in all kinds of different orders. If in the end the indices k_1, k_2 and k_3 are still free, this would be a valid tensor network for T. We see that there is a lot of freedom when it comes to finding a tensor network.

Consider now a one-dimensional spin chain of N-particles. From (1.1) we know that this system can be described by a tensor $T_{k_1,k_2,\cdots,k_N}$. Which in turn can be described by a tensor network shown below in Figure 2b. This is an example of a holographic description. A one-dimensional state (the spin chain) has an alternative description as a two-dimensional tensor network. This can be seen from the fact that when we restrict to the boundary, (i.e. we take all tensors in the bulk to be zero) we obtain something like Figure 2a. This is just the one-dimensional spin chain again. Some tensor networks show a lot of resemblance with the AdS/CFT holography. A particular tensor network that contains an AdS structure in its bulk is the MERA network [6, 7]. This network is also thought of as 'discretizing AdS space'. However, this means that at small distances this analogy breaks down. More on this will be covered in the discussion 5. Some other important networks are [8, 9, 10].

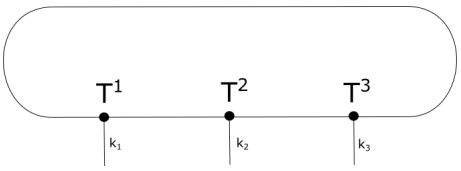

(a) Tensor network of T_{k_1,k_2,k_3}.

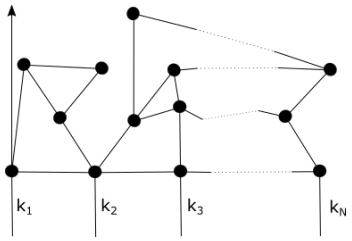

(b) Tensor network of a one-dimensional spin chain. The dotted lines indicate an arbitrary continuation of the network. The arrow points into the holographic emergent direction.

Figure 2: Some tensor networks

One example of a quantity that has a holographic description is entanglement entropy. This is a quantity that measures the amount of entanglement between a given region and its surroundings. In the holographic description, this quantity is represented by the area of some surface called the *RT-surface*. An analog in tensor networks exists as well. This is called the minimal cut and will briefly be mentioned in the discussion 5. We see here that quantum mechanical entanglement relates to geometry in the bulk. It is thought that the geometry of the bulk spacetime is actually emergent from the quantum correlations in the boundary quantum theory. This is why we are so interested in finding the entanglement entropy of certain regions. It could teach us about how the geometry of spacetime can emerge from holography [11, 12, 13]. But not only the geometry, also Einstein's equation holographically emerges from the dynamics of entanglement [14, 15, 16], which is truly remarkable. One final importance of entanglement entropy are the entropy inequalities[17, 18, 19]. These are inequalities that must hold for the entanglement entropy of several regions. When considered holographically, these inequalities follow from basic geometric properties. This means that, when these inequalities are not satisfied, we know the QFT does not have a holographic dual.

This thesis is written in such a way that it should be understandable for any student in theoretical physics with a basic understanding of quantum field theory and general relativity. It is structured as follows. In the next chapter, an introduction to AdS/CFT is given. This is followed by an introduction to holographic entanglement entropy and bit threads. In chapter four the results are stated, presented in the chronological order of the research. This is done to give some insight into our thought processes and how we made the discoveries. Readers who are familiar with AdS/CFT, holographic entanglement entropy, and bit threads can go directly to chapter four

2 AdS/CFT

In this first chapter, we want to start with an introduction to the AdS/CFT correspondence. This duality between a theory of quantum gravity and a quantum field theory was first proposed by Juan Maldacena in [5]. This was remarkable finding, firstly, because he found a duality between a theory of gravity and a quantum theory, but also because this duality is of holographic nature. This is because the dual quantum field theory is proposed to live on the conformal boundary of an AdS space.

This chapter will be structured as follows. We will begin by introducing the concept of a CFT, followed by an example of a two-dimensional CFT. This two-dimensional case is discussed because it gives an elegant look into the world of CFT's, apart from being very relevant for string theory. After this, we will bring up the notion of an AdS space, followed again by a lower-dimensional example. Finally, we bring the two together and elaborate upon the AdS/CFT correspondence.

2.1 Conformal Field Theory

In this subchapter, we will introduce the concept of a conformal field theory or CFT. But before we can do this, we need to comprehend conformal transformations and conformal symmetry. After we understand this, we see that a CFT is just a special case of a quantum field theory. We will discuss in detail a two-dimensional CFT. By first computing the energy-momentum tensor, followed by scratching the surface of the concept of OPE's. Finally, we will calculate some propagators of the theory.

2.1.1 Conformal transformations and conformal symmetry

We wish to begin by defining a conformal transformation. Let us start with an arbitrary manifold, this should be a Riemannian (or Lorentzian) manifold. A *conformal transformation* applied to the manifold would be a coordinate transformation where the metric changes by an overall factor. Thus if we change the coordinates $x \to x'$ we get that

$$g_{\mu\nu}(x) \to \Omega^2(x) g_{\mu\nu}(x) = g'_{\mu\nu}(x'). \tag{2.1}$$

It can be seen that this transformation preserves angles, since the length scale (metric) of each coordinate is changed by the same factor. The relative length scales between the coordinates remain unchanged. One can think of this transformation as 'zooming' in or out while keeping the angles fixed.

An object or manifold which enjoys a *conformal symmetry* would be invariant under this transformation. This means that one would obtain the same object before and after a conformal transformation. An example of this would be the infinite one-dimensional line. 'Zooming' in and out does not change the line at all.

On to the definition of a CFT. As we now understand, manifolds can enjoy a conformal symmetry. In physics, it would make sense to consider the spacetime manifold. The metric in consideration would then of course be the spacetime metric. A *conformal field theory* is a quantum field theory that possesses conformal symmetry. In the sense that the action of the theory is invariant under this conformal transformation. When we consider the spacetime metric to be dynamic (i.e. to depend on the coordinates of spacetime) the transformation will be a diffeomorphism[3] and the conformal symmetry will be a gauge symmetry.[4] This can be seen by noting that (2.1) is just a diffeomorphism that can be undone by a Weyl transformation.[5] If we keep the background metric fixed, this symmetry will be an actual physical symmetry.

2.1.2 Two-dimensional conformal field theory

Next, we want to give an example of a CFT. Namely, a two-dimensional free field theory. We start with the two-dimensional plane with a flat Euclidean metric. This metric is non-dynamic, so the conformal transformations will be of physical nature. We work out this theory in detail for

[3] This is a coordinate transformation such that the metric changes is a 'tensorial' way.

[4] As a reminder, a gauge symmetry is a symmetry of the Lagrangian under the transformations of a certain gauge group, dependent on spacetime. It is a non-physical symmetry, hence a redundancy of the theory.

[5] This is a transformation where the metric again changes with an overall factor, but the coordinates remain the same.

two reasons. One is that two spatial dimensions allow for a convenient transformation to complex coordinates. This way the formulation of the theory becomes easy to work with. This is due to the holomorphic nature of the conformal transformations and the fields as we shall see in a moment. Another reason is that this theory shows some resemblance with the world sheet in string theory. Because it is two-dimensional, the action of the world sheet enjoys Weyl symmetry. This is because in two dimensions the Weyl factor of $\sqrt{-g}$ cancels the one from $g_{\mu\nu}$. As mentioned before this Weyl symmetry can be used to undo a conformal transformation, making the world sheet a two-dimensional CFT. Although the metric signature does not agree with our calculations here, a similar derivation can be done in Minkowski spacetime.

We start by introducing complex coordinates to describe the plane.[6] Let

$$z := x^1 + ix^2 \qquad\qquad \bar{z} := x^1 - ix^2 \tag{2.2}$$

and in these coordinates the metric becomes

$$g_{\mu\nu} = \frac{1}{2}\begin{pmatrix} 0 & 1 \\ 1 & 0 \end{pmatrix}. \tag{2.3}$$

The derivatives change as well due to the change in coordinates and they become

$$\partial := \partial_z = \frac{1}{2}(\partial_1 - i\partial_2) \qquad\qquad \bar{\partial} := \partial_{\bar{z}} = \frac{1}{2}(\partial_1 + i\partial_2). \tag{2.4}$$

As a reminder, a function $f(z)$ that only depends on z (and is differential with respect to z) is called *holomorphic*, any function that depends only on $\bar{z}$ is called *anti-holomorphic*. Any holomorphic change of coordinates is a conformal transformation. This can be seen easily, let us apply the change of coordinates

$$z \to f(z) \qquad\qquad \bar{z} \to \bar{f}(\bar{z}) \tag{2.5}$$

then the metric changes

$$g'_{\mu\nu} = \frac{\partial z'^{\alpha}}{\partial z^{\mu}} \frac{\partial z'^{\beta}}{\partial z^{\nu}} g_{\alpha\beta} = \partial f(z) \bar{\partial} \bar{f}(\bar{z}) g_{\mu\nu} = |\partial f(z)|^2 g_{\mu\nu} \tag{2.6}$$

and we see it satisfies (2.1). Notice that there are an infinite number of conformal transformations in two dimensions. Indeed any holomorphic function $f(z)$ does the trick. This is special for two-dimensional CFT's. In general the *conformal group*, the group of conformal transformations, is $SO(p+1, q+1)$ for an theory living on $\mathbb{R}^{p,q}$ with $p + q > 2$.

Next, we will show some nice properties of the energy-momentum tensor. Some may be known and some are special for a conformal field theory. We impose an infinitesimal translation of our coordinates

$$\delta x^{\mu} = \epsilon^{\mu}. \tag{2.7}$$

Our action should be invariant under this transformation. But say now we pretend that $\epsilon^{\mu} = \epsilon(x^{\mu})$ is a function of the coordinates. The variation of the action will now become

$$\delta S = \int J^{\mu} \partial_{\mu} \epsilon \; d^2x \tag{2.8}$$

for some function J^{μ} of the fields. We see that if ϵ is constant, the action is invariant as desired. But what if the equations of motion are fulfilled? Then we should have that $\delta S = 0$ regardless of ϵ. From this, it follows that $\partial_{\mu} J^{\mu} = 0$ when the EOM are satisfied. Hence, J^{μ} is the conserved current. Remember now that $\epsilon(x^{\mu})$ is a translation dependent on spacetime. It can be seen as a diffeomorphism transformation so we know how the metric changes

$$\delta g_{\mu\nu} = \partial_{\mu} \epsilon_{\nu} + \partial_{\nu} \epsilon_{\mu}. \tag{2.9}$$

[6] We will treat z and $\bar{z}$ as independent coordinates, even though they are related by complex conjugation of course. By doing so we extend our calculations to $\mathbb{C}^2$ when in reality our two-dimensional plane is sitting inside $\mathbb{R}^2 \subset \mathbb{C}^2$.

From this, we get that

$$\delta S = -\int \frac{\delta S}{\delta g_{\mu\nu}} \delta g_{\mu\nu} \; d^2x = -2 \int \frac{\delta S}{\delta g_{\mu\nu}} \partial_\mu \epsilon_\nu \; d^2x \tag{2.10}$$

and we see that

$$T_{\mu\nu} := -\frac{4\pi}{\sqrt{g}} \frac{\delta S}{\delta g^{\mu\nu}} \tag{2.11}$$

is a conserved current. Furthermore, we want to show that for a conformal field theory, the energy-momentum tensor is traceless. Let us make a new transformation. This time we scale the metric by a constant. Such that

$$\delta g_{\mu\nu} = \epsilon g_{\mu\nu} \tag{2.12}$$

and we look at the variation of the action

$$\delta S = -\int \frac{\delta S}{\delta g_{\mu\nu}} \delta g_{\mu\nu} \; d^2x = -\int \frac{\delta S}{\delta g_{\mu\nu}} \epsilon g_{\mu\nu} \; d^2x = \frac{1}{4\pi} \int \sqrt{g} T^\mu_\mu \epsilon \; d^2x. \tag{2.13}$$

The action should be invariant under this transformation since we are dealing with a conformal field theory. So we conclude that the energy-momentum tensor must be traceless. Coming back to our two-dimensional theory in complex coordinates, we see that this means that

$$g^{\mu\nu} T_{\mu\nu} = 2T_{z\bar{z}} + 2T_{\bar{z}z} = 4T_{z\bar{z}} = 0 \tag{2.14}$$

since $T_{\mu\nu}$ should be symmetric of course. Then from the fact that it should be a conserved current we see that $\partial_\mu T^{\mu\nu} = 0$ and hence

$$\partial T^{zz} = 0 \qquad\qquad \bar{\partial} T^{\bar{z}\bar{z}} = 0 \tag{2.15}$$

which implies $\partial T_{\bar{z}\bar{z}} = 0$ and $\bar{\partial} T_{zz} = 0$. Thus $T(z) := T_{zz}$ and $\bar{T}(\bar{z}) := T_{\bar{z}\bar{z}}$ are holomorphic and anti-holomorphic respectively.

After we calculated some properties of the energy-momentum tensor, it is time to return to the action. The action for a free field theory is given by

$$S = \frac{1}{4\pi} \int \partial_\mu \phi(x) \partial^\mu \phi(x) \; d^2x = \frac{1}{4\pi} \int (\partial\phi)^2 \; d^2x. \tag{2.16}$$

where the square above $\partial\phi$ indicates the contraction over spacetime indices. We can now use (2.11) to compute the energy-momentum tensor, or equivalently

$$\begin{aligned} T_{\mu\nu} &= -\frac{4\pi}{\sqrt{g}} \frac{\delta \sqrt{g}\mathcal{L}}{\delta g^{\mu\nu}} = -\left(\frac{1}{\sqrt{g}} \frac{\delta \sqrt{g}}{\delta g^{\mu\nu}} (\partial\phi)^2 + \frac{\delta (\partial\phi)^2}{\delta g^{\mu\nu}} \right) \\ &= -\left(\frac{1}{2g} \frac{\delta g}{\delta g^{\mu\nu}} (\partial\phi)^2 + \frac{\delta}{\delta g^{\mu\nu}} g^{\mu\nu} \partial_\mu \phi \partial_\nu \phi \right) \\ &= -\left(\partial_\mu \phi \partial_\nu \phi - \frac{1}{2} g_{\mu\nu} (\partial\phi)^2 \right) \end{aligned} \tag{2.17}$$

where we use the functional derivative on a fixed point in spacetime. This way there is no delta function to kill the integral. We see now that it is indeed traceless and in complex coordinates, we see that

$$T_{z\bar{z}} = -\partial\phi\bar{\partial}\phi + \frac{1}{4} 4 \partial\phi\bar{\partial}\phi = 0 \tag{2.18}$$

and

$$T_{zz} = -\partial\phi\partial\phi \qquad\qquad T_{\bar{z}\bar{z}} = -\bar{\partial}\phi\bar{\partial}\phi. \tag{2.19}$$

From (2.16) it is also easy to see that the equation of motion for the field ϕ is $\partial\bar{\partial}\phi(z,\bar{z}) = 0$. This means that the field can be decomposed in a holomorphic and an anti-holomorphic part

$$\phi(z,\bar{z}) = \phi(z) + \bar{\phi}(\bar{z}). \tag{2.20}$$

It is now clear that T_{zz} and $T_{\bar{z}\bar{z}}$ are also holomorphic and anti-holomorphic, respectively, as promised.

2.1.3 Operator product expansion

Until this point, most of what we have done regarding our conformal field theory has been classical. To make it really a quantum field theory we need to promote our field to an operator field. This does however come with a price. We lose Weyl symmetry when we make the leap to quantization.[7] This has the consequence that the energy-momentum tensor is not necessarily traceless anymore. When a symmetry of a theory does not survive the journey to quantization, this is called an anomaly. As it is with the Weyl anomaly just described.

An important feature of any quantum field theory is the *operator product expansion* or OPE. As we know the fields in QFT become operator fields. They can thus be inserted at points in spacetime. The OPE is an expression where the time-ordered correlation function of two operators inserted at different nearby points, can be approximated as the sum over operators inserted at one of these points. Formally this looks like

$$\langle \mathcal{O}_i(z,\bar{z})\mathcal{O}_j(w,\bar{w})\ldots\rangle = \sum C_{ij}^k(z-w,\bar{z}-\bar{w})\,\langle \mathcal{O}_k(w,\bar{w})\ldots\rangle \tag{2.21}$$

where the brackets mean we are looking at the time-ordered correlation function and the "..." represent the insertion of arbitrary other operators. This can be any operator as long as the distance of insertion is large compared to $|z-w|$. It turns out the OPE is actually an exact statement in a CFT. With the radius of convergence equal to the distance to the next arbitrary insertion, see Figure 3. The $C_{ij}^k(z-w,\bar{z}-\bar{w})$ are coefficient functions of the expansion that depend only in the difference of the points $z-w$ and $\bar{z}-\bar{w}$.

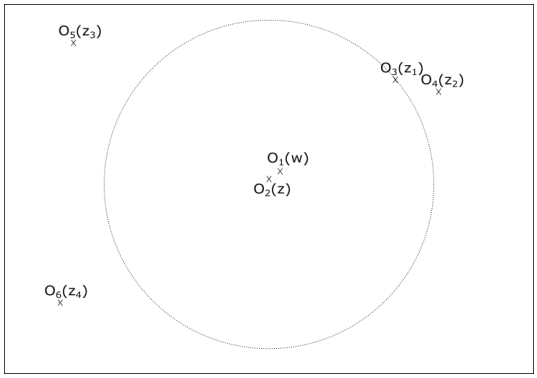

Figure 3: Convergence disk of an OPE in a CFT.

Using the OPE we can now give the following definition. A *primary operator* as an operator whose OPE with the energy-momentum tensor contains no singular terms of higher-order then $(z-w)^{-2}$ or $(\bar{z}-\bar{w})^{-2}$. More precisely, the OPE should be of the form

$$T(z)\mathcal{O}(w,\bar{w}) = h\frac{\mathcal{O}(w,\bar{w})}{(z-w)^2} + \frac{\partial\mathcal{O}(w,\bar{w})}{z-w} + \text{ non-singular} \tag{2.22}$$

$$\bar{T}(\bar{z})\mathcal{O}(w,\bar{w}) = \tilde{h}\frac{\mathcal{O}(w,\bar{w})}{(\bar{z}-\bar{w})^2} + \frac{\bar{\partial}\mathcal{O}(w,\bar{w})}{\bar{z}-\bar{w}} + \text{ non-singular} \tag{2.23}$$

where h and $\tilde{h}$ make up the conformal weights of the operator. They tell us how the operator transforms under conformal transformations. Namely, it holds that

$$\mathcal{O}(z,\bar{z}) \to \tilde{\mathcal{O}}(\tilde{z},\bar{\tilde{z}}) = \left(\frac{\partial\tilde{z}}{\partial z}\right)^{-h}\left(\frac{\partial\bar{\tilde{z}}}{\partial\bar{z}}\right)^{-\tilde{h}}\mathcal{O}(z,\bar{z}) \tag{2.24}$$

under a general conformal transformation $z \to \tilde{z}$. From the conformal weights we can define new quantities. For instance,

$$s = h - \tilde{h} \qquad\qquad \Delta = h + \tilde{h} \tag{2.25}$$

[7] One has to introduce a length scale to regularize the theory. Meaning the theory depends on this length scale and we lose Weyl symmetry.

the conformal *spin* and *scaling dimension* of the operator. They represent the eigenvalues of the operator under rotation and scaling. In general, the two-point functions of primary operators actually take the form

$$\langle \mathcal{O}(z,\bar{z})\mathcal{O}'(w,\bar{w})\rangle \propto |(z,\bar{z})-(w,\bar{w})|^{-2\Delta} \tag{2.26}$$

for primary operators $\mathcal{O}$ and $\mathcal{O}'$ with scaling dimension Δ.

2.1.4 Free scalar field theory

Let us return to the free scalar field theory. Our goal will be to try and calculate two-point functions of different operators and specifically, the propagator of the field. This is done in a QFT by inserting operators in the partition function of the theory. In the path integral formalism, this is given by

$$Z = \int \mathcal{D}\phi \; e^{-S} \tag{2.27}$$

where S is the action of the theory given in (2.16). Now a total derivative under the integral should vanish as with regular integrals so we get that

$$0 = \int \mathcal{D}\phi \frac{\delta}{\delta\phi} \; e^{-S} = -\int \mathcal{D}\phi \; e^{-S}\frac{\delta S}{\delta\phi} = \int \mathcal{D}\phi \; e^{-S}\left(\frac{1}{2\pi}\partial_\mu\partial^\mu\phi\right) \tag{2.28}$$

where in the last equality we used partial integration for the action integral. We see that the equation of motion transfers to the quantum version namely,[8]

$$\langle \partial_\mu\partial^\mu\phi\rangle = 0. \tag{2.29}$$

To find the propagator we will use the same trick. Note that we omitted the spacetime point in the functional derivative in (2.28), but it is implicitly there to kill the integral over spacetime coming from the action. We will reintroduce it now and insert an operator field at a different point in the partition function. We get that

$$0 = \int \mathcal{D}\phi \; \frac{\delta}{\delta\phi(x)}\left(e^{-S}\phi(x')\right) = \int \mathcal{D}\phi \; e^{-S}\left(\frac{1}{2\pi}\big(\partial_\mu\partial^\mu\phi(x)\big)\phi(x') + \delta(x-x')\right) \tag{2.30}$$

hence we obtain

$$\langle\big(\partial_\mu\partial^\mu\phi(x)\big)\phi(x')\rangle = -2\pi\delta(x-x'). \tag{2.31}$$

To solve this differential equation we need equation (4.21) from [20],

$$\partial^2 \log\left((x-x')^2\right) = 4\pi\delta(x-x'). \tag{2.32}$$

From this, we can see that the solution to (2.31) is

$$\langle\phi(x)\phi(x')\rangle = -\frac{1}{2}\log\left((x-x')^2\right) \tag{2.33}$$

and in complex coordinates this becomes

$$\langle\phi(z,\bar{z})\phi(w,\bar{w})\rangle = -\frac{1}{2}\log(z-w) - \frac{1}{2}\log(\bar{z}-\bar{w}). \tag{2.34}$$

We see again the presence of a holomorphic and an anti-holomorphic part. We remember the same form the field ϕ and conclude that the nonzero propagators between all (anti-)holomorphic parts of the field are

$$\langle\phi(z)\phi(w)\rangle = -\frac{1}{2}\log(z-w) \qquad\qquad \langle\bar{\phi}(\bar{z})\bar{\phi}(\bar{w})\rangle = -\frac{1}{2}\log(\bar{z}-\bar{w}). \tag{2.35}$$

[8] We normalize the partition function to be unity. We then see that (2.28) and (2.29) agree.

To get the propagators of $\partial\phi$ we can now just take the derivatives with respect to z and w. The same goes for their anti-holomorphic counterparts. We get

$$\langle \partial\phi(z)\partial\phi(w)\rangle = \partial_z\partial_w\langle\phi(z)\phi(w)\rangle = -\frac{1}{2}\frac{1}{(z-w)^2} \tag{2.36}$$

and analog for the anti-holomorphic part.

Moving on to the energy-momentum tensor in the quantum theory. We are interested in the OPE of $T(z)$ with operators derived from the field. This way we can determine whether these operators are primary. We will focus on the holomorphic parts for the moment. The calculations for the anti-holomorphic parts are analogous.

For the classical free field theory, we derived that

$$T(z) = -\partial\phi(z)\partial\phi(z). \tag{2.37}$$

Looking at (2.36) we can see right away that we can not just take the expectation value of this to get the quantum energy-momentum tensor. We need to define normal ordering

$$T(z) = -:\partial\phi(z)\partial\phi(z): \equiv -\lim_{w\to z}\left(\partial\phi(z)\partial\phi(w) - \langle\partial\phi(z)\partial\phi(w)\rangle\right). \tag{2.38}$$

For this definition of normal ordering, we still have that $\langle T\rangle = 0$ and Wick's theorem holds.[9] We will now try to find

$$\langle T(z)\partial\phi(w)\rangle = -\langle :\partial\phi(z)\partial\phi(z):\partial\phi(w)\rangle \tag{2.39}$$

and we will use Wick's theorem. Since we take the the time ordered correlation function, the normal ordering of two operators vanishes and the contractions become just the propagators. Since contractions inside the normal ordering in an OPE do not contribute we end up with [10]

$$\begin{aligned}\langle T(z)\partial\phi(w)\rangle &= \langle -2\partial\phi(z)\langle\partial\phi(z)\partial\phi(w)\rangle\rangle = \left\langle -2\partial\phi(z)\left(-\frac{1}{2}\frac{1}{(z-w)^2}\right)\right\rangle \\ &= \frac{\langle\partial\phi(w)\rangle}{(z-w)^2} + \frac{\langle\partial^2\phi(w)\rangle}{z-w} + \cdots\end{aligned} \tag{2.40}$$

where in the last step we expanded the field $\partial\phi(z)$ around w. The dots represent that there might be non-singular terms involved, but this is not of interest. We can see already that $\partial\phi(z)$ is a primary operator of conformal weight $h = 1$ and $\tilde{h} = 0$. Also, we notice that (2.36) agrees with (2.26).

A natural question that now arises: is the energy tensor a primary operator? The answer is 'no'. One can do a similar calculation using Wick's theorem to compute the OPE of the energy-momentum tensor with itself. One would find that

$$\begin{aligned}T(z)T(w) &= :\partial\phi(z)\partial\phi(z)::\partial\phi(w)\partial\phi(w): \\ &= 2\left(-\frac{1}{2}\frac{1}{(z-w)^2}\right)^2 - \frac{4}{2}\frac{:\partial\phi(z)\partial\phi(w):}{(z-w)^2} \\ &= \frac{1/2}{(z-w)^4} + \frac{T(w)}{(z-w)^2} + \frac{\partial T(w)}{z-w} + \cdots\end{aligned} \tag{2.41}$$

where again in the last line we expanded $\partial\phi(z)$ around w. The factor of 2 in the first term comes from the two ways to take the product of two propagators. The factor of 4 in the second term comes from the four ways to take one propagator. Also, we omitted the expectation value brackets in the calculation, but they should be implicitly there. We see now straight away that $T(z)$ is not a primary operator. The extra $(z-w)^{-4}$ term does however possess some special information about the theory. In general the constant in the numerator is equal to $c/2$ ($\tilde{c}/2$ for the anti-holomorphic part) where we call c (or $\tilde{c}$) the *central change* of the theory. It turns out it is actually equal to the number of degrees of freedom of the theory. Hence it makes sense that we have that $c = \tilde{c} = 1$ for the free scalar field. We will encounter this central change again when we calculate entanglement entropy.

[9] Normally, normal ordering is defined by commuting the operators such that all annihilation operators are to the right of creation operators.

[10] This is because the expectation value of a normal ordered set of operators is always zero.

2.2 Anti-de Sitter space

In this section, we will get familiar with anti-de Sitter space. We will first mention a few of its properties. Then we will describe it using different coordinates, partially or as a whole. Finally, we will calculate its curvature tensors and scalar.

An anti-de Sitter space is a Riemannian (or Lorentzian) manifold that is maximally symmetric with negative curvature. As a reminder, a maximally symmetric space has the maximum number of Killing vectors.[11] For a d-dimensional manifold this number is $d(d+1)/2$. AdS space is also a solution to Einstein's equation in vacuum with a negative cosmological constant.

$$G_{\mu\nu} = R_{\mu\nu} - \frac{1}{2}Rg_{\mu\nu} = -\Lambda g_{\mu\nu} \tag{2.42}$$

To give a bit of perspective, a sphere is a maximally symmetric space with positive curvature. Just like a sphere, an AdS space also has a radius, which we will call l. In order for the AdS space to be a solution of (2.42), the cosmological constant and the anti-de Sitter radius should be related as

$$\Lambda = -\frac{d(d-1)}{2l^2} \tag{2.43}$$

for a $d+1$-dimensional AdS space.

Just as with the sphere, it is possible to embed the AdS_{d+1} space in a $d+2$-dimensional flat space. The equation constraining the AdS surface in the ambient space will be

$$-(x_1)^2 - (x_2)^2 + (x_3)^2 + \cdots + (x_{d+2})^2 = -l^2 \tag{2.44}$$

where x_i are the coordinates of the flat space. We see again the resemblance with the sphere. If all signs in (2.44) were plus signs it would give us the $d+1$-dimensional sphere in $\mathbb{R}^{d+2}$ of radius l. It is thus not surprising that the isometry group of AdS_{d+1} is $SO(d,2)$. Note that AdS_{d+1} is locally diffeomorphic to $\mathbb{R}^{d,1}$. Since the boundary is of one spatial dimension lower, it can thus be mapped to $\mathbb{R}^{d-1,1}$. A theory living on the boundary would then have conformal group $SO(d,2)$ as mentioned in Section 2.1.2. This is the same group as the isometry group of AdS_{d+1}!

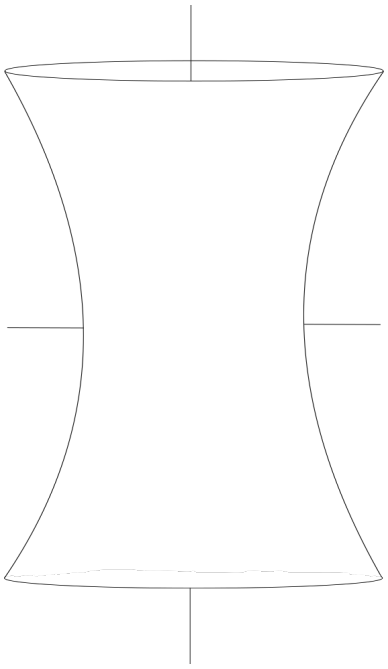

Figure 4: Graphic illustration of the embedding of AdS space.

Embedded in flat space, we can give global coordinates that describe the whole AdS space. Let

[11] Killing vectors are the generating vector fields of isometries.

$$\begin{cases} x_1 = l\cosh\chi\cos\tau \\ x_2 = l\cosh\chi\sin\tau \\ x_i = l\sinh\chi\ \tilde{x}_i \quad i \in \{3,\dots,d+2\} \end{cases} \tag{2.45}$$

where $\tilde{x}_i$ are the coordinates of a $d-1$-dimensional sphere. Replacing (2.44) with these coordinates we see that the equation is satisfied. In these coordinates the metric becomes

$$ds^2 = l^2(-\cosh^2\chi d\tau^2 + d\chi^2 + \sinh^2\chi d\Omega_{d-1}^2) \tag{2.46}$$

where $d\Omega_{d-1}$ is the metric of a $d-1$-dimensional sphere. The domains of these coordinates are

$$\chi \in \mathbb{R}^+ \qquad\qquad \tau \in [0, 2\pi). \tag{2.47}$$

One can describe AdS space in different coordinates as well. One example of this would be to use Poincaré coordinates. In these coordinates, the metric takes a much more approachable form. It does however come with a price. Poincaré coordinates only describe a path of the AdS space. Let us choose a different parameterization

$$\begin{cases} x_1 = \frac{l^2}{2r}\left(1 + \frac{r^2}{l^4}\left(l^2 + \vec{x}^2 - t^2\right)\right) \\ x_2 = \frac{r}{l}t \\ x_i = \frac{r}{l}\tilde{x}_i \quad i \in \{3,\dots,d+1\} \\ x_{d+2} = \frac{l^2}{2r}\left(1 - \frac{r^2}{l^4}\left(l^2 - \vec{x}^2 + t^2\right)\right). \end{cases} \tag{2.48}$$

It is not hard to check that this parameterization satisfies (2.44). Now the metric becomes

$$ds^2 = -\frac{r^2}{l^2}dt^2 + \frac{l^2}{r^2}dr^2 + \frac{r^2}{l^2}d\vec{x}^2 \tag{2.49}$$

and if we make the final substitution $z \equiv l^2/r$ the metric takes the form

$$ds^2 = \frac{l^2}{z^2}\left(dz^2 + dx_\mu dx^\mu\right) \tag{2.50}$$

where x^μ are the coordinates of d-dimensional Minkowski space. The convenience of describing AdS space in these coordinates is that the boundary now corresponds to taking the limit $z \to 0$. Apart from this, the boundary (constant z) appears to have a flat geometry. This is why these coordinates are most frequently used in the AdS/CFT correspondence. We will be using these coordinates as well since we will use the fact that the boundary is effectively Minkowski in these coordinates.

Finally we will compute the curvature tensors and scalar. To get the intrinsic curvature or Ricci-scalar there is clever trick we can do using (2.42). Take the contraction on both sides of the equation with $g^{\mu\nu}$. We end up with

$$\begin{aligned} R - \frac{1}{2}R(d+1) &= -\Lambda(d+1) \\ R\left(1 - \frac{1}{2}(d+1)\right) &= -\Lambda(d+1) \\ R = -\frac{\Lambda(d+1)}{\frac{1}{2}(1-d)} &= 2\frac{\Lambda(d+1)}{d-1} = -\frac{d(d+1)}{l^2} \end{aligned} \tag{2.51}$$

and substituting this again in (2.42) we see that

$$\begin{aligned} R_{\mu\nu} &= \frac{1}{2}Rg_{\mu\nu} - \Lambda g_{\mu\nu} = \left(-\frac{d(d+1)}{2l^2} + \frac{d(d-1)}{2l^2}\right)g_{\mu\nu} \\ &= \frac{d(d-1) - d(d+1)}{2l^2}g_{\mu\nu} = -\frac{d}{l^2}g_{\mu\nu}. \end{aligned} \tag{2.52}$$

Now it is shown on page 382 of [21] that for a maximally symmetric space the Riemann tensor is proportional to the appropriate combinations of the metric. Namely,

$$R_{\mu\nu\rho\sigma} = \frac{R}{d(d+1)}(g_{\sigma\nu}g_{\mu\rho} - g_{\rho\nu}g_{\mu\sigma}) = -\frac{1}{l^2}(g_{\sigma\nu}g_{\mu\rho} - g_{\rho\nu}g_{\mu\sigma}) \tag{2.53}$$

which gives us the Riemann tensor.

2.3 The AdS/CFT correspondence

Now that we have familiarized ourselves with the concepts of a conformal field theory and an anti-de Sitter space, we can begin to give a detailed introduction to Maldecena's AdS/CFT duality [5]. Although this duality is found in string theory, it now 'stands on its own' as a powerful tool for calculations, and to learn more about quantum gravity. We start by introducing some terms from string theory, where this duality was found. We continue by giving a brief description of the original findings. Finally, we state the main conjecture of the AdS/CFT correspondence.

2.3.1 String theory

To give a detailed description of how the AdS/CFT conjecture was first discovered, we need to introduce a few concepts from string theory. In string theory, the 0-dimensional point-like particle is generalized to a 1-dimensional *string*. The world line (the path a particle travels through spacetime) is then generalized to a 2-dimensional world sheet. There are two different types of strings. *Open* and *Closed* string, where the latter is a string with its endpoints identified with each other. There are different kinds of boundary conditions one can impose on the endpoints of an open string. They are called *Dirichlet* or *Neumann* boundary conditions. Where the former means the endpoint is kept fixed and the latter represents an endpoint that is free to move. Later, the Dirichlet boundary condition was also interpreted as a higher-dimensional objects on which the strings end called a *D-brane*. Depending of course on the type of string and its boundary conditions, the strings can vibrate. Different particles are then represented by different modes propagating through the strings. Unfortunately, it was discovered that the vacuum strings (non-vibrating strings) have negative mass. These are called *tachyons* and they are unphysical. However, the first excited states are massless if the spacetime dimension around the string is chosen to be $D = 26$. So they could represent massless gauge bosons (open strings) and gravitons (closed strings).

The problem of the tachyons was resolved by imposing something called *supersymmetry*. This is a symmetry of changing bosons into fermions and vise versa. Adding this symmetry to the action removes the tachyonic states and reduces the critical dimension to $D = 10$. The way this is done is not unique and depending on the choice one makes here, one ends up in different types of string theory. A *type I* string theory is a theory that allows both open and closed strings. Considering only closed strings we get a *type II* string theory. The latter can again be classified as *type IIA* and *type IIB*. There are more such different kinds of varieties but they are all part of an 11-dimensional theory called *M-theory*.

2.3.2 Findings of a duality

To see the first example of a duality between a highly interacting effective quantum field theory and a higher dimensional theory of quantum gravity we need to focus on type IIB string theory. This theory allows for D-branes and in the low energy limit, it reduces to an effective quantum field theory called *type IIB supergravity*. Here only the first excitations of the strings become relevant. We propose now that we stack N 3-dimensional D-branes (D3-branes) on top of each other. We will denote the string coupling by g_s, the string length l_s, and the distance between the branes d. As mentioned before, the D-branes can serve as boundary conditions for open strings between them. We now take the low energy limit. Meaning that $l_s \to 0$ and $d \to 0$ while keeping $U = d/l_s^2$ (the mass of the strings between the branes) constant. We can see the strings between the branes as perturbations of the branes themselves and we get an effective quantum field theory. This theory is a gauge theory called $\mathcal{N} = 4$ supersymmetric Yang-Mills theory. Where $\mathcal{N}$ is the number of supercharges of the theory.[12] The gauge group of the QFT is $U(N)$ and it enjoys conformal symmetry! In this low energy limit, the interactions between the closed strings and the branes are removed. Thus making sure that the gauge theory decouples from the background type IIB supergravity, see Figure 5a.

Now an alternative viewpoint for this situation is to see the D-branes as massive perturbations of the type IIB supergravity theory. The metric of such a gravity theory for N D3-branes is given in [22],

$$\mathrm{d}s^2 = \frac{\mathrm{d}x^2}{\sqrt{1 + 4\pi N g_\mathrm{s} \left(l_\mathrm{s}/r\right)^4}} + \sqrt{1 + 4\pi N g_\mathrm{s} \left(l_\mathrm{s}/r\right)^4} \left(\mathrm{d}r^2 + r^2 \, \mathrm{d}\Omega_5^2 \right) \tag{2.54}$$

[12] Supercharges are the charges arising from Noether's theory belonging to the supersymmetry.

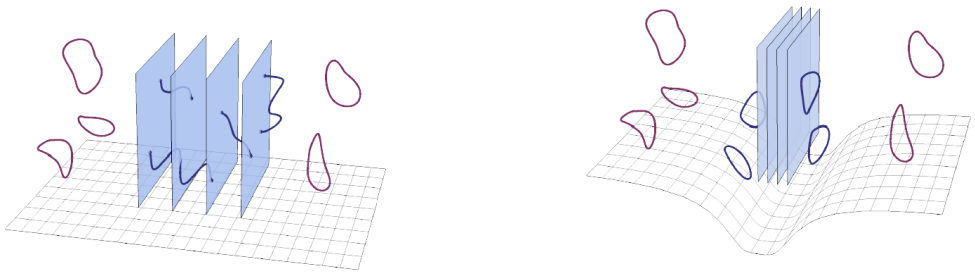

(a) At small coupling Ng_s, open strings between N D-branes form an effective $U(N)$ gauge theory in the low-energy limit, with decoupled closed strings described by IIB supergravity in a flat $\mathbb{R}^{9,1}$ background.

(b) At large Ng_s, the D-branes deform the spacetime background filled with closed strings. At low energies, strings near to and far away from the D-branes decouple; both are approximated by IIB supergravity, with the metric described by $\mathrm{AdS}_{4+1} \times S^5$ and flat $\mathbb{R}^{9,1}$, respectively.

Figure 5: Visualization of two perspectives on the AdS/CFT setup. [22]

where x are the coordinates along the brane and r the radial coordinate away from the brane. If we now define $\alpha = (4\pi N g_s)^{\frac{1}{4}} l_s$ we get that the metric becomes

$$\mathrm{d}s^2 = \frac{r^2}{\alpha^2}\,\mathrm{d}x^2 + \frac{\alpha^2}{r^2}\,\mathrm{d}r^2 + \alpha^2\,\mathrm{d}\Omega_5^2 \tag{2.55}$$

we recognise (2.49) and see this is the metric of $\mathrm{AdS}_{4+1} \times S^5$. Taking again the low energy limit we see that once more that the closed strings near $r = 0$ decouple from the ones far away, see Figure 5b. Now the closed strings away from the branes reduce to the same type IIB supergravity theory on a flat background metric. Again close to the branes we obtain a similar type IIB theory, but this time on an AdS space, instead of the conformal field theory we previously arrived at. Since both viewpoints of the branes should be equivalent, both theories should be equivalent and we arrive at the duality between

$$\mathcal{N} = 4\ SU(N) \text{ SYM theory on } \mathbb{R}^{3,1} \iff \text{Type IIB superstring theory on } AdS_5 \times S^5 \tag{2.56}$$

Now the coupling constants are related $g_{YM}^2 = 2\pi g_s$ and $\lambda \equiv N g_{YM}^2 = \alpha^4/2l_s^4$. Where λ is known as the *'t Hooft coupling*, the effective coupling in the gauge theory. Since we are taking a limit such that $l_s \ll \alpha$ we see that this coupling is strong. We can take another limit called the *'t Hooft limit*, where we take $N \to \infty$ but we keep λ fixed. We see that $g_s = \lambda/2\pi N$ will tend to zero. Hence the string coupling becomes very small. At the end of the day, we have a duality between a strongly coupled gauge theory and a weakly coupled gravity theory. This is why this gauge/gravity duality is also called a *strong/weak duality*. This is also why it is such a powerful tool. The stronger the coupling (or interactions) in the QFT, the weaker the string coupling in the gravity theory. In the limit of very large coupling in the CFT, the supergravity becomes so weakly coupled that we can treat it as a classical gravity theory i.e. Einstein's theory of general relativity. This is a great advantage since very strongly coupled QFT's cannot be calculated in the normal way, by expanding in the coupling constant and calculating the Feynman diagrams. Using this duality we can translate these strongly coupled QFT's to a classical theory of gravity and do the calculations there!

2.3.3 General AdS/CFT duality

The calculations previously described in Section 2.3.2 were done first by Juan Maldacena in [5]. He discovered that using the right limits in string theory, one finds a duality between a gravity theory on an $\mathrm{AdS}_{4+1} \times S^5$ space and a conformal field theory living on the AdS boundary of that space. This calculation can be repeated with different D-branes, leading to similar dualities of different dimensions. This of course suggests a more general duality between a gravity theory living on AdS and a conformal field theory on its boundary. That is why the general AdS/CFT conjecture reads

$$Z_{AdS_{d+1}}[\phi] = Z_{CFT_d}[\mathcal{O}]. \tag{2.57}$$

It is stated that the two theories are equivalent in the sense that their partition functions agree. Here the field ϕ is the bulk field and $\mathcal{O}$ is the operator on the boundary. This conjecture has been proposed by Edward Witten in [23]. It is still a conjecture, hence a formal proof of the statement has yet to be given.

In [24, 25] it is shown that the field ϕ in the bulk can be constructed from the boundary conditions on the AdS boundary. This is called *bulk reconstruction*. Let us denote ϕ_0 as this field restricted to the boundary. This then implies that the bulk action is a function of ϕ_0. Hence

$$Z_{AdS_{d+1}}[\phi] = Z_{AdS_{d+1}}[\phi_0] = \left\langle \exp \int d^d x \ \phi_0 \mathcal{O} \right\rangle_{CFT} \tag{2.58}$$

and we see the fields act as source terms for each other. After some calculations, this relation leads to

$$\Delta = \frac{1}{2}\left(d + \sqrt{d^2 + 4m^2}\right) \tag{2.59}$$

a relation between the scaling dimension of the operator Δ, the dimension of the theory d, and the mass of the bulk field m, according to [23]. This is the first example of the so-called AdS/CFT dictionary. This is a dictionary that relates quantities of the bulk to quantities of the boundary. We will see that entanglement entropy is also part of this dictionary. It is still very much under construction and learning more about the representations of entanglement entropy in the bulk and boundary can teach us about the rest of this dictionary.

Because of this fact that field ϕ 'emerges' from the conditions on the boundary, it is interpreted that the gravity theory and the extra dimension emerge from the conformal field theory. The conformal symmetry implies that the CFT is invariant under a change of length scale. Since length is inversely proportional to energy in natural units, this then implies an invariance in energy scale. The energy scale is then seen as the extra dimension that emerges. We have previously seen that, if the coupling in the CFT is strong, the coupling in the quantum gravity theory becomes weak. The inverse of this statement is true as well. If the coupling in the CFT becomes weak, we obtain a dual theory of quantum gravity with strong coupling. This situation can be studied to learn more about the nature of quantum gravity. One can now take a big leap and say that the gravity in our own universe is holographic, and it emerges from a CFT at the boundary of our universe. The problem is of course that our universe does not have the AdS geometry. The cosmological constant appears to be positive and our universe becomes asymptotically de-Sitter in the infinite past and future. There however also exists a dS/CFT conjecture and this might be applicable to our universe [26].

3 Holographic entanglement entropy

We now have a basic understanding of the ADS/CFT correspondence. This is an example of a holographic duality. This chapter will introduce entanglement entropy. A quantity that has an equivalent holographic description. We will introduce three ways of calculating this quantity. In the first section, we will introduce what entanglement entropy is and see how we can calculate it directly. After that we will give the first holographic description of entanglement entropy, using the AdS/CFT duality. We will see that this entanglement entropy can equivalently be calculated in the bulk. Finally, we will look at an alternative way to interpret and calculate entanglement entropy in the holographic sense, using something called bit threads. This will be the main goal of this thesis.

3.1 Entanglement entropy

Before we dive straight into entanglement entropy, we like to review the two concepts on their own. We start with our familiar notion of thermodynamic entropy and see this can be introduced more generally as Shannon entropy. Then we move over to the quantum world to discuss von Neumann entropy. Furthermore, we review two equivalent definitions of entanglement. After that, we define what we mean by entanglement entropy and show that it is the same for a subsystem, and its complement. Finally, we will work out an example. Calculating the entanglement entropy in a two-dimensional CFT.

Say we consider a thermodynamics system. Remember that the macrostates of the system are specified by measurable quantities like temperature, volume, pressure, etc. The microstates of the system are all the different ways one can order the individual particles, depending on the position and velocity of the particles. Recall now the definition of thermodynamic entropy

$$S = k_{\mathrm{B}} \log \Omega \tag{3.1}$$

where Ω is the number of microstates that represent the same macrostate and k_{B} is Boltzmann's constant. This form of entropy is actually a specific form of a more general information-theoretical entropy, which comes from the probability-based definition of information. Namely, if one finds the value of a random variable X, the information obtained from knowing this value is defined as

$$I = -k \log P(X) \tag{3.2}$$

for a constant k and probability P of fining this value a priory. Expressed in bits one uses $k = 1$ and $\log_2$. The entropy is then the average of the information over the probability distribution of X. Thus

$$S = \langle I \rangle = -k \sum_i P(X_i) \log P(X_i). \tag{3.3}$$

This definition is called *Shannon entropy* [27]. It tells us the uncertainty of the outcome of a classical random variable. Under one of the postulates of thermodynamics, the fact that every microstate is equally probable, this entropy reduces to the thermodynamic entropy of (3.1).

Until now everything was classical. We move to quantum mechanics and there is another form of entropy one can introduce. In general, a probability distribution like the one just given $P(X_i)$ can be related to an ensemble of states in quantum mechanics. Say one has a system that is not in one particular state, but has a certain probability to be in a number of states. The system is then best described by a density matrix

$$\rho = \sum_j p_j |j\rangle\langle j| \tag{3.4}$$

with p_j the probability that the system is in state $|j\rangle$. This is of course normalized such that $\sum_j p_j = 1$. If we have that there is a j such that $p_j = 1$, hence $\rho = |j\rangle\langle j|$, we then say that it is a *pure* ensemble. Otherwise, it is a *mixed* ensemble. The *von Neumann entropy* is defined as

$$S = -\mathrm{Tr}\rho \log \rho. \tag{3.5}$$

Now we can see that if we substitute (3.4) back into the von Neumann entropy we get

$$S = -\sum_j p_j \log p_j \tag{3.6}$$

and we recover the Shannon entropy again.

We have now introduced all relevant definitions of entropy. The von Neumann entropy was the most general of these definitions. We will see this entropy again shortly. Let us focus on entanglement for the moment. Remember that in quantum mechanics, we said that a state $|\Psi\rangle$ is *entangled* if it is part of the combined Hilbert space of two systems $\mathcal{H}_A \otimes \mathcal{H}_B$ and can **not** be written as the product of two states $|\psi\rangle_A \otimes |\psi\rangle_B$ each in there respective Hilbert space. An alternative definition would be the following. Recall that in the formulation of density operators, we may write the full known state $|\Psi\rangle$ as $\rho = |\Psi\rangle\langle\Psi|$. If one now wants to find the density matrix of one of the subsystems, say A. We can take the partial trace over B and define

$$\rho_A \equiv \sum_j \big(I_A \otimes \langle j|_B\big)|\Psi\rangle\langle\Psi|\big(I_A \otimes |j\rangle_B\big) = \mathrm{Tr}_B(\rho) \tag{3.7}$$

where $|j\rangle$ form a basis for $\mathcal{H}_B$ and I_A the identity on $\mathcal{H}_A$. For an entangled state, this *reduced density matrix* will then be a mixed ensemble rather than a pure ensemble.

Using the von Neumann entropy we can now give the definition of entanglement entropy. For a given quantum system made up of two subsystems A and B, the ground state $|\Psi\rangle$ can be expressed as a pure ensemble $\rho = |\Psi\rangle\langle\Psi|$. The *entanglement entropy* of the region A (or B for that matter) is defined as the von Neumann entropy of the reduced density matrix. Hence

$$S_A = -\mathrm{Tr}\rho_A \log \rho_A. \tag{3.8}$$

We can see straight away that if there is no entanglement between A and B, the reduced density matrix will be pure and the entanglement entropy will be zero. Also, note that the entanglement entropy is the same for the complement B. To see this, use the Schmidt decomposition of a pure state $|\Psi\rangle = \sum_i \alpha_i |\tilde{i}\rangle \otimes |i\rangle$[27]. Here $|\tilde{i}\rangle$ and $|i\rangle$ are orthonormal states who agree with the ones from the partial trace in (3.7). We compute the reduced density matrix

$$\begin{aligned}
\rho_A &= \sum_j \big(I \otimes \langle j|\big)|\Psi\rangle\langle\Psi|\big(I \otimes |j\rangle\big) \\
&= \sum_j \big(I \otimes \langle j|\big)\left(\sum_i \alpha_i |\tilde{i}\rangle \otimes |i\rangle\right)\left(\sum_k \alpha_k \langle\tilde{k}| \otimes \langle k|\right)\big(I \otimes |j\rangle\big) \\
&= \sum_j \left(\sum_i \alpha_i |\tilde{i}\rangle \otimes \langle i|j\rangle \sum_k \alpha_k \langle\tilde{k}| \otimes \langle k|j\rangle\right) \\
&= \sum_j |\alpha_j|^2 |\tilde{j}\rangle\langle\tilde{j}|
\end{aligned} \tag{3.9}$$

and we see

$$S_A = -\mathrm{Tr}\rho_A \log \rho_A = -\sum_j |\alpha_j|^2 \log\left(|\alpha_j|^2\right). \tag{3.10}$$

From this, it is clear that for a pure state $|\Psi\rangle$ we have that $S_A = S_B$.

3.1.1 Entanglement entropy in a two-dimensional CFT

As we have seen above, entanglement entropy or EE has a quite general definition. It can be defined for any quantum system that can be decomposed into two parts. What we want to do is try to find the EE in a QFT. In this subsection, we will focus on finding the EE of an interval in a time slice of a 1+1-dimensional CFT.

For these calculations, we will closely follow [28]. We start by choosing two points u and v on a time slice ($t = 0$) of a two-dimensional euclidean space. Then $A = [u, v]$ and we need to find the ground state $|\Psi\rangle$ of the CFT. This is best formulated in the path integral formalism. For a field

$\phi(t,x)$ representing the static CFT, the ground state of the system will be found by integrating from $t=-\infty$ to $t=0$

$$|\Psi(\phi_0)\rangle = \int_{\phi(-\infty,x)}^{\phi(0,x)\equiv\phi_0(x)} \mathcal{D}\phi \exp(-S(\phi)) \tag{3.11}$$

where S is the action. We know $\rho = |\Psi(\phi_0)\rangle\langle\Psi(\phi_0')|$ with ϕ' the field of the conjugate Ψ. To find ρ_A we need to trace over the subsystem B. In the QFT picture this means that we have to integrate over B with the condition that $\phi_0(x) = \phi_0'(x)$ for $x \in B$. When this is done we obtain ρ_A.

Next we perform a clever trick. We take n copies of ρ_A and perform the trace to obtain $\mathrm{Tr}\rho_A^n$. In the path integral formalism this is obtained by taking n-sheets of the CFT and gluing them together in an appropriate way. Namely, by demanding that $\phi_i'(x) = \phi_{i+1}(x)$ where the index i runs over the fields associated to the different sheets. This way $\mathrm{Tr}\rho_A^n$ is given by the path integral over a so called n-sheeted Riemann surface $\mathcal{R}_n$. Hence,

$$\mathrm{Tr}\rho_A^n = (Z_1)^{-n} \int_{\mathcal{R}_n} \mathcal{D}\phi \exp(-S(\phi)) = \frac{Z_n}{(Z_1)^n} \tag{3.12}$$

where Z_i is the partition function of i copies of ρ_A. Z_1 was introduced already in the path integral for ρ_A to normalize $\mathrm{Tr}\rho_A = 1$. Now if we take the derivative of the LHS with respect to n we get

$$\frac{\partial}{\partial n}\mathrm{Tr}\rho_A^n = \mathrm{Tr}\rho_A^n \log \rho_A \tag{3.13}$$

and taking the limit $n \to 1$ we obtain

$$S_A = -\left.\frac{\partial}{\partial n}\mathrm{Tr}\rho_A^n\right|_{n=1} = -\left.\frac{\partial}{\partial n}\frac{Z_n}{(Z_1)^n}\right|_{n=1}. \tag{3.14}$$

We now see the advantage of this trick as the problem that remains is finding these partition functions.

They show in [28] that by making some clever transformations of the energy-momentum tensor, they were able to calculate the vacuum expectation value (VEV) of the energy-momentum tensor on $\mathcal{R}_n$. They related this to the standard form of the OPE of the energy-momentum tensor with two primary operators $\Phi_n(u)$ and $\Phi_{-n}(v)$ inserted at the boundary points of A. These primary operators are called *twist fields* and have scaling dimension $\Delta_n = c/12(1-(1/n)^2)$ where c is the central charge. They obtained

$$\langle T(w)\rangle_{\mathcal{R}_n} \equiv \frac{\int \mathcal{D}\phi T(w) e^{-S(\mathcal{R}_n)}}{\int \mathcal{D}\phi e^{-S(\mathcal{R}_n)}} = \frac{\langle T(w)\Phi_n(u)\Phi_{-n}(v)\rangle_{\mathbf{C}}}{\langle \Phi_n(u)\Phi_{-n}(v)\rangle_{\mathbf{C}}} \tag{3.15}$$

as this relation. Infinitesimal conformal transformations were performed and from the way both sides of the equation transformed they deduced that

$$\frac{Z_n}{(Z_1)^n} \propto \langle \Phi_n(u)\Phi_{-n}(v)\rangle_{\mathbf{C}}^n \propto \left(\frac{u-v}{a}\right)^{-2n\Delta_n} = \left(\frac{\ell}{a}\right)^{-\frac{c}{6}(n-\frac{1}{n})} \tag{3.16}$$

where ℓ is the length of the interval and a a UV cut-off or lattice spacing, introduced to make it dimensionless. In the second step, we used equation (2.26) giving the two-point function of primary operators. The proportionality constant can be fixed by normalization. Finally, we obtain

$$S_A = -\left.\frac{\partial}{\partial n}\frac{Z_n}{(Z_1)^n}\right|_{n=1} = -\lim_{n\to 1}\log\left(\frac{\ell}{a}\right)\left(\frac{\ell}{a}\right)^{-\frac{c}{6}(n-\frac{1}{n})}\left(-\frac{c}{6}(1+\frac{1}{n^2})\right) = \frac{c}{3}\log\frac{\ell}{a}. \tag{3.17}$$

3.2 Holographic entanglement entropy

Having calculated the EE of a specific region in a $1+1$-dimensional CFT, an obvious question arises. As we have seen in the previous chapter, this CFT has a dual description in the form of a gravity theory living in AdS space. But in this gravity theory, what is the equivalent of the EE just calculated? This is an important question and the answer is quite elegant. It turns out that

the way we just calculated the EE (directly, using partition functions in the CFT) is actually the hardest! To find out what should be the bulk dual of EE, we first give a more intuitive idea of what EE actually represents. After that, we will give the holographic description of EE. Finally, we will give an example of how to calculate the same EE from the previous section, but now in the holographic description.

Say we consider again a CFT divided into two regions A and B. As we have seen before, the EE of region A is equal to that of region B. It measures the uncertainty of the ensemble ρ_A, as the Shannon entropy measures the uncertainty of a probability distribution. This Shannon entropy is given by the average information. But since we have traced over the subsystem B, the EE will represent the defect in the exchange in information between the subsystems. Thus a trivial EE $S_A = 0$ means there is a maximal exchange of information possible between A and B. But if the EE is maximal, this means that there is no exchange of information between the two regions. This reminds us of a black hole!

This already hints towards a holographic description. The entropy of a black hole is known to scale with the area of the horizon, not its volume. Does this statement find its origin in a holographic description of entropy? We could consider a black hole in AdS spacetime. We know there will be a CFT living on its conformal boundary. The black hole region will have a dual region on the boundary, say A. As just discussed, this EE should be maximal. Does it make sense to say that the entropy of the black hole is in some sense dual to the EE of the region A? If this is the case, then the EE will be proportional to the area of the black hole horizon

$$S_{BH} = \frac{A}{4G_N}. \tag{3.18}$$

Of course, in the above description, a lot of details are neglected. The overall idea, however, turns out to be not too far off. In general, there might not be a black hole present in the AdS spacetime. Hence the formal holographic duality of EE is formulated a bit differently. The original two finders of this description are Ryu and Takayanagi in [29, 30]. One can find an overview in [31]. They conjectured[13] that

$$S_A = \frac{\text{Area}(\gamma_A)}{4G_N} \tag{3.19}$$

where γ_A is the minimal surface in a time-slice of AdS homologous to A. Homologous means that the boundaries of the two surfaces agree $\partial\gamma_A = \partial A$. It is minimal in the sense that we minimize the area functional (using the Einstein-Hilbert action) over all surfaces in AdS homologous to A. This γ_A surface is therefore called the *Ryu-Takayanagi surface* or *RT surface* displayed in Figure 6.

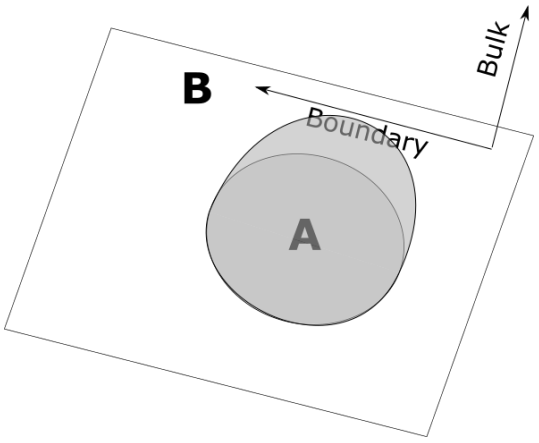

Figure 6: The grey "cap" is the RT surface of an entangling region A.

This was a remarkable finding. How is it that something so quantum-mechanical as entanglement has such an elegant geometric representation. Because of this it is natural to wonder what

[13] It was later also proven.

this quantity can teach us about the holographic map, the AdS/CFT dictionary and the emergence of spacetime. In [32] an example is given how entanglement creates geometry. One takes two copies of the same Hilbert space of some QFT and call them left and right theories. We can then write down the thermofield or Hartle-Hawking state by entangling energy eigenstates $|\mathrm{r}_i\rangle \in \mathcal{H}_R$ and $|\mathrm{l}_i\rangle \in \mathcal{H}_L$ respectively, weighted by a Boltzmann factor,

$$|\Psi\rangle = \frac{1}{\sqrt{Z(\beta)}} \sum_i e^{-\frac{1}{2}\beta E_i} |\mathrm{r}_i \mathrm{l}_i\rangle \,. \tag{3.20}$$

Tracing out one of the copies leaves the other in a mixed thermal state, say

$$\rho_R = \frac{1}{Z(\beta)} \sum_i e^{-\beta E_i} |\mathrm{r}_i\rangle \langle \mathrm{r}_i| \,. \tag{3.21}$$

For small β or equivalently large temperatures, the state is maximally entangled. At any non-vanishing β the entanglement entropy is given by the thermal entropy of a single theory as it turns out. At low temperatures $\beta \gg 1$ however, the ground state dominates and there is low entanglement. What do the different values of β represent in the bulk? For thermal states like this, the bulk contains a Schwarzschild-AdS black hole. However, in the case of low entanglement, the left and right black holes are disconnected geometrically. Only when the high entanglement case is considered, a causal 'bridge' is built between the two black holes. This is an example of how entanglement creates geometry and this is why it is sometimes thought that 'entanglement builds bridges'.

This holographic description of EE has a lot of advantages. For instance, we see that it should be the same for the complement B since $\partial A = \partial B$. The interpretation of EE is also more clear in this picture, since γ_A represents a partition of the bulk into two regions, just as the entangling surface or ∂A represents a partition of the boundary. This way it makes sense that the RT surface should be homologous to A. From the information-theoretical perspective, γ_A can be seen as some kind of horizon, dividing the two regions of the bulk such that the exchange of information is limited. Although this interpretation is not perfect, we shall see in the next section that it does come close. One can also see from this formulation that the entropy inside a certain region (and hence the total amount of information) is bounded by its surface area, not its volume.

It is important to note that the RT-formula is only valid for a time slice of holographic spacetime. If one wants to find the holographic entanglement entropy in a covariant situation, a slight adjustment to the RT-formula is needed [33]. One then, instead of a minimal surface, has to find an *extremal surface* in the bulk homologous to A. This extremal surface should be a local extremum of the area functional. Apart from this, restricted to the boundary it should agree with the entangling surface (as was for the RT-surface). It should be retractable to the entangling region, in the sense of homology. Finally, of all surfaces satisfying these conditions, we should pick the one that has the least area. This formulation is called the *HRT formula* and it reduces to the minimal surface if we take a static time slice.

The HRT and RT formula have both been proven in [34] and [35] respectively. Important to remember is that these formulas only hold in a specific limit. If we remember the couplings form Section 2.3.2, the (H)RT formulae are only valid in the limit of large N and large 't Hooft coupling (λ). In this limit the quantum gravity in the bulk becomes classical and we can use Einstein's equation. However, if one of these couplings are small, we can include corrections to obtain a valid answer. Corrections in $1/\lambda$ are given by higher curvature gravities [36, 37]. Corrections in $1/N$ are given by semi-classical gravity or quantum corrections [38, 39].

There is still one final detail that requires our attention. The area of the minimal surface and hence the EE is actually infinite. This is because the metric diverges at the boundary. This can easily be seen in Poincare coordinates from (2.50) and remembering that the boundary is at $z \to 0$. It is not a major problem because one can simply introduce a cut-off in the z direction. This means that we will calculate the area of the minimal surface until $z = \epsilon$ (some parameter) close to 0.

3.2.1 Holographic entanglement entropy of a CFT

We now want to put the method previously introduced to use. Let us consider the same CFT as in Section 3.1.1. We again consider the same region A. This will be given by the interval from

$(-\ell/2, 0)$ to $(\ell/2, 0)$ in a time slice of the CFT. Here ℓ is again the length of the interval. We now need to find the minimal surface in a time slice of AdS_3. The metric will be given by

$$ds^2 = \frac{R^2}{z^2}(dx^2 + dz^2) \tag{3.22}$$

on the hyperbolic half-plane. We need to find a line in this hyperbolic half-plane that has minimal length and has endpoints $(-\ell/2, 0)$ and $(\ell/2, 0)$. This minimal length will correspond to a geodesic. The non-vanishing Christoffel symbols are

$$\Gamma^z_{xx} = \frac{1}{z} \qquad\qquad \Gamma^x_{zx} = \Gamma^x_{xz} = \Gamma^z_{zz} = -\frac{1}{z}. \tag{3.23}$$

Remembering the geodesic equation

$$\frac{d^2x^\mu}{ds^2} + \Gamma^\mu_{\alpha\beta}\frac{dx^\alpha}{ds}\frac{dx^\beta}{ds} = 0 \tag{3.24}$$

we find two differential equations

$$\frac{d^2x(s)}{ds^2} - \frac{2}{z}\frac{dx(s)}{ds}\frac{dz(s)}{ds} = 0 \tag{3.25}$$

$$\frac{d^2z(s)}{ds^2} + \frac{1}{z}\left(\left(\frac{dx(s)}{ds}\right)^2 - \left(\frac{dz(s)}{ds}\right)^2\right) = 0 \tag{3.26}$$

and (3.25) implies that

$$z\frac{d^2x}{ds^2} = 2\frac{dx}{ds}\frac{dz}{ds}. \tag{3.27}$$

Consider now the following quantity

$$x_0 \equiv z\frac{dz}{ds}\left(\frac{dx}{ds}\right)^{-1} + x \tag{3.28}$$

and take the derivative with respect to s. We obtain

$$\begin{aligned}
\frac{dx_0}{ds} &= \left(\frac{dz}{ds}\right)^2\left(\frac{dx}{ds}\right)^{-1} + z\frac{d^2z}{ds^2}\left(\frac{dx}{ds}\right)^{-1} - z\frac{dz}{dx}\left(\frac{dx}{ds}\right)^{-2}\frac{d^2x}{ds^2} + \frac{dx}{ds} \\
&= \left(\frac{dz}{ds}\right)^2\left(\frac{dx}{ds}\right)^{-1} + z\frac{d^2z}{ds^2}\left(\frac{dx}{ds}\right)^{-1} - 2\frac{dz}{dx}\left(\frac{dx}{ds}\right)^{-2}\frac{dx}{ds}\frac{dz}{ds} + \frac{dx}{ds} \\
&= z\frac{d^2z}{ds^2}\left(\frac{dx}{ds}\right)^{-1} + \frac{dx}{ds} - \left(\frac{dz}{ds}\right)^2\left(\frac{dx}{ds}\right)^{-1} = 0
\end{aligned} \tag{3.29}$$

where in the second step we substituted (3.27) and the last line is just (3.26) multiplied by $z(dx/ds)^{-1}$, hence zero. We conclude that x_0 is a constant and that

$$z\frac{dz}{ds} + x\frac{dx}{ds} = x_0\frac{dx}{ds}, \tag{3.30}$$

by multiplying (3.28) by $(dx/ds)^{-1}$. We notice that this is just the derivative of

$$z^2 + (x - x_0)^2 = r_0^2 \tag{3.31}$$

the semi-circle centered at $(x_0, 0)$ with radius r_0. We conclude that the geodesics will be semi-circles. What remains is to compute the length of a semi-circle with endpoints $(-\ell/2, 0)$ and $(\ell/2, 0)$. That means that $r_0 = \ell/2$ and $x_0 = 0$. Since the metric diverges as $z \to 0$, we have to introduce a cut-off parameter a and calculate the length from $z = a$. We choose a parameterization

$$\mathbf{r}(s) = \frac{\ell}{2}(\cos s, \sin s) \tag{3.32}$$

and define $\epsilon = 2a/\ell$ as a cut-off for the parameterization. Remember the formula for arc length

$$\begin{aligned}\text{Length}(\gamma_A) &= \int d\mathbf{r}(s) = \int \left|\frac{d\mathbf{r}}{ds}\right| ds = \int \sqrt{g_{\mu\nu}\frac{dr^\mu}{ds}\frac{dr^\nu}{ds}}ds \\ &= \int_\epsilon^{\pi-\epsilon} \sqrt{\frac{R^2}{\left(\frac{\ell}{2}\sin s\right)^2}\left(\frac{\ell^2}{4}\sin^2 s + \frac{\ell^2}{4}\cos^2 s\right)}ds \\ &= 2R\int_\epsilon^{\frac{\pi}{2}} \frac{ds}{\sin s} = 2R\left[-\log\left|\frac{1+\cos s}{\sin s}\right|\right]_\epsilon^{\pi/2} \\ &= 2R\log\left|\frac{1+\cos\epsilon}{\sin\epsilon}\right| \approx 2R\log\frac{2}{\epsilon} = 2R\log\frac{\ell}{a}\end{aligned} \tag{3.33}$$

where in the last step we used the small-angle approximations $\sin x \approx x$ and $\cos x \approx 1$. We conclude that since the central charge of the CFT is related to the AdS radius and Newton's constant via the AdS/CFT dictionary, $c = 3R/2G_N$, we obtain

$$S_A = \frac{\text{Length}(\gamma_A)}{4G_N} = \frac{c}{3}\log\frac{\ell}{a}. \tag{3.34}$$

This is the same result as obtained in Section 3.1.1.

3.3 Bit threads

The new holographic description of the EE, as being proportional to the RT surface, already has its computational advantages. However, there are still some things that conflict with this interpretation from the information-theoretical point of view. At this moment the interpretation of RT formula is that the information of the region A, associated with the maximum EE S_A, is encoded by one bit per four Planck areas on the minimal surface.[14] Just as in the holographic principle of t' Hooft in [3] concerning the black hole entropy. A problem with this, pointed out in [40], arises when we consider A to be a partition of two disconnected regions $A = A_1 \cup A_2$. If the two regions are far away form each other, the RT surface will be given by the union of the RT surfaces of each of the two regions $\gamma_A = \gamma_{A_1} \cup \gamma_{A_2}$ (Figure 7a). But moving the two regions closer together continuously, there is a point where the RT surface changes discontinuously. Since at close range we have that $\gamma_A \neq \gamma_{A_1} \cup \gamma_{A_2}$ (Figure 7b). This can be seen in Figure 7. What happens to the bits in this situation? Is there a discontinuous transfer of bits, or is our interpretation of the RT surface wrong?

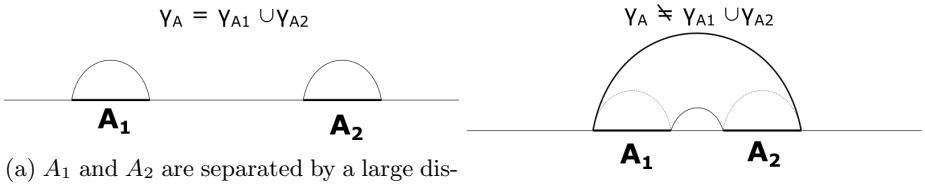

(a) A_1 and A_2 are separated by a large distance. The union of their minimal surfaces is equal to the minimal surface of A, the union of A_1 and A_2.

(b) A_1 and A_2 are close to each other. The union of their minimal surfaces is now not equal to the minimal surface of A.

Figure 7: The discontinuity in the RT surface as we move the entangling regions closer to each other.

In [40] a new way of looking at the RT formula is proposed. By introducing the so called *bit threads*. These are threads that start and end at the boundary and move through the bulk, containing one bit of information. Threads starting in A contain one bit of information about the microstate of A. So S_A is the maximal number of bits that can leave A. More rigorously, the threads are the flow lines of a certain vector field i.e. for a vector field v^μ a thread would be a curve $\gamma(t)$ satisfying

$$\frac{d\gamma^\mu(t)}{dt} = v^\mu|_{\gamma(t)} \qquad \forall t \in \text{dom}(\gamma). \tag{3.35}$$

[14] A Planck area is the Planck length squared.

However, this vector field can not just be any vector field, it has to satisfy certain conditions. Namely, it has to be divergenceless and bounded

$$\nabla_\mu v^\mu = 0 \qquad\qquad |v| \leq C \tag{3.36}$$

where C is a constant. A vector field satisfying these conditions is called a *flow*.

What is the connection of these bit threads with the RT surface? To see this we first have to investigate the flux of this flow through the surface A. Note that due to Stokes' Theorem and the fact that the vector field is divergenceless, we get that

$$\int_A v \equiv \int_A \sqrt{h} n_\mu v^\mu = \int_{\gamma_A} v \tag{3.37}$$

where h is the induced metric on the surface of integration and n_μ is the normal vector to the surface, pointing outward on the RT surface. Due to the fact that the RT surface is homologous to A, the net flux entering the volume enclosed by A, and the RT surface has to be zero. Meanwhile, the flow is bounded thus so is the flux through the region A

$$\int_A v = \int_{\gamma_A} v \leq C \text{ area}(\gamma_A). \tag{3.38}$$

There is a theorem originally from network theory called the *max-flow min-cut theorem* [40, 41]. It says that if one now maximizes the LHS over all possible flows, the inequality becomes saturated. We end up with

$$\max_v \int_A v = C \text{ area}(\gamma_A) \tag{3.39}$$

and if we choose the constant $C = 1/4G_N$ we get a new formulation of the EE as

$$S_A = \max_v \int_A v. \tag{3.40}$$

We see that the flow saturates at the RT surface. This is the way we want to interpret the RT surface, as a bottleneck for the more fundamental bit threads. If we remember that bit threads represent one bit of information, we can now see that RT-surface is the bottleneck for the number of bit threads leaving the entangling region. Restricting the EE to one bit per four Planck areas. It is now clear that the bit thread configuration in the bulk is a global property. Moving two disjoint regions of the boundary closer to each other will not induce a discontinuous jump in the threads, although the bottleneck of the threads might change discontinuously.

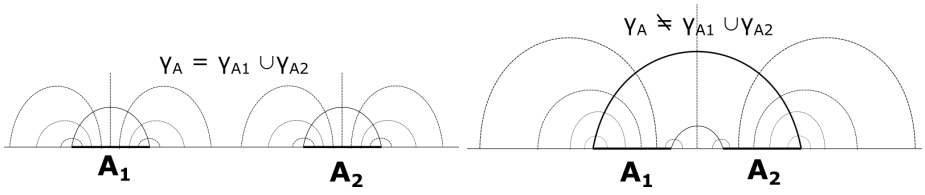

Figure 8: A similar picture as figure 7, but now with the bit threads. We see the RT surface as the bottleneck for the bit threads. This still changes discontinuously as we move the entangling regions closer together, but the bit threads can have a smooth transitions into there new configuration.

It is important to note at this point, that there is no unique flow whose flux corresponds to the EE. The global maximum of the flux in the space of all flows is degenerate. Thus there is still some freedom left for the flow, even if one has found a flow that maximizes the flux. In principle one of the degenerate flows would be enough to calculate the EE. There is an interpretation for this freedom given in [40]. First of all, there is the freedom to move the starting points of the threads around on the entangling surface. As long as threads start and end on the boundary, and do not split or join each other. This is excluded because of the divergenceless condition. There is also the freedom to add more threads that start and end at the entangling region. As long as

they stay away from the RT-surface, since the number of threads is maximized there to be one per four Planck areas. In the former case, this freedom represents classical correlations within the entangling region. In the latter case, this is due to entanglement within the entangling region. A bit thread is really thought to represent entanglement between different boundary points.

Just as with the (H)RT formula, this description of the bit threads is only valid in the classical gravity ($N, \lambda \to \infty$) limit. For corrections in $1/\lambda$ i.e. higher curvature gravity, see [42]. For quantum corrections ($1/N$ corrections) see [43, 44]. There are also some interesting applications to the this bit thread description. In [45], Einstein's equation is derived in the bulk from the bit thread dynamics. The tools used to prove the entropy inequalities in the bit thread formulation can be found in [46]. Finally so literature on the connection between bit threads and tensor networks [47, 48, 49]

What happens to the problem that the metric diverges at the boundary? The RT surface is divergent because of this fact. This is solved by imposing a cut-off in the z direction and calculating the area of the RT surface from $z = \epsilon$ upward. In the bit threat picture, this problem arises due to the fact that the vector field diverges on the entangling surface ∂A. This can be resolved by introducing a cut-off δ in the interior of A and calculating the flux until $r = R - \delta$. where r is some kind of radial coordinate in the boundary and R is then the location of the entangling surface.[15] Another advantage to the bit thread picture is that, this way the vector field itself is actually non-divergent, only the flux is. Whereas in the RT formulation the whole RT surface itself is divergent.

In this thesis, we want to use this interpretation of the EE to see if we can find a method for computing the EE. We can already see that the problem now lies with maximizing the flux functional over the space of flows, a problem in convex optimization.[16] We note however that the vector field is still defined in AdS space. We want to investigate if we can move the problem to flat Minkowski space and optimize the flux there. Keeping track of course, of the conditions that one has to impose on the vector field.

[15] R can depend on the other coordinates in the boundary or course.
[16] This is a field in mathematics that is focused on maximizing in general settings.

4 Results

In this chapter, we will discuss the result of this thesis. Its primary focus is to calculate the EE of several regions in a time-slice of a two and three-dimensional CFT. We use the holographic bit thread description introduced in the previous two chapters. The ultimate goal is to find a general algorithm for calculating the EE of general regions in two and three-dimensional CFT's. We hope that our method helps with analytic and numerical calculations. The idea rests on the assumption that the global maximum of the flux over the space of flows can be found by considering the same optimization problem in Minkowski space, this is done by relating the vector field in AdS and Minkowski space by an overall conformal factor. If successful, the divergenceless condition on the space of vector fields in Minkowski space would indicate that one might consider magnetic fields as candidates for the max-flow. The magnetic field would be generated by a current running through the entangling surface.

The chapter is structured as follows. We start by imposing that there is a vector field in Minkowski space which is related to the max-flow by a conformal factor. We follow the conditions for a flow and arrive at similar conditions for the vector field. A magnetic field is considered as candidate for this vector field, we focus our attention on specific regions in a three-dimensional CFT. We see that this does not work however, if we make a small change to the law generating the field, we are able to find a max-flow for specific examples. After this, we will try to justify our change by maximizing the flux functional. We discover a lot of degeneracy when maximizing the flux. We continue by taking a detour to the two-dimensional CFT and see that we can find a working description there as well. Realizing that the bounded condition was not imposed yet, we combine the degenerate states for the flux maximizing vector fields with the bounded condition to conclude that this fixes a lot of degeneracies. Finally, we test our newfound algorithm on a case that is not yet known and discover that a general law should depend on the extrinsic curvature of the entangling surface.

4.1 Flows from AdS to Minkowski

Given a region A on the boundary of a d-dimensional CFT there must be a bit thread configuration that corresponds to the flow lines of a max-flow. We want to find a vector field in Minkowski space that is related to this max-flow by a conformal factor. We then have to carry the conditions of a flow (divergenceless and bounded) to the new vector field. Investigating what happens to these conditions, we get a new set of conditions on the vector field in Minkowski space. These should be equivalent to the conditions of a flow on AdS space.

We start with the metric of AdS_{d+1} in Poincaré coordinates

$$ds^2 = \frac{l^2}{z^2}(-dt^2 + dx_1^2 + \cdots + dx_{d-1}^2 + dz^2) = g(z)ds^2_{\mathrm{Min}}, \tag{4.1}$$

and write it as a function $g(z)$ times the metric in Minkowski space. This motivates us to make the following assumption for the maximizing vector field: We impose that there exists a max-flow in AdS and a vector field in Minkowski space that is related by a conformal factor. Hence,

$$V_{\mathrm{AdS}} = f(z)V_{\mathrm{Min}} \tag{4.2}$$

where the subscript indicates where the vector field lives and $f(z)$ is the conformal factor. We consider a constant time slice and compute the divergence in AdS space to set it equal to zero. The only non zero components of the Christoffel symbol for this conformal metric are

$$\Gamma^{\mu}_{\mu z} = \frac{1}{2}g^{\mu\mu}\partial_z g_{\mu\mu} = \frac{1}{2}g(z)^{-1}\eta^{\mu\mu}\partial_z g(z)\eta_{\mu\mu} = \frac{d}{2}\frac{g'(z)}{g(z)} \tag{4.3}$$

where the greek index μ is still free and $g(z) = \frac{l^2}{z^2}$. This makes the divergence

$$\begin{aligned}
\nabla_\mu V^{\mu}_{\mathrm{AdS}} &= \partial_\mu V^{\mu}_{\mathrm{AdS}} + \Gamma^{\mu}_{\mu\nu}V^{\nu}_{\mathrm{AdS}} = \partial_\mu(f(z)V_{\mathrm{Min}}) + \frac{d}{2}\frac{g'(z)f(z)}{g(z)}V^{z}_{\mathrm{Min}} \\
&= f'(z)V^{z}_{\mathrm{Min}} + f(z)\partial_\mu V^{\mu}_{\mathrm{Min}} + \frac{d}{2}\frac{g'(z)f(z)}{g(z)}V^{z}_{\mathrm{Min}} \qquad (4.4) \\
&= \left(f'(z) + \frac{dg'(z)f(z)}{2\ g(z)}\right)V^{z}_{\mathrm{Min}} \overset{!}{=} 0 \qquad (4.5)
\end{aligned}$$

where the second term in (4.4) is set to zero by demanding that the vector field is divergenceless in Minkowski-space as well. Apart from the fact that, we do this because now we get a simple differential equation for $f(z)$

$$f'(z) + \frac{d}{2}\frac{g'(z)f(z)}{g(z)} = 0,$$

it is also convenient that the divergenceless condition is preserved in the transition to Minkowski space. It is easy to check that this differential equation is solved by

$$f(z) = \frac{c_1}{g(z)^{\frac{d}{2}}} = \frac{c_1}{(\frac{l^2}{z^2})^{\frac{d}{2}}} = \frac{c_1}{l^d} z^d \tag{4.6}$$

for c_1 an arbitrary constant. This constant can be fixed by imposing the second condition.

The second condition that needs to be satisfied in order for V_{AdS} to be a flow is boundedness. We impose that

$$\begin{aligned}
|V_{\text{AdS}}| &\leq \frac{1}{4G_N} \\
\sqrt{g_{\mu\nu}V^\mu_{\text{AdS}}V^\nu_{\text{AdS}}} &\leq \frac{1}{4G_N} \\
\sqrt{g(z)\eta_{\mu\nu}f(z)V^\mu_{\text{Min}}f(z)V^\nu_{\text{Min}}} &\leq \frac{1}{4G_N} \\
\sqrt{g(z)}f(z)|V_{\text{Min}}| &\leq \frac{1}{4G_N} \\
c_1 g(z)^{\frac{1-d}{2}}|V_{\text{Min}}| &\leq \frac{1}{4G_N} \\
c_1 \frac{z^{d-1}}{l^{d-1}}|V_{\text{Min}}| &\leq \frac{1}{4G_N} \\
z^{d-1}|V_{\text{Min}}| &\leq \frac{l^{d-1}}{4c_1 G_N}
\end{aligned} \tag{4.7}$$

and we see that we can fix the constant $c_1 = l^{d-1}/4G_N$. This way we get that the function $f(z)$ is completely fixed for each dimension of AdS. In conclusion, we can summarize the new conditions as

$$\boxed{V_{\text{AdS}} = \frac{z^d}{4lG_N}V_{\text{Min}} \qquad \partial_\mu V^\mu_{\text{Min}} = 0 \qquad z^{d-1}|V_{\text{Min}}| \leq 1} \tag{4.8}$$

and we know that if these conditions are satisfied, the vector field in AdS space will be a flow.

This result now allows us to translate the conditions to Minkowski-space and look for flux maximizing vector fields there. There are two reasons why we think that magnetic fields could be serious candidates for this vector field in Minkowski. The first one is the fact that the bit threads look like magnetic field lines. This can be seen in Figures 12 and 13 in Appendix A. The second reason is the fact that the divergenceless condition is preserved when we make the transformation go to Minkowski, and we know magnetic fields are divergenceless. These things make us curious to see if magnetic field could generate a max-flow. But, where do we put the wire generating the magnetic field? Since the max-flow diverges **on** the entangling surface, this would be a natural place for us to place the current.

4.2 Magnetic fields

For the moment we will focus on a time slice of a three-dimensional CFT. This will be a two-dimensional surface. We will try to find the bit tread configurations and hence the EE of a disk and the half-plane. The corresponding entangling surface will then be a circle and an infinite straight line respectively. We will try running a current through the entangling surface and investigate the magnetic field. This will be compared with calculations of bit threads in AdS in appendix A. These calculations have been done by Dr. Juan F. Pedraza in [50] and are known to give the right bit thread configuration and EE.

4.2.1 The magnetic field for the disk

We start with $A = D^2(R)$ a disk of radius R. The entangling surface will be a circle of radius R. We let a current run through this circle and find the magnetic field using Biot-Savart's law

$$\mathbf{B}(\mathbf{r}) = I \int \frac{d\mathbf{l} \times \mathbf{r}'}{|\mathbf{r}'|^3} \tag{4.9}$$

where we have omitted the the factor of $\mu_0/4\pi$ since we are not considering a real magnetic field. The current I is arbitrary at this point. We can later determine how much current we run through the wire such that the flux will match the area of the RT surface. We have that $\mathbf{r}' = \mathbf{r} - \mathbf{l}$ and $\mathbf{l}$ the position of the current. The current will be parameterized by ϕ thus in cylindrical coordinates(r, θ, z) we have that $\mathbf{r} = (r\cos\theta, r\sin\theta z)^T$ and $\mathbf{l} = (R\cos\phi, R\sin\phi, 0)^T$. This gives

$$d\mathbf{l} = \begin{pmatrix} -R\sin\phi \\ R\cos\phi \\ 0 \end{pmatrix} d\phi \qquad \text{and} \qquad \mathbf{r}' = \begin{pmatrix} r\cos\theta - R\cos\phi \\ r\sin\theta - R\sin\phi \\ z \end{pmatrix}. \tag{4.10}$$

The cross product between the two then becomes

$$\begin{aligned} d\mathbf{l} \times \mathbf{r}' &= \begin{pmatrix} -R\sin\phi \\ R\cos\phi \\ 0 \end{pmatrix} \times \begin{pmatrix} r\cos\theta - R\cos\phi \\ r\sin\theta - R\sin\phi \\ z \end{pmatrix} d\phi \\ &= \begin{pmatrix} zR\cos\phi \\ zR\sin\phi \\ -rR\sin\theta\sin\phi + R^2\sin^2\phi - rR\cos\theta\cos\phi + R^2\cos^2\phi \end{pmatrix} d\phi \\ &= \begin{pmatrix} zR\cos\phi \\ zR\sin\phi \\ R^2 - rR\cos(\phi - \theta) \end{pmatrix} d\phi \end{aligned} \tag{4.11}$$

and

$$\begin{aligned} |\mathbf{r}'|^3 &= \left((r\cos\theta - R\cos\phi)^2 + (r\sin\theta - R\sin\phi)^2 + z^2\right)^{\frac{3}{2}} \\ &= \left(r^2\cos^2\theta - 2rR\cos\theta\cos\phi + R^2\cos^2\phi + r^2\sin^2\theta - 2rR\sin\theta\sin\phi + R^2\sin^2\phi + z^2\right)^{\frac{3}{2}} \\ &= \left(r^2 - 2rR\cos(\phi - \theta) + R^2 + z^2\right)^{\frac{3}{2}}. \end{aligned} \tag{4.12}$$

Substituting this into $\mathbf{B}(\mathbf{r})$ we get

$$\mathbf{B}(\mathbf{r}) = I \int_0^{2\pi} \begin{pmatrix} zR\cos\phi \\ zR\sin\phi \\ R^2 - rR\cos(\phi - \theta) \end{pmatrix} \frac{d\phi}{(r^2 + R^2 - 2rR\cos(\phi - \theta) + z^2)^{\frac{3}{2}}}. \tag{4.13}$$

Looking at the expression we see that something might be wrong with this field. An indication for this is the following. If we look at the z-component of the field. We see that it has a polynomial of degree two in R in the numerator. In the denominator, we have also a degree two polynomial, but to the power of 3/2. This gives that the overall order of magnitude of the z-component is proportional to $\mathcal{O}(R^{-1})$. If we now compare this to (A.1) (with $d = 2$ the dimension of the boundary time slice) we see that the z-component has order of magnitude $\mathcal{O}(R^{-2})$ in R. This suggests that we might need to change the power in the denominator to of (4.9) to match this.

4.2.2 The magnetic field for the half-plane

Having looked at a specific current configuration, a circular current, we will now look at another entanglement region. In this case $A = H^2 = \{(x, y) \in \mathbb{R} \mid y \geq 0\}$ such that the entangling surface will be the x-axis. We let a current run through the x-axis and we will calculate the magnetic field it produces. We again calculate the magnetic field in the space with Biot-Savart's law (4.9). In this case, will just use Cartesian coordinates and let l parametrize the current. Then $\mathbf{r} = (x, y, z)^T$

and $\mathbf{l} = (l, 0, 0)^T$. This yields $\mathbf{r}' = (x - l, y, z)^T$ and $\mathbf{dl} = (dl, 0, 0)^T$. We get that the cross product becomes

$$\mathbf{dl} \times \mathbf{r}' = \begin{pmatrix} x - l \\ y \\ z \end{pmatrix} \times \begin{pmatrix} dl \\ 0 \\ 0 \end{pmatrix} = \begin{pmatrix} 0 \\ -z dl \\ y dl \end{pmatrix} \tag{4.14}$$

and

$$|\mathbf{r}'|^3 = \left((x - l)^2 + y^2 + z^2\right)^{\frac{3}{2}}. \tag{4.15}$$

Substituting this again into the integral for the magnetic field one obtains

$$\mathbf{B}(\mathbf{r}) = I \int_{-\infty}^{\infty} \frac{dl}{((x - l)^2 + y^2 + z^2)^{\frac{3}{2}}} \begin{pmatrix} 0 \\ -z \\ y \end{pmatrix} = I \int_{-\infty}^{\infty} \frac{dl}{(l^2 + y^2 + z^2)^{\frac{3}{2}}} \begin{pmatrix} 0 \\ -z \\ y \end{pmatrix} \tag{4.16}$$

where in the second step we used the fact that the problem is symmetric in the x-coordinate and we choose $x = 0$. Taking a look at (B.6) from Appendix B with $\alpha = 3/2$ we get

$$\int_{-\infty}^{\infty} \frac{dx}{(x^2 + c^2)^{\frac{3}{2}}} = \sqrt{\pi} \frac{\Gamma(1)}{\Gamma(\frac{3}{2})} (c^2)^{-1} = \frac{2}{c^2}. \tag{4.17}$$

With $c^2 = y^2 + z^2$ in this case, we can perform the integral and the magnetic field becomes

$$\mathbf{B}(\mathbf{r}) = \frac{2I}{(y^2 + z^2)} \begin{pmatrix} 0 \\ -z \\ y \end{pmatrix}. \tag{4.18}$$

We see again that this does not agree with (A.18), where we set $d = 2$ and replace x with y.

4.3 Modifying the law for the flow

There is a clear issue with the magnetic fields as we have just calculated them. The power in the denominator seems to be consistently off from the one in Appendix A. So what would be sensible to do now? Can we change the power in the denominator of Biot-Savart's law? Will we keep the divergenceless property? This is something we will investigate in the next section. We would like to modify Biot-Savart's law a bit so that we can match the field in the appendix A, but keep the divergenceless property. Our suggestion now is to modify the denominator from a third to a fourth power. This is based on the fact that if the power in the denominator in (4.13) were two, the order of magnitude in R would match the field in (A.1). This results in

$$\mathbf{B}(\mathbf{r}) = I \int \frac{d\mathbf{l} \times \mathbf{r}'}{|\mathbf{r}'|^4}. \tag{4.19}$$

What happens to the divergence of the field? Let us straightforwardly compute it. For this, we use the following vector calculus identity

$$\nabla \cdot \left(\frac{\mathbf{A}}{\phi}\right) = \frac{\phi \nabla \cdot \mathbf{A} - \nabla\phi \cdot \mathbf{A}}{\phi^2} \tag{4.20}$$

for a general vector field $\mathbf{A}$ and scalar field ϕ. We will interchange between considering the derivatives with respect to $\mathbf{r}$ and $\mathbf{r}'$ since the derivative of $\mathbf{r}'$ with respect to $\mathbf{r}$ is one. Using this we see that

$$\begin{aligned} \nabla \cdot \mathbf{B}(\mathbf{r}) &= I \int \nabla \cdot \frac{d\mathbf{l} \times \mathbf{r}'}{|\mathbf{r}'|^4} = I \int \frac{|\mathbf{r}'|^4 \nabla \cdot (d\mathbf{l} \times \mathbf{r}') - \nabla |\mathbf{r}'|^4 \cdot (d\mathbf{l} \times \mathbf{r}')}{|\mathbf{r}'|^8} \\ &= I \int \frac{\nabla \cdot (d\mathbf{l} \times \mathbf{r}') - 4|\mathbf{r}'|^{-2} \mathbf{r}' \cdot (d\mathbf{l} \times \mathbf{r}')}{|\mathbf{r}'|^4}. \end{aligned} \tag{4.21}$$

Using another vector calculus identity

$$\nabla \cdot (\mathbf{A} \times \mathbf{B}) = (\nabla \times \mathbf{A}) \cdot \mathbf{B} - \mathbf{A} \cdot (\nabla \times \mathbf{B}) \tag{4.22}$$

to obtain

$$\nabla \cdot (d\mathbf{l} \times \mathbf{r}') = (\nabla \times d\mathbf{l}) \cdot \mathbf{r}' - d\mathbf{l} \cdot (\nabla \times \mathbf{r}') = 0 \tag{4.23}$$

since $d\mathbf{l}$ does not depend on $\mathbf{r}$ and the curl of $\mathbf{r}'$ is obviously zero. Finally we use the fact that for any vector $\mathbf{r}'$,

$$\mathbf{r}' \cdot (d\mathbf{l} \times \mathbf{r}') = 0 \tag{4.24}$$

since $(d\mathbf{l} \times \mathbf{r}')$ is perpendicular to $\mathbf{r}'$. We see that indeed the field is still divergenceless.

4.3.1 The circular current

With this new expression for the vector field, let us now return to our specific cases. We want to apply this modified law for the magnetic field, to see if we can match the expression in Appendix A. We start again with the case where A is the disk. We let a current run through the entangling surface which is again a circle of radius R. This time we compute the $\mathbf{B}(\mathbf{r})$ field using (4.19) hence

$$\mathbf{B}(\mathbf{r}) = I \int_0^{2\pi} \begin{pmatrix} zR\cos\phi \\ zR\sin\phi \\ R^2 - rR\cos(\phi - \theta) \end{pmatrix} \frac{d\phi}{\left(r^2 + R^2 - 2rR\cos(\phi - \theta) + z^2\right)^2}. \tag{4.25}$$

and since the magnetic field is symmetric in θ it should not depend on this. We set $\theta = 0$, so computing the field in the x, z-plane with $x > 0$. We will examine each component of the field, starting with the x-component

$$\begin{aligned} B_x(\mathbf{r}) &= I \int_0^{2\pi} \frac{zR\cos\phi}{\left(r^2 + R^2 + z^2 - 2rR\cos\phi\right)^2}\, d\phi \\ &= \frac{IzR}{4r^2R^2} \int_0^{2\pi} \frac{\cos\phi\ d\phi}{\left(\frac{r^2+z^2+R^2}{2rR} - \cos\phi\right)^2} \\ &= \frac{Iz}{4r^2R} \frac{2\pi}{\left(\left(\frac{r^2+z^2+R^2}{2rR}\right)^2 - 1\right)^{\frac{3}{2}}} \\ &= \frac{\pi Iz}{2r^2R} \left(\frac{(r^2+z^2+R^2)^2 - 4r^2R^2}{4r^2R^2}\right)^{-\frac{3}{2}} \\ &= \frac{\pi Iz\ 8r^3R^3}{2r^2R\ \left((r^2+z^2+R^2)^2 - 4r^2R^2\right)^{\frac{3}{2}}} \\ &= \frac{4\pi IzrR^2}{\left((r^2+z^2+R^2)^2 - 4r^2R^2\right)^{\frac{3}{2}}} \end{aligned} \tag{4.26}$$

where in the second line we used an integral identity (B.2) with $c = (r^2 + z^2 + R^2)/2rR$, which is greater than zero everywhere except on the entangling surface. The y-component of the field is zero. This can be seen from the fact that the numerator of the integrand is anti-symmetric from 0 to 2π and the denominator is symmetric on this region. It can also be seen from Figure 9 of the

flow lines. Finally, we compute the z-component of the field

$$\begin{aligned}
B_z(\mathbf{r}) &= I\int_0^{2\pi}\frac{R^2-rR\cos\phi\ d\phi}{\left(r^2+R^2+z^2-2rR\cos\phi\right)^2}\\
&= \frac{I}{4r^2R^2}\left(R^2\int_0^{2\pi}\frac{d\phi}{\left(\frac{r^2+z^2+R^2}{2rR}-\cos\phi\right)^2}-rR\int_0^{2\pi}\frac{\cos\phi\ d\phi}{\left(\frac{r^2+z^2+R^2}{2rR}-\cos\phi\right)^2}\right)\\
&= \frac{I}{4r^2R^2}\left(R^2\frac{2\pi\frac{r^2+z^2+R^2}{2rR}}{\left(\left(\frac{r^2+z^2+R^2}{2rR}\right)^2-1\right)^{\frac{3}{2}}}-rR\frac{2\pi}{\left(\left(\frac{r^2+z^2+R^2}{2rR}\right)^2-1\right)^{\frac{3}{2}}}\right)\\
&= \frac{2\pi I}{4r^2R}\frac{\frac{r^2+z^2+R^2}{2r}-r}{\left(\left(\frac{r^2+z^2+R^2}{2rR}\right)^2-1\right)^{\frac{3}{2}}} = \frac{2\pi I}{4r^2R}\frac{8r^3R^3\frac{r^2+z^2+R^2-2r^2}{2r}}{((r^2+z^2+R^2)^2-4r^2R^2)^{\frac{3}{2}}}\\
&= \frac{2\pi IR^2\ (R^2-r^2+z^2)}{((r^2+z^2+R^2)^2-4r^2R^2)^{\frac{3}{2}}}
\end{aligned}\tag{4.27}$$

where again we used the integral identities (B.2) and (B.3) in the third line with the same value for c. We now need to transform this field to AdS space. We use (4.8) and obtain

$$\begin{aligned}
V_{\mathrm{AdS}} &= \frac{z^3}{4lG_N}V_{\mathrm{Min}} = \frac{z^3}{4lG_N}\frac{2\pi IR^2}{((r^2+z^2+R^2)^2-4r^2R^2)^{\frac{3}{2}}}\begin{pmatrix}2zr\\0\\R^2-r^2+z^2\end{pmatrix}\\
&= \frac{\pi I}{8lG_N}\frac{4z^3R^2}{((r^2+z^2+R^2)^2-4r^2R^2)^{\frac{3}{2}}}\begin{pmatrix}2zr\\0\\R^2-r^2+z^2\end{pmatrix}
\end{aligned}\tag{4.28}$$

where we put the field in cylindrical components.

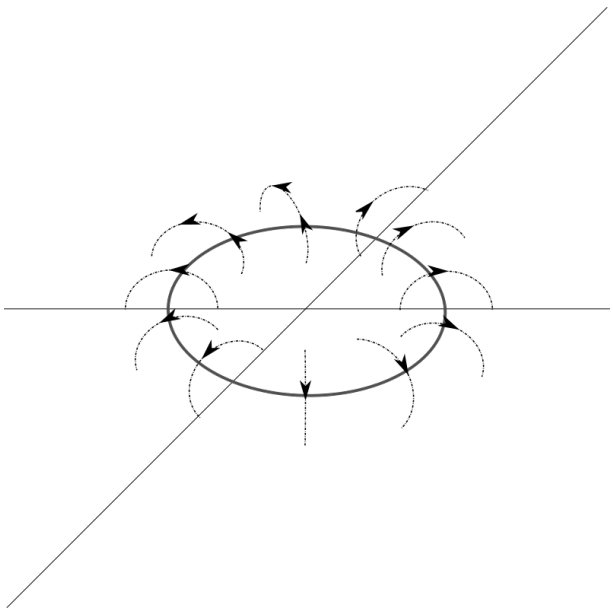

Figure 9: Magnetic field lines of a circular current.

Let us now compare this result with the appendix A or [50]. The vector field in AdS_{d+1} from [50] for boundary region of a $(d-1)$ - dimensional disk is given by

$$V = \left(\frac{2Rz}{\sqrt{\left(R^2+r^2+z^2\right)^2-4R^2r^2}}\right)^d\left(\frac{rz}{R},\frac{R^2-r^2+z^2}{2R}\right)^T\tag{4.29}$$

where the first component is the radial direction of the $(d-1)$-dimensional disk. The angular directions are suppressed. The second component is the z-direction. In our case we take $d = 3$ to get:

$$V = \frac{8R^3z^3}{\left((R^2+r^2+z^2)^2 - 4R^2r^2\right)^{\frac{3}{2}}} \left(\frac{rz}{R}, \frac{R^2-r^2+z^2}{2R}\right)^T. \tag{4.30}$$

We see that our field (4.28) agrees with this if we set $I = 8lG_N/\pi$. But in [50] they set the norm bound to be saturated at l. We set it to be $1/4G_N$ (in AdS) and hence we will need to set $I = 2/\pi$ to obtain the right EE.

4.3.2 The straight current

We continue with the second entangling region. Let now again the entangling region be the upper half-plane and hence the entangling surface the x-axis. We let again a current flow through the entangling surface and calculate the magnetic field, but this time using (4.19). By copying the expression from (4.16) and changing the power in the denominator we obtain

$$\mathbf{B}(\mathbf{r}) = I \int_{-\infty}^{\infty} \frac{dl}{\left(l^2+y^2+z^2\right)^2} \begin{pmatrix} 0 \\ -z \\ y \end{pmatrix}. \tag{4.31}$$

Using again the identity (B.6), but this time for $\alpha = 2$ we get

$$\int_{-\infty}^{\infty} \frac{dx}{(x^2+c^2)^2} = \sqrt{\pi}\frac{\Gamma(\frac{3}{2})}{\Gamma(2)}(c^2)^{-\frac{3}{2}} = \frac{\pi}{2(c^2)^{\frac{3}{2}}} \tag{4.32}$$

and for $c^2 = y^2 + z^2$ again we get

$$\mathbf{B}(\mathbf{r}) = \frac{I\pi}{2(y^2+z^2)^{\frac{3}{2}}} \begin{pmatrix} 0 \\ -z \\ y \end{pmatrix}. \tag{4.33}$$

Now we will make the transformation to AdS space for the second time. Using (4.8) we see that

$$V_{\text{AdS}} = \frac{z^3}{4lG_N} V_{\text{Min}} = \frac{z^3}{4lG_N} \frac{I\pi}{2(y^2+z^2)^{\frac{3}{2}}} \begin{pmatrix} 0 \\ -z \\ y \end{pmatrix} \tag{4.34}$$

$$= \frac{I\pi}{8lG_N} \frac{z^3}{(y^2+z^2)^{\frac{3}{2}}} \begin{pmatrix} 0 \\ -z \\ y \end{pmatrix} \tag{4.35}$$

After comparing this to the Appendix A, (A.18) gives us

$$V_{\text{AdS}} = \left(\frac{z}{\sqrt{y^2+z^2}}\right)^d (z,-y)^T = \frac{z^3}{(y^2+z^2)^{\frac{3}{2}}}(z,-y)^T. \tag{4.36}$$

We see that again if $I = -8lG_N/\pi$ the two fields agree. The extra minus sign comes from the fact that in A the lower half-plane is considered, where we consider the upper half-plane. In our case, we obtain again that $I = 2/\pi$.

4.4 Flux maximization

In the previous section, we have found an interesting result. We modified the law from Biot and Savart for the magnetic field, by changing the power in the denominator. This way we were able to recover the same flow as in [50] for two specific cases of entangling regions. What we would like to do next is justify our seemingly random choice to turn a three into a four in the denominator. To do so we will maximize the flux. As we have seen in (3.40), the flow that will be saturated at the RT surface should be the one that maximizes the flux through the entangling region. What we want to do is write down a functional of the flux. This functional will depend on a function in

the denominator of some generalized Biot-Savart's law. We will then maximize this flux functional with respect to the function in the denominator.[17] Hopefully, we will obtain the function $|\cdot|^4$ as the global maximum of the flux. This will justify our initial right guess. By doing so we need to be careful. We want to maximize over the space of flows. This means that the vector field we will be considering should be divergenceless. To make sure that this is always the case, we will start with a vector potential. In electromagnetism, the magnetic field is obtained by taking the curl of the vector potential. This way one makes sure that the magnetic field is always divergenceless. This is exactly what we will do as well. For a current distribution over a volume V this vector potential is given by

$$A(\mathbf{r}) = \frac{\mu_0}{4\pi} \int_V \frac{J(\mathbf{r}')}{|\mathbf{r} - \mathbf{r}'|} \, d\mathbf{v}'. \tag{4.37}$$

What we will do is replace the denominator with a general function $f(\mathbf{r} - \mathbf{r}')$ and change the factor in front to 1/2. The factor 1/2 is such that if $f(\mathbf{r} - \mathbf{r}') = |\mathbf{r} - \mathbf{r}'|^2$ the curl of the field matches (4.19). We will then calculate the $\mathbf{B}(\mathbf{r})$ field and maximize its flux through a specific surface, with respect to the function f. This way it is guaranteed that the field is still divergenceless.

The magnetic field is given by

$$B(\mathbf{r}) = \nabla \times A(\mathbf{r}) = \nabla \times \frac{1}{2} \int_V \frac{J(\mathbf{r}')}{f(\mathbf{r} - \mathbf{r}')} \, d\mathbf{v}' = \frac{1}{2} \int_V \nabla \times \frac{J(\mathbf{r}')}{f(\mathbf{r} - \mathbf{r}')} \, d\mathbf{v}' \tag{4.38}$$

and hence the flux through a surface S will be given by

$$F[f] = \frac{1}{2} \int_V \int_S \nabla \times \frac{J(\mathbf{r}')}{f(\mathbf{r} - \mathbf{r}')} \cdot d\mathbf{S} \, d\mathbf{v}' \tag{4.39}$$

We vary this functional with respect to $f(\mathbf{r_0} - \mathbf{r_0'})$

$$\frac{\delta F}{\delta f(\mathbf{r_0} - \mathbf{r_0'})} = -\frac{1}{2} \int_V \int_S \nabla \times \frac{J(\mathbf{r}')}{f^2(\mathbf{r} - \mathbf{r}')} \frac{\delta f(\mathbf{r} - \mathbf{r}')}{\delta f(\mathbf{r_0} - \mathbf{r_0'})} \cdot d\mathbf{S} \, d\mathbf{v}'$$

and use Stokes' theorem to get rid of the curl

$$\begin{aligned} \frac{\delta F}{\delta f(\mathbf{r_0} - \mathbf{r_0'})} &= -\frac{1}{2} \int_V \int_{\partial S} \frac{J(\mathbf{r}')}{f^2(\mathbf{r} - \mathbf{r}')} \delta(\mathbf{r} - \mathbf{r}' - \mathbf{r_0} + \mathbf{r_0'}) \cdot d\mathbf{l} \, d\mathbf{v}' \\ &= -\frac{1}{2} \int_{\partial S} \frac{J(\mathbf{r} - \mathbf{r_0} + \mathbf{r_0'})}{f^2(\mathbf{r_0} - \mathbf{r_0'})} \cdot d\mathbf{l}, \end{aligned} \tag{4.40}$$

where we can replaced $\mathbf{r}$ with $\mathbf{l}$ since the integral runs over the variable $\mathbf{r}$. So for the flux to be maximal f should be such that

$$-\frac{1}{2} \int_{\partial S} \frac{J(\mathbf{l} - \mathbf{r_0} + \mathbf{r_0'})}{f^2(\mathbf{r_0} - \mathbf{r_0'})} \cdot d\mathbf{l} = 0. \tag{4.41}$$

4.4.1 The circular current

Now that we have an integral equation for stationary points of the flux, we will try to look at our specific examples. For the disk, we had that

$$J(\mathbf{l}) = I \begin{cases} (-r\sin\theta, r\cos\theta, 0)^T & \text{if } r = R \text{ and } z = 0 \\ \mathbf{0} & \text{otherwise} \end{cases} \tag{4.42}$$

where again we use cylindrical coordinates for $\mathbf{l}$. We now define $\mathbf{r_0} - \mathbf{r_0'} = \boldsymbol{\imath} = (\imath_x, \imath_y, \imath_z)^T$ and we know $d\mathbf{l} = (-R\sin\theta, R\cos\theta, 0)^T d\theta$ since $d\mathbf{l}$ is restricted to run over a circle of radius R. This

[17] Actually, this flux is divergent. However, we can introduce a cut-off δ in the r direction. This way the flux is finite and we can maximize it. This also means that the surface we will consider the flux through is slightly smaller than the entangling region. We will however ignore this subtlety here. For the simple reason that it is quite tedious to keep track of this, and it has no effect on the calculations. But keep in mind that this is actually what we want to maximize.

leads to

$$\begin{aligned} J(\mathbf{l}-\mathbf{r_0}+\mathbf{r'_0})\cdot d\mathbf{l} &= J\begin{pmatrix} r\cos\theta-\boldsymbol{\imath}_x \\ r\sin\theta-\boldsymbol{\imath}_y \\ z-\boldsymbol{\imath}_z\end{pmatrix}\cdot\begin{pmatrix}-R\sin\theta\\ R\cos\theta\\0\end{pmatrix}d\theta \\ &= I\begin{pmatrix}-r\sin\theta+\boldsymbol{\imath}_y\\ r\cos\theta-\boldsymbol{\imath}_x\\0\end{pmatrix}\cdot\begin{pmatrix}-R\sin\theta\\R\cos\theta\\0\end{pmatrix}d\theta \\ &= I(rR\sin^2\theta-\boldsymbol{\imath}_y R\sin\theta+rR\cos^2\theta-\boldsymbol{\imath}_x R\cos\theta)\,d\theta \\ &= IR\big(r-(\boldsymbol{\imath}_y\sin\theta+\boldsymbol{\imath}_x\cos\theta)\big)\,d\theta \end{aligned} \tag{4.43}$$

under the condition that

$$\begin{aligned} R^2 &= (r\cos\theta-\boldsymbol{\imath}_x)^2+(r\sin\theta-\boldsymbol{\imath}_y)^2 \qquad \text{and} \qquad z=\boldsymbol{\imath}_z \\ R^2 &= r^2-r(\boldsymbol{\imath}_y\sin\theta+\boldsymbol{\imath}_x\cos\theta)+\boldsymbol{\imath}_x^2+\boldsymbol{\imath}_y^2 \end{aligned} \tag{4.44}$$

which we assumed in the second equality of (4.43). Since if this is not the case, by (4.42) $J=0$ and this will give us no information about the function f. At the same time, l is restricted to the circle of radius R since this is the domain of integration. This means that $r=R$ and $z=0$ and we get

$$R(\boldsymbol{\imath}_y\sin\theta+\boldsymbol{\imath}_x\cos\theta)=|\boldsymbol{\imath}|^2 \qquad \text{and} \qquad \boldsymbol{\imath}_z=0 \tag{4.45}$$

we now write $\boldsymbol{\imath}=(r_0\cos\theta_0, r_0\sin\theta_0, 0)^T$ in polar coordinates. We get the condition

$$\begin{aligned} R(r_0\sin\theta_0\sin\theta+r_0\cos\theta_0\cos\theta)&=r_0^2 \\ R\cos(\theta-\theta_0)&=r_0 \end{aligned} \tag{4.46}$$

and (4.43) becomes

$$\begin{aligned} J(\mathbf{l}-\boldsymbol{\imath})\cdot d\mathbf{l} &= IR(R-r_0\cos(\theta-\theta_0))d\theta = IR^2(1-\cos^2(\theta-\theta_0)) \\ &= IR^2\sin^2(\theta-\theta_0). \end{aligned} \tag{4.47}$$

The integral equation (4.41) now becomes

$$\frac{\delta F}{\delta f(\boldsymbol{\imath})}=-\frac{IR^2}{2}\int_0^{2\pi}\frac{\sin^2(\theta-\theta_0)d\theta}{f^2(\boldsymbol{\imath})}=0. \tag{4.48}$$

If we now try the function $f(\boldsymbol{\imath})=|\boldsymbol{\imath}|^2=r_0^2=R^2\cos^2(\theta-\theta_0)$ we would get that

$$\frac{\delta F}{\delta f(\boldsymbol{\imath})}=-\frac{I}{2R^2}\int_{-\theta_0}^{2\pi-\theta_0}\frac{\tan^2\theta}{\cos^2\theta}d\theta=-\frac{I}{2R^2}\frac{\tan^3\theta}{3}\Big|_{-\theta_0}^{2\pi-\theta_0}=0 \tag{4.49}$$

where we used the identity (B.4). We see that $f(\mathbf{r}-\mathbf{r}')=|\mathbf{r}-\mathbf{r}'|^2$ would then be valid function f that would maximize the flux. We also notice that this does not indicate that the function is unique. Indeed we see the integral equation is very degenerate, in the sense that there would be a lot of functions f that could give zero. This could be a degeneracy from the fact that the flux maximizing flow is degenerate, as we have stated before. It can however also be a degeneracy from the fact that there might be other (non-global) maxima of the flux.

4.4.2 The straight current

We move on to our second case, the half-plane. In this case, we know that the current will be given by

$$J(\mathbf{l})=I\begin{cases}\hat{\mathbf{e}}_\mathbf{x} & \text{if } y=z=0\\ 0 & \text{otherwise.}\end{cases} \tag{4.50}$$

We return to (4.41) and let $l = (x, 0, 0)^T$ so that $d\mathbf{l} = dx$ and see that it gives

$$\frac{\delta F}{\delta f(\textbf{z})} = -\frac{I}{2}\begin{cases}\int_{-\infty}^{\infty}\frac{dx}{f^2(\textbf{z})} & \text{if } \textbf{z}_y = \textbf{z}_z = 0\\ 0 & \text{otherwise.}\end{cases} \tag{4.51}$$

We see that for this functional to be stationary we need to require that $f(\textbf{z}) \sim (\textbf{z}_y^2 + \textbf{z}_z^2)^{\frac{n}{2}}$ for $n \in \mathbb{N}$. This is because in that case, $\textbf{z}_y = \textbf{z}_z = 0$ is not in the domain of the integrand and the variation of the functional will be identically zero. Due to the fact that the problem is symmetric in the x-axis, we can set $x = 0$ and focus on the yz-plane. Using this we see that

$$f(\textbf{z}) \propto |\textbf{z}|^n. \tag{4.52}$$

This is even more degenerate than before, although our function $n = 2$ is still valid. We will however use this statement to kill the degeneracies later on.

4.5 Two-dimensional CFT

In this section, we want to see if we can formulate a similar law in one dimension lower. So this time we will be focusing on our familiar case of a two-dimensional CFT. We know that if we take a time slice, we are left with just one dimension. We will again look at the case where $A = [-\ell/2, \ell/2]$ an interval of length ℓ. We can see this as the disk but in a lower dimension. After all $D^1(\ell/2)$ the one-dimensional disk of radius $\ell/2$ is just the interval. We will suppress the y coordinate such that the remaining coordinates will be denoted x and z. The current running through the circle is now reduced to two-point charges that carry opposite but equal charges. These two points will now be the entangling surface. What does the field look like in two spatial dimensions with a point-like charge source? We propose the following law

$$B(\mathbf{r}) = Q\left(\frac{\epsilon_{ij}\mathbf{r_1}^j}{|\mathbf{r_1}|^2} - \frac{\epsilon_{ij}\mathbf{r_2}^j}{|\mathbf{r_2}|^2}\right) \tag{4.53}$$

where Q (the charge) is a constant, ϵ_{ij} is the two dimensional Levi-civita-symbol[18] and $\mathbf{r_k} = \mathbf{r} - \mathbf{l_k}$ with $\mathbf{l_k}$ the location of the k-th point-like charge. Note that this expression is actually similar to the higher dimensional expression (4.19). The only differences are the fact that the integral is replaced by a sum over the charges, the cross product is now a contraction with the epsilon tensor and the power in the denominator is two. Let us check if it is indeed divergenceless. First we note that $\partial_i \mathbf{r_k} = \partial_i \mathbf{r}$ and that $\partial_i \epsilon^i_j \mathbf{r}^j = 0$ since we take the derivative of the opposite coordinate. This gives us

$$\partial_i B^i(\mathbf{r}) = \sum_k \partial_i\left(\frac{\epsilon^i_j \mathbf{r_k}^j}{|\mathbf{r_k}|^2}\right) = \sum_k \partial_i\left(\frac{1}{|\mathbf{r_k}|^2}\right)\epsilon^i_j \mathbf{r_k}^j = \sum_k \frac{-2}{|\mathbf{r_k}|^4}\mathbf{r_k}_i \epsilon^i_j \mathbf{r_k}^j = 0 \tag{4.54}$$

since $\epsilon_{ij}\mathbf{r_k}^i\mathbf{r_k}^j = 0$.

Now the charges are located at $\mathbf{l_1} = (\ell/2, 0)^T$ and $\mathbf{l_2} = (-\ell/2, 0)^T$. This gives us $\mathbf{r}_i = \mathbf{r} + (-1)^i\ \ell/2\ \hat{\mathbf{e}}_\mathbf{x} = (x + (-1)^i\ \ell/2, z)^T$. The magnetic field thus becomes

$$B(\mathbf{r}) = Q\left(\frac{1}{(x-\frac{\ell}{2})^2 + z^2}\begin{pmatrix} z \\ \frac{\ell}{2} - x\end{pmatrix} - \frac{1}{(x+\frac{\ell}{2})^2 + z^2}\begin{pmatrix} z \\ -(x+\frac{\ell}{2})\end{pmatrix}\right). \tag{4.55}$$

Making again the transformation to AdS space we see

$$V_{\text{AdS}} = \frac{z^2}{4lG_N}V_{\text{Min}} = \frac{z^2 Q}{4lG_N}\left(\frac{1}{(x-\frac{\ell}{2})^2 + z^2}\begin{pmatrix} z \\ \frac{\ell}{2} - x\end{pmatrix} - \frac{1}{(x+\frac{\ell}{2})^2 + z^2}\begin{pmatrix} z \\ -(x+\frac{\ell}{2})\end{pmatrix}\right). \tag{4.56}$$

Looking back at (4.29) we see that for $d = 2$ we get

$$V_{\text{AdS}} = \frac{4R^2 z^2}{\left(R^2 + r^2 + z^2\right)^2 - 4R^2 r^2}\left(\frac{rz}{R}, \frac{R^2 - r^2 + z^2}{2R}\right)^T \tag{4.57}$$

[18] where $\epsilon_{ii} = 0$ and $\epsilon_{12} = -\epsilon_{21} = 1$

and in our case, we have $R = \ell/2$ and $x = r$. Renaming these and multiplying the two denominators in (4.55) with each other we get that the common denominator becomes

$$\begin{aligned}((r-R)^2+z^2)((r+R)^2+z^2) &= ((r-R)(r+R))^2 + z^2(r-R)^2 + z^2(r+R)^2 + z^4 \\ &= (r^2-R^2)^2 + z^2((r-R)^2+(r+R)^2) + z^4 \\ &= (r^2-R^2)^2 + 2z^2(r^2+R^2) + z^4 \\ &= (r^2+R^2)^2 - 4r^2R^2 + 2z^2(r^2+R^2) + z^4 \\ &= (R^2+r^2+z^2)^2 - 4R^2r^2 \end{aligned} \tag{4.58}$$

which agrees with the denominator of (4.57). The numerator of the z-component of (4.55) (or the part within the brackets of (4.56)) becomes

$$\begin{aligned}&(R-r)((r+R)^2+z^2) + (r+R)((r-R)^2+z^2) \\ &\quad = (R^2-r^2)(r+R) + z^2(R-r) + (r^2-R^2)(r-R) + z^2(r+R) \\ &\quad = 2R(R^2-r^2) + 2Rz^2 = 2R(R^2-r^2+z^2)\end{aligned} \tag{4.59}$$

and the x-component yields

$$z((r+R)^2+z^2) - z((r-R)^2+z^2) = z((r+R)^2-(r-R)^2) = 4zrR \tag{4.60}$$

hence we see they agree with (4.57) up to the factor of z^2. Thus if we pick $Q = 4lG_N$ the two fields exactly agree. We however set the norm bound to $1/4G_N$ so we set $Q = 1$.

We will now try to use the field just obtained, to get the right EE for the interval. We have already calculated this using two different methods so we hope that the flux of this field through the entangling regions matches this. We will perform the calculation in AdS space. The induced metric on a constant z surface is $h = l^2/z^2$ and the unit vector normal to such is surface is $n_\mu = (0, l/z)^T$. To compute the flux we need to compute

$$\int_A \sqrt{h}\; n_\mu V^\mu_{\text{AdS}} \tag{4.61}$$

where we set $z = 0$ and the integrand simplifies to

$$\frac{l}{4G_N}\left(\frac{\frac{\ell}{2}-x}{(\frac{\ell}{2}-x)^2} + \frac{\frac{\ell}{2}+x}{(\frac{\ell}{2}+x)^2}\right) = \frac{l}{4G_N}\left(\frac{1}{\frac{\ell}{2}-x} + \frac{1}{\frac{\ell}{2}+x}\right). \tag{4.62}$$

Let us now compute the flux through the line $z = 0$ for $-\frac{\ell}{2} < x < \frac{\ell}{2}$. We again introduce a UV cut-off parameter a as before in section 3.2.1[19] and the integral becomes

$$\begin{aligned}\int_{a-\ell/2}^{\ell/2-a} \sqrt{h}\; n_\mu V^\mu_{\text{AdS}}\, dx &= \int_{a-\ell/2}^{\ell/2-a} \frac{l}{4G_N}\left(\frac{1}{\frac{\ell}{2}-x} + \frac{1}{\frac{\ell}{2}+x}\right) dx \\ &= \frac{l}{4G_N}\left[-\log(\frac{\ell}{2}-x) + \log(\frac{\ell}{2}+x)\right]_{a-\frac{\ell}{2}}^{\frac{\ell}{2}-a} \\ &= \frac{l}{4G_N}\left[-\log a + \log(\ell-a) + \log(\ell-a) - \log a\right] \\ &= 2\frac{l}{4G_N}\log\left(\frac{\ell-a}{a}\right) \approx \frac{l}{2G_N}\log\left(\frac{\ell}{a}\right).\end{aligned} \tag{4.63}$$

We see that we get the same value as in (3.33) and as we have seen before we can use that $c = 3l/2G_N$ to obtain

$$S_A = \int_A \sqrt{h}\; n_\mu V^\mu_{\text{AdS}} = \frac{c}{3}\log\frac{\ell}{a}. \tag{4.64}$$

This agrees with (3.34), (3.17) and we see we get a similar result as in [51].

[19] Before we introduced a as the cut-off in the z direction. We then imposed ϵ as the cut-off in the r direction. In this case it exactly turns out that the two cut-offs agree. So we can use a as a cut-off in the r direction as well.

4.5.1 Flux maximization in lower dimensions

We have again obtained a nice result. Still, there is an obvious question. Where did the law for the vector field (yielding the right maximum for the flux and hence EE) come from? It was again just proposed in (4.53) without any justification. We would like to set it on a more solid ground, attempting the same approach as before in the higher dimensional case, by maximizing the flux functional with respect to some potential. This time we start with a general scalar potential $\phi(\mathbf{r})$. This is because, in two dimensions, the curl will be equivalent to a contraction of a partial with an epsilon tensor. So if we would consider a vector potential again, we would be left with one too many indices. Hence we start with

$$B^j(\mathbf{r}) = \sum_k \epsilon^{ij}\partial_i\phi(\mathbf{r_k}). \tag{4.65}$$

where $\mathbf{r_k} = \mathbf{r} - \mathbf{l_k}$ again with $\mathbf{l_k}$ the location of the charge. This ensures the divergenceless property of the B-field since

$$\partial_j B^j(\mathbf{r}) = \sum_k \partial_j\epsilon^{ij}\partial_i\phi(\mathbf{r_k}) = 0 \tag{4.66}$$

for any continuous function $\phi(\mathbf{r})$. The flux of this field through some interval I will now be

$$F[\phi] = \int_I B^j(\mathbf{r})d\mathbf{S}_j = \sum_k \int_I \epsilon^{ij}\partial_i\phi(\mathbf{r_k})d\mathbf{S}_j. \tag{4.67}$$

In our case we will always have $d\mathbf{S}_j = dx(\hat{\mathbf{e}}_\mathbf{z})_j$. Yielding

$$F[\phi] = \sum_k \int_I \partial_x\phi(\mathbf{r_k})dx = \sum_k \phi(\mathbf{r_k})\Big|_{\partial I} \tag{4.68}$$

$\phi(\mathbf{r})$ evaluated at the boundary of the interval. Taking the functional derivative with respect to the function ϕ we see

$$\frac{\delta F}{\delta\phi(\mathbf{r}')} = \sum_k \frac{\delta\phi(\mathbf{r_k})}{\delta\phi(\mathbf{r}')}\Big|_{\partial I} = \sum_k \delta(\mathbf{r_k} - \mathbf{r}')\Big|_{\partial I}. \tag{4.69}$$

Hence any function that is not defined on the boundary points of I will maximize the flux. This is again a very degenerate result, as we have seen before. We can not extract any information from this, but there is hope. Note that through all calculations we did so far the bounded condition was not imposed anywhere. Maybe this additional piece of information will kill some of the degeneracy that we have seen.

4.6 Boundedness

Until now we have neglected one property of the vector field we seek. Aside from the divergenceless property, the vector field also has to be bounded in AdS-space. What happens to the degeneracy if we impose this condition. This section will investigate one specific case from the two and three-dimensional CFT. Imposing that the vector field (generated by a general potential) should be bounded. We will see how this condition restricts the potential and hence the degeneracies that we have encountered previously.

4.6.1 The half-line

We stated already before that in AdS_3 the field should have the form of (4.65) to be divergenceless. We will compute the norm of this field for a specific case. This case is when there is one charge at the origin and the entangling region $A = [0, \infty)$ is half of the x-axis. This can be seen as the lower-dimensional case of the half-plane. The field will be given by

$$B^j(\mathbf{r}) = \epsilon^{ij}\partial_i\phi(\mathbf{r}). \tag{4.70}$$

We know that the norm bound in AdS is equivalent to the third equation in (4.8). So this is what we will compute

$$4G_N|V_{\text{AdS}}| = z|V_{\text{Min}}| \leq 1. \tag{4.71}$$

In this case

$$z|V_{\text{Min}}| = z\sqrt{B^j(\mathbf{r})B_j(\mathbf{r})} = z\sqrt{\epsilon^{ij}\partial_i\phi(\mathbf{r})\epsilon^k_j\partial_k\phi(\mathbf{r})}$$
$$= z\sqrt{(\partial_x\phi(\mathbf{r}))^2 + (\partial_z\phi(\mathbf{r}))^2}. \tag{4.72}$$

Assuming now that $\phi(\mathbf{r}) = \phi(|\mathbf{r}|)$, we get that

$$\partial_i\phi(|\mathbf{r}|) = \phi'(|\mathbf{r}|)\frac{\mathbf{r}_i}{|\mathbf{r}|}. \tag{4.73}$$

Inserting this in (4.72) we end up with

$$z|V_{\text{Min}}| = z\sqrt{\left(\phi'(|\mathbf{r}|)\frac{x}{|\mathbf{r}|}\right)^2 + \left(\phi'(|\mathbf{r}|)\frac{z}{|\mathbf{r}|}\right)^2} = z\frac{\phi'(|\mathbf{r}|)}{|\mathbf{r}|}\sqrt{x^2+z^2} = z\phi'(|\mathbf{r}|). \tag{4.74}$$

We see right away that $\phi'(|\mathbf{r}|) \sim 1/z$ for the norm to be bounded. Indeed if we pick $\phi(|\mathbf{r}|) = Q\log(|\mathbf{r}|)$ we get that

$$z|V_{\text{Min}}| = \frac{zQ}{|\mathbf{r}|} \leq Q = 1 \tag{4.75}$$

if again $Q = 1$.

What does this imply for the field? Let us plug $\phi(|\mathbf{r}|) = Q\log(|\mathbf{r}|)$ into (4.65) to get

$$B^j(\mathbf{r}) = \epsilon^{ij}\partial_i Q\log(|\mathbf{r}|) = Q\frac{\epsilon^{ij}\mathbf{r}_i}{|\mathbf{r}|^2} \tag{4.76}$$

and we see that this matches the proposed law for this specific example. This is a good result. We did make an assumption about the scalar potential. Namely, it should be a function of the norm only. But under this assumption, we were able to kill a lot of degeneracy and found out what the potential should be in this specific case. Let us see if this also works in the higher dimensional case.

4.6.2 The half-plane

We would like to return to the higher dimensional cases now. Let us focus on the half-plane for the moment. We want to impose the norm bound again according to (4.8). Could we also limit the possibilities of the function $f(r-r')$ from (4.38) by imposing the bounded condition? We start again with (4.71), but this time with a factor of z^2. We get that

$$z^2|V_{\text{Min}}| = z^2\sqrt{B(r)\cdot B(r)}$$
$$= \frac{z^2}{2}\sqrt{\int_{V_1}\int_{V_2}\left(\nabla\times\frac{J(\mathbf{r_1})}{f(\mathbf{r}-\mathbf{r_1})}\right)\cdot\left(\nabla\times\frac{J(\mathbf{r_2})}{f(\mathbf{r}-\mathbf{r_2})}\right)d\mathbf{v_1}\,d\mathbf{v_2}} \tag{4.77}$$

using (4.38) for the field. First let us work out the integrand underneath the square root. Since

$$\nabla\times\frac{J(\mathbf{r_i})}{f(\mathbf{r}-\mathbf{r_i})} = \frac{-1}{f^2(\mathbf{r}-\mathbf{r_i})}\nabla f(\mathbf{r}-\mathbf{r_i})\times J(\mathbf{r_i})$$
$$= \frac{-1}{f^2(\mathbf{r}-\mathbf{r_i})}\begin{pmatrix}\partial_y f(\mathbf{r}-\mathbf{r_i})J_z(\mathbf{r_i}) - \partial_z f(\mathbf{r}-\mathbf{r_i})J_y(\mathbf{r_i})\\ \partial_z f(\mathbf{r}-\mathbf{r_i})J_x(\mathbf{r_i}) - \partial_x f(\mathbf{r}-\mathbf{r_i})J_z(\mathbf{r_i})\\ \partial_x f(\mathbf{r}-\mathbf{r_i})J_y(\mathbf{r_i}) - \partial_y f(\mathbf{r}-\mathbf{r_i})J_x(\mathbf{r_i})\end{pmatrix} \tag{4.78}$$

we get that the integrand should be

$$\frac{\begin{pmatrix}\partial_y f(\mathbf{r}-\mathbf{r_1})J_z(\mathbf{r_1}) - \partial_z f(\mathbf{r}-\mathbf{r_1})J_y(\mathbf{r_1})\\ \partial_z f(\mathbf{r}-\mathbf{r_1})J_x(\mathbf{r_1}) - \partial_x f(\mathbf{r}-\mathbf{r_1})J_z(\mathbf{r_1})\\ \partial_x f(\mathbf{r}-\mathbf{r_1})J_y(\mathbf{r_1}) - \partial_y f(\mathbf{r}-\mathbf{r_1})J_x(\mathbf{r_1})\end{pmatrix}\cdot\begin{pmatrix}\partial_y f(\mathbf{r}-\mathbf{r_2})J_z(\mathbf{r_2}) - \partial_z f(\mathbf{r}-\mathbf{r_2})J_y(\mathbf{r_2})\\ \partial_z f(\mathbf{r}-\mathbf{r_2})J_x(\mathbf{r_2}) - \partial_x f(\mathbf{r}-\mathbf{r_2})J_z(\mathbf{r_2})\\ \partial_x f(\mathbf{r}-\mathbf{r_2})J_y(\mathbf{r_2}) - \partial_y f(\mathbf{r}-\mathbf{r_2})J_x(\mathbf{r_2})\end{pmatrix}}{f^2(\mathbf{r}-\mathbf{r_1})f^2(\mathbf{r}-\mathbf{r_2})}. \tag{4.79}$$

Since the entangling surface of the half-plane is just the x-axis. We get that for this example we can take $\mathbf{r_i} = (x_i, 0, 0)^T$, $J_x(\mathbf{r_i}) = I$ and $J_y(\mathbf{r_i}) = J_z(\mathbf{r_i}) = 0$. The integrand will then be

$$\begin{aligned}
&\frac{I^2}{f^2(\mathbf{r}-\mathbf{r_1})f^2(\mathbf{r}-\mathbf{r_2})}\begin{pmatrix}0\\ \partial_z f(\mathbf{r}-\mathbf{r_1})\\ -\partial_y f(\mathbf{r}-\mathbf{r_1})\end{pmatrix}\cdot\begin{pmatrix}0\\ \partial_z f(\mathbf{r}-\mathbf{r_2})\\ -\partial_y f(\mathbf{r}-\mathbf{r_2})\end{pmatrix}\\
&= \frac{I^2}{f^2(\mathbf{r}-\mathbf{r_1})f^2(\mathbf{r}-\mathbf{r_2})}\big(\partial_z f(\mathbf{r}-\mathbf{r_1})\partial_z f(\mathbf{r}-\mathbf{r_2}) + \partial_y f(\mathbf{r}-\mathbf{r_1})\partial_y f(\mathbf{r}-\mathbf{r_2})\big). \qquad (4.80)
\end{aligned}$$

We now look back at (4.52) from which we knew that in this particular case we need that $f(\mathbf{r}-\mathbf{r_i}) = |\mathbf{r}-\mathbf{r_i}|^n$. This made sure that the flux was maximized. We can simplify this further now using that

$$\partial_j f(|\mathbf{r}-\mathbf{r_i}|) = f'(|\mathbf{r}-\mathbf{r_i}|)\frac{(\mathbf{r}-\mathbf{r_i})_j}{|\mathbf{r}-\mathbf{r_i}|}$$

we find that the integrand is equal to

$$\begin{aligned}
&\frac{I^2 f'(\mathbf{r}-\mathbf{r_1})f'(\mathbf{r}-\mathbf{r_2})}{f^2(\mathbf{r}-\mathbf{r_1})f^2(\mathbf{r}-\mathbf{r_2})|\mathbf{r}-\mathbf{r_1}||\mathbf{r}-\mathbf{r_2}|}(y^2+z^2) = \frac{I^2n^2|\mathbf{r}-\mathbf{r_1}|^{n-1}|\mathbf{r}-\mathbf{r_2}|^{n-1}}{|\mathbf{r}-\mathbf{r_1}|^{2n+1}|\mathbf{r}-\mathbf{r_2}|^{2n+1}}(y^2+z^2)\\
&= I^2n^2(y^2+z^2)(|\mathbf{r}-\mathbf{r_1}||\mathbf{r}-\mathbf{r_2}|)^{-n-2}\\
&= \frac{I^2n^2(y^2+z^2)}{((x-x_1)^2+y^2+z^2)^{\frac{n}{2}+1}((x-x_2)^2+y^2+z^2)^{\frac{n}{2}+1}}. \qquad (4.81)
\end{aligned}$$

For reasons that will become clear later, we redefine $r^2 = y^2+z^2$. Putting the integrand back into (4.77) we get

$$z^2|V_{\text{Min}}| = \frac{z^2In}{2}\sqrt{\int_{-\infty}^{\infty}\int_{-\infty}^{\infty}\frac{r^2}{((x-x_1)^2+r^2)^{\frac{n}{2}+1}((x-x_2)^2+r^2)^{\frac{n}{2}+1}}dx_1\,dx_2}. \qquad (4.82)$$

We will solve these integrals using an identity from appendix B. In (B.6) we find

$$I_\alpha = \sqrt{\pi}\frac{\Gamma\left(\alpha-\frac{1}{2}\right)}{\Gamma(\alpha)}\left(r^2\right)^{\frac{1}{2}-\alpha} \qquad (4.83)$$

where

$$I_\alpha \equiv \int_{-\infty}^{\infty}\frac{dx}{(x^2+r^2)^\alpha}. \qquad (4.84)$$

From this we see that if we pick $\alpha = n/2+1$ we get

$$\int_{-\infty}^{\infty}\frac{dx}{(x^2+r^2)^{\frac{n}{2}+1}} = \sqrt{\pi}\,\frac{\Gamma(\frac{n}{2}+\frac{1}{2})}{\Gamma(\frac{n}{2}+1)}(r^2)^{-\frac{n}{2}-\frac{1}{2}} \qquad (4.85)$$

We realize that in this specific example, the magnetic field should not depend on x. So we can set $x = 0$ from now on. The two integrals in (4.82) both become equal to (4.85) and for the norm of the vector field we now get

$$z^2|V_{\text{Min}}| = \frac{z^2In}{2}\sqrt{\pi}\frac{\Gamma(\frac{n}{2}+\frac{1}{2})}{\Gamma(\frac{n}{2}+1)}\frac{1}{(r^2)^{\frac{n}{2}}} = \frac{\sqrt{\pi}In}{2}\frac{\Gamma(\frac{n}{2}+\frac{1}{2})}{\Gamma(\frac{n}{2}+1)}\frac{z^2}{|\mathbf{r}|^n}. \qquad (4.86)$$

This is a great result. For this expression to be bounded, the integer n is limited. The first two factors in the expression are just constants. In the third factor we see that of $n > 2$, we obtain divergencies at small $\mathbf{r}$. If $n < 2$ we see the field blows up when $z \to \infty$. Only if $n = 2$ the vector field is bounded, since then $z^2/|\mathbf{r}|^2 \leq 1$. Using the fact that $\Gamma(\frac{3}{2}) = 1/2\sqrt{\pi}$ and $\Gamma(2) = 1$ indeed for this value we get

$$z^2|V_{\text{Min}}| = \sqrt{\pi}I\frac{\frac{1}{2}\sqrt{\pi}}{1}\frac{z^2}{|\mathbf{r}|^2} = \frac{\pi Iz^2}{2|\mathbf{r}|^2} \leq \frac{\pi I}{2} = 1 \qquad (4.87)$$

again if $I = 2/\pi$.

What does this mean for the magnetic field? Using again (4.38) and taking the curl we see that

$$B(\mathbf{r}) = \frac{I}{2}\int_V \frac{1}{f^2(\mathbf{r}-\mathbf{r}')}\nabla f(\mathbf{r}-\mathbf{r}')\times J(\mathbf{r}')\ d\mathbf{v}' \tag{4.88}$$

Now plugging in $f(\mathbf{r}-\mathbf{r}') = |\mathbf{r}-\mathbf{r}'|^2$ we see that we get

$$B(\mathbf{r}) = I\int_V \frac{(\mathbf{r}-\mathbf{r}')\times J(\mathbf{r}')}{|\mathbf{r}-\mathbf{r}'|^4}d\mathbf{v}'. \tag{4.89}$$

This is indeed the 4^{th} power law we guessed correctly in (4.19). Starting with a general vector potential generated by a current running through the entangling surface. We have shown that, for this specific case, the half-plane, the denominator in the law is fixed by a combination of the divergenceless, bounded and flux maximizing conditions. What can we say about the other case, the disk? The circle can conformally be mapped to the x-axis by the stereographic projection. This means that we can conformally map one of our examples to the other one. This implies that the law (4.19) for the flow should also be valid for the disk. But what can we say about shapes that can not be related to the half-plane by conformal mapping, like an ellipse, for instance? Can the same law be applied in more general cases? This is what we will be investigating next.

4.7 The ellipse

We want to use the presumed description to find a max flow (4.19), to see if we can find the EE of an ellipse. To do so we will again create a magnetic field using a current in the shape of the ellipse. This field is calculated using the law (4.19) instead of the regular law. But before we find the closed-form of this field we encounter a problem.

Recall that an ellipse is described by the points in the x, y-plane satisfying the following equation

$$\frac{x^2}{a^2}+\frac{y^2}{b^2} = 1 \tag{4.90}$$

where a and b are the semi-major and semi-minor axes respectively. A parameterization of the ellipse is then

$$\mathbf{l} = (a\cos\phi, b\sin\phi, 0), \quad 0 \le \phi < 2\pi$$

this makes

$$d\mathbf{l} = (-a\sin\phi, b\cos\phi, 0)d\phi.$$

With $\mathbf{r} = (x, y, z)$ we get that

$$\mathbf{r}' = \mathbf{r}-\mathbf{l} = (x - a\cos\phi, y - b\sin\phi, z)$$

and hence

$$\begin{aligned} d\mathbf{l}\times\mathbf{r}' &= \begin{pmatrix} -a\sin\phi \\ b\cos\phi \\ 0 \end{pmatrix} \times \begin{pmatrix} x - a\cos\phi \\ y - b\sin\phi \\ z \end{pmatrix} d\phi \\ &= \begin{pmatrix} zb\cos\phi \\ za\sin\phi \\ -ay\sin\phi + ab\sin^2\phi - bx\cos\phi + ab\cos^2\phi \end{pmatrix} d\phi \\ &= \begin{pmatrix} zb\cos\phi \\ za\sin\phi \\ ab - ay\sin\phi - bx\cos\phi \end{pmatrix} d\phi. \end{aligned} \tag{4.91}$$

We see that the field becomes

$$\mathbf{B}(\mathbf{r}) = \int \frac{d\mathbf{l}\times\mathbf{r}'}{|\mathbf{r}'|^4} = \int_0^{2\pi} \begin{pmatrix} zb\cos\phi \\ za\sin\phi \\ ab - ay\sin\phi - bx\cos\phi \end{pmatrix} \frac{d\phi}{((x - a\cos\phi)^2 + (y - b\sin\phi)^2)^2}. \tag{4.92}$$

In appendix C we find the closed-form of the vector potential of this field. This calculation was already done before we encountered a problem described by the following sanity check.

The sanity check is to see if the surface that maximizes the norm of the field is exactly homologous to the entangling region. We will calculate the integral numerically in Mathematica. We do this to see where the field saturates. If it is a max-flow, the field should saturate at the RT surface which is homologous to the entangling region. We will compute the norm of the field (multiplied by z^2 as we know from (4.8)) and try to find its maximum. We do this by discretizing the x, y and z coordinates from $-a$ to a, $-b$ to b and 0 to a respectively. The steps δ in between each new value of the coordinates will be around $1/20$ in each direction. This way we create a three-dimensional grid. In each grid point, we calculate the value of the integral (4.92) numerically. We then calculate the norm (times z^2) and look for the maximum over all points on the grid. We collected all grid points for which this norm is ϵ close to the maximum. Where ϵ is some small parameter. The resulting grid points were plotted and are shown in figure 6 below.

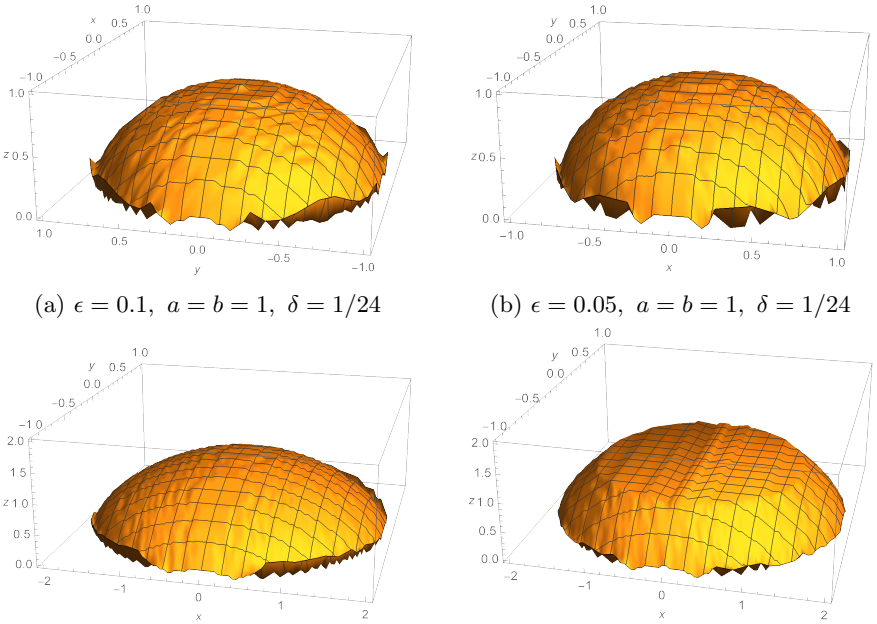

(a) $\epsilon = 0.1,\ a = b = 1,\ \delta = 1/24$ (b) $\epsilon = 0.05,\ a = b = 1,\ \delta = 1/24$

(c) $\epsilon = 0.1,\ a = 2,\ b = 1,\ \delta = 1/22$ (d) $\epsilon = 0.05,\ a = 2,\ b = 1,\ \delta = 1/22$

Figure 10: The surface of maximal field norm for different values of the parameters.

What we see is the following. The top two Figures 10a and 10b are simulations of the circle. We set $a = b = 1$ and the steps $\delta = 1/24$. We do not see a lot of difference between the two figures. The left one corresponds to $\epsilon = 0.1$ and the right one to $\epsilon = 0.05$. Both surfaces look a lot like the RT surface of the disk and are homologous to this entangling region. Now have a look at the bottom two images, Figures 10c and 10d. These are simulations of the ellipse. We choose $a = 2$, $b = 1$ and the steps $\delta = 1/22$ in both cases. There is a clear difference between these two figures. The left surface looks good, but there is a problem with the right one. This is the case where we set $\epsilon = 0.05$, we see that it is completely flat at the top. This actually means that these points are missing from the grid. This is how ListPlot3D works in Mathematica. We give it a list of points in 3D space and it connects all the points, making a surface. If there is a gap in the surface (no points of small x and y values in this case) Mathematica will just connect the remaining points with straight lines. The points that are missing have been taken out when we set $\epsilon = 0.05$ instead of 0.1. This means that the values of the norm for these points are somewhere between 0.05 and 0.1 away from the maximum. This means that the norm of the field is smaller in the middle as opposed to close to the boundary. The surface of maximizing norm is not homologous to an ellipse! There is a big hole in this surface. This is a very big problem. If the surface of maximizing norm of a flow is not homologous to the entangling region, then the flow can not be a max-flow. This means that the algorithm we proposed on finding a max-flow for a given entangling region, might not be correct for general cases.

4.8 Calculating entanglement entropy

We wanted to use our description to work out the field for an ellipse and calculate the EE by integrating the flux over the surface inside the ellipse. This would have been the final goal of the thesis, to give an analytic expression of the EE of an ellipse. Unfortunately, as described above, the field is not a max-flow in the case of an ellipse. We did however find the right field in the case where $a = b = R$, the circle. So instead of finding a new result to conclude this project, we will use our new approach to recover a known result, the EE of the disk in a time-slice of a three-dimensional CFT. Recall from (4.28) the flow we found for the disk. We will compute its flux through the disk at $z = 0$. In order to make this finite, we need to introduce a cut-off. In the literature this cut-off ϵ is used in the z direction to make the RT surface finite. One calculates the area of the RT surface for $z > \epsilon$. We will introduce a cut-off δ in the r direction. So calculating the flux of the field through a disk of radius $R - \delta$ in the $z = 0$ plane. Both choices should be equivalent as long as $\delta = \epsilon - \epsilon^2/2R$.[20]

We will perform the calculation in AdS space. The determinant of the induced metric on a surface of constant z and the unit normal vector are

$$h = \frac{l^4 r^2}{z^4} \qquad\qquad n_\mu = \frac{l}{z}\delta^z_\mu. \tag{4.93}$$

The flux of the field through this surface is

$$\begin{aligned} S_{D^2} &= \int_{D^2} \sqrt{h}\; n_\mu V^\mu_{\text{AdS}} = \int_{D^2} \frac{l^2 r}{z^2}\frac{l}{z} V^z_{\text{AdS}} \\ &= \int_{D^2} \frac{l^3 r}{z^3}\frac{\pi I}{8 l G_N}\frac{4z^3R^2(R^2 - r^2 + z^2)}{((r^2 + z^2 + R^2)^2 - 4r^2R^2)^{\frac{3}{2}}} \end{aligned} \tag{4.94}$$

and after we set $I = 2/\pi$ and take the limit $z \to 0$ to obtain

$$\begin{aligned} S_{D^2} &= \frac{l^2}{4G_N}\int_{D^2} \frac{r4R^2(R^2 - r^2)}{((r^2 + R^2)^2 - 4r^2R^2)^{\frac{3}{2}}} = \frac{2\pi l^2 R^2}{G_N}\int_0^{R-\delta} \frac{r(R^2 - r^2)dr}{((R^2 - r^2)^2)^{\frac{3}{2}}} \\ &= \frac{2\pi l^2 R^2}{G_N}\int_0^{R-\delta} \frac{rdr}{(R^2 - r^2)^2}. \end{aligned} \tag{4.95}$$

Now let $u = R^2 - r^2$ so that $du = -2rdr$ and the upper bound of the integral becomes $R^2 - (R-\delta)^2 = 2R\delta - \delta^2$. We get that the flux is

$$\begin{aligned} S_{D^2} &= -\frac{\pi l^2 R^2}{G_N}\int_{R^2}^{2R\delta - \delta^2} \frac{du}{u^2} = \frac{\pi l^2 R^2}{G_N}\left[\frac{1}{u}\right]_{R^2}^{2R\delta - \delta^2} = \frac{\pi l^2 R^2}{G_N}\left[\frac{1}{2R\delta - \delta^2} - \frac{1}{R^2}\right] \\ &= \frac{\pi l^2}{G_N}\frac{R^2 - 2R\delta + \delta^2}{\delta(2R - \delta)} = \frac{\pi l^2}{G_N}\frac{(R - \delta)^2}{\delta(2R - \delta)} \end{aligned} \tag{4.96}$$

and if we now convert the cut-off to ϵ using $\delta = \epsilon - \epsilon^2/2R$ we get that the flux becomes

$$\begin{aligned} S_{D^2} &= \frac{\pi l^2}{G_N}\frac{(R - \epsilon + \epsilon^2/2R)^2}{(\epsilon - \epsilon^2/2R)(2R - \epsilon + \epsilon^2/2R)} \\ &= \frac{\pi l^2}{\epsilon G_N}\frac{(R - \epsilon + \epsilon^2/2R)^2}{(1 - \epsilon/2R)(2R - \epsilon + \epsilon^2/2R)} \simeq \frac{\pi l^2}{\epsilon G_N}\left[\frac{R^2}{2R} + \frac{2R2R(-1) - R^2(-\frac{1}{2R}2R - 1)}{4R^2}\epsilon\right] \\ &= \frac{l^2}{4G_N}\left[\frac{2\pi R}{\epsilon} + \frac{4\pi}{\epsilon}\frac{2R^2 - 4R^2}{4R^2}\epsilon\right] = \frac{l^2}{4G_N}\left[\frac{2\pi R}{\epsilon} - 2\pi\right]. \end{aligned} \tag{4.97}$$

If we now take a look at [52], we see that there the area of the RT surface is calculated. Using this ϵ cut-off in the z-direction they calculated that

$$\mathcal{A}_A = \frac{2\pi R}{\epsilon} - 2\pi \tag{4.98}$$

[20] This result comes from calculations done by Juan. He related the different cut-offs in several dimensions. This was done using the expression for the maximum of the norm of the field i.e. the RT surface. By investigating the r coordinate of the RT surface at the $z = \epsilon$ cut-off, he was able to deduce this relation.

where again $A = D^2(R)$ a disk of radius R and $\mathcal{A}$ is the area of the RT surface. This quantity is made dimensionless so we have to multiply it by a factor of l^2 to give it the dimension of area again. Remembering that the EE is the area of the RT surface divided by $4G_N$ we see that

$$S_A = \frac{\mathcal{A}_A}{4G_N} = \frac{l^2}{4G_N}\left[\frac{2\pi R}{\epsilon} - 2\pi\right] \tag{4.99}$$

the same result we obtained. It is interesting to note that there could be terms linear in ϵ, but these are not of our interest since $\epsilon \to 0$. We have two terms left, a finite piece, and a $1/\epsilon$ piece. We see that this $1/\epsilon$ piece follows the area law for the entropy. A scales as the area of its boundary $2\pi R$ instead of its volume. In [52] it is actually stated that this term should always be proportional to ∂A.

5 Discussion

In the discussion of this thesis, we would like to start by reviewing our results. Let us summarize what we have discovered in this project. We started with the assumption that the max-flow of a particular entangling region could be related to a different vector field in Minkowski space. We deduced the conditions for this field. We proceeded by stating an algorithm to find this field in two and three dimensions. It should be found by letting a current run through the entangling surface and calculating its magnetic field using a modified version of Biot-Savart's law. With this algorithm, we were able to recover the correct flows for the disk, the half-plane, and the interval as entangling regions. We showed the validity of this law in two specific cases explicitly. By starting with a general field, maximizing its flux, and applying the conditions we carried over from the flow. We then naively assumed this law should produce a max-flow in more general cases. Unfortunately, this turned out not to be the case. We saw that for the case of an ellipse, the surface where the flow is maximal was not homologous to the entangling surface.

What we would like to do next is discuss this problem. The first thing we tried to fix this is to make a coordinate transformation from the ellipse to the circle. By changing our coordinates as $u = x/a$ and $v = y/b$, we see that (4.90) becomes just the equation for a circle of radius one. We know our law works for a circular entangling surface. This would change of course the metric and in its turn the denominator of the law. Unfortunately, the results show that this does not work as well. The problem was even worse than in Figure 10. This can be explained by the fact that the coordinate transformation just described is not conformal. Hence we might need a different law altogether to describe these regions.

Looking at some other simulations done by Guim Planella (similar to the ones in Figure 10) we saw that the norm of the field drops off faster in the direction where the curvature of the entangling surface is larger. This gave us the indication that the problem might arise with a non-constant curvature of the entangling surface. Since the situations that we calculated explicitly (and gave the correct result) all have an entangling surface of constant curvature. Also, it seems to be that the field is not strong enough, away from the entangling surface. This means that we might solve the problem in two different ways. Change the numerator of the expression, hence the current running through the entangling surface. Or change the denominator in the law again to increase the field at larger distances.

The former solution would mean we vary the amount of current running through the entangling surface from point to point. Depending on the curvature at each point we would let more or less current flow through that point. There is however a problem with changing the current on different points of the entangling surface. This is the fact that the field will have different values close to different points on the entangling surface. This means that the norm of the field will also vary between points just above the entangling surface. Hence the norm can not be maximal just above the **whole** entangling surface. Only this has to be the case for the maximal surface to be homologous to the entangling surface. What if we change the denominator then? This will be difficult as well. The power of the denominator is completely fixed by the same asymptotic behavior. If we move close to the entangling surface, it can be approximated by a straight line. But we already know what the field should be for the straight line! The fourth power in the denominator is completely fixed by requiring that the field is divergenceless, bounded and that it maximizes the flux. We can now see why this problem is quite huge and in fact, we were not able to fix it yet.

Basically, the only thing that one can do at this point is, try to make small perturbations of the entangling surface around a known case. Thereafter try to see how the law for the field changes depending on the change in the entangling surface. One thing that is in active research at the moment by Guim Planella is to try and invert this process. So start with a know max-flow and make a small perturbation. Demand the conditions such as divergenceless and norm bound. Then try and see how the RT surface and hence the entangling surface changes. If one can find a relation like this it could be inverted to discover how the field changes when we make small perturbations to the entangling surface.

All in all we still believe there is something to gain here. Our first discovery (changing a number in the denominator of Biot-Savart's law resulting in a max-flow for two different chases) gave us a lot of hope. This was going to be a much more accessible way of calculating the EE of a certain region. This turned out to be 'too good to be true'. However, we still believe that there should be a general description of finding the max-flow. This should then reduce to our description when the

curvature of the entangling surface is taken to be constant. One way of finding a hint towards this more universal law might be to look at disconnected regions as well. Starting with two intervals as the entangling region in a two-dimensional CFT. If one could find a max-flow there, this could maybe be generalized to higher dimensions to find this universal law.

Now there are several ways one could continue in future research. One of them would be to relax the condition of a static spacetime. So instead of considering a time slice in the CFT and AdS, one could try and calculate a more covariant description of EE. It would be interesting to see what happens to the bit threads in this case. Since the RT formula and hence the bit treads are only valid for static spacetimes. One would need the so-called HRT formula in this case. More on this can be found in [33].

Another direction one could generalize this project would be to investigate the direct connection between the CFT and the bit threads. By this, we mean without taking the detour to the RT surface. EE can be calculated, as we have seen, directly in the CFT using partition functions and path integrals. It makes sense to propose that there is a connection between the bit threads and this straightforward description of the EE. After all, the RT surface is just the bottleneck for the max-flow.

We continue with the fact that one can investigate the dynamics of entanglement. For perturbed excited states, the change in the EE is mapped in the bulk to linear Einstein equations [14, 15, 16]. It would be interesting to see how this translates to the bit thread picture. Especially since the emergence of gravity and Einstein's equations might help us understand gravity in our own (non AdS) universe.

We have neglected another important thing. The RT formula and the bit thread description are only valid to leading order in the CFT's coupling and central charge. If one wants to consider higher-order corrections, we have to take into account bulk entanglement entropy contributions. This is an extra term given by the EE of a volume $\sigma(A)$ such that $\partial\sigma(A) = A \cup \gamma_A$. One could find these contributions using quantum bit threads [43]. These would be bit threads that could start and end at the bulk instead of the boundary. To find these quantum bit threads one could resort to theories of double holography. In these theories, the EE of the bulk region $\sigma(A)$ can in its turn again be described using 'classical' bit threads but in one dimension higher.

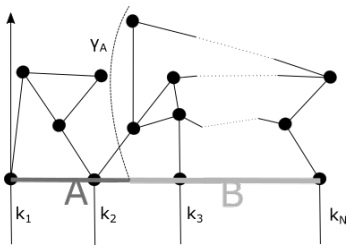

(a) Tensor network from figure 2b with a minimal cut.

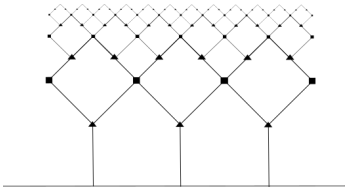

(b) The MERA network.

Figure 11: Some tensor networks

Finally, we like to note the connection to tensor networks. Remember the one-dimensional spin chain from the introduction 1. It is discussed in [22] that there is a clever way to find the maximal EE from a tensor network. Say one divides the chain up into two pieces (A and B) as shown in Figure 11a. Then one makes a minimal cut through the network, such that it cuts through the least amount of contractions. The maximal EE of A (or B) is then shown to be proportional to the minimal number of cuts one makes through the network. Here we can see the resemblance with the RT formula. This is also a minimal cut but through a continuous space. However, in this case, the maximal EE is constant in the size of A. The minimal cut does not depend on the size of the region A. This is different than what we have seen for a time slice of a two-dimensional CFT. We computed in three ways that the EE of an interval scales with the log of the size of the interval. There are however tensor networks that show this property as well. An example of this is the *multi-scale entanglement renormalization ansatz* or MERA network (also mentioned in the introduction 1) first introduced by Guifré Vidal [6, 7] shown in Figure 11b. Here the number of cuts of the minimal cut scales logarithmically with the size of the considered region. Also, the MERA network can produce conformally invariant states at the boundary. This indicates that this

network, is the right candidate to express a time slice of AdS space as a tensor network. What would be interesting for future research, is to investigate the connection of these tensor networks with the bit threads. The minimal cut through the network already shows a lot of resemblance with the bottleneck of the bit thread configuration. Maybe one can formulate a tensor network, where the contractions coincide with the bit threads.

Appendix A Analytic flows in AdS

In [50], a specific flow was constructed for the sphere in empty AdS based, taking space-like geodesics as integral curves and imposing the divergenceless condition to fix the norm. In the following we will review the main result and obtain a similar flow for the case of the semi-infinite plane in empty AdS.

A.1 The sphere

For the sphere, the resulting vector field was [50]:

$$V^a = \left(\frac{2Rz}{\sqrt{(R^2+r^2+z^2)^2-4R^2r^2}}\right)^{d+1}\left(\frac{rz}{R}\,,\,\frac{R^2-r^2+z^2}{2R}\right)\,. \tag{A.1}$$

with

$$|V| = \left(\frac{2Rz}{\sqrt{(R^2+r^2+z^2)^2-4R^2r^2}}\right)^{d}\,, \tag{A.2}$$

$$\hat{\tau}^a \equiv \frac{V^a}{|V|} = \frac{2Rz}{\sqrt{(R^2+r^2+z^2)^2-4R^2r^2}}\left(\frac{rz}{R}\,,\,\frac{R^2-r^2+z^2}{2R}\right)\,. \tag{A.3}$$

In Figure 12 we show the integral curves and magnitude of V for $d=1$, $d=2$ and $d=3$ spatial dimensions.

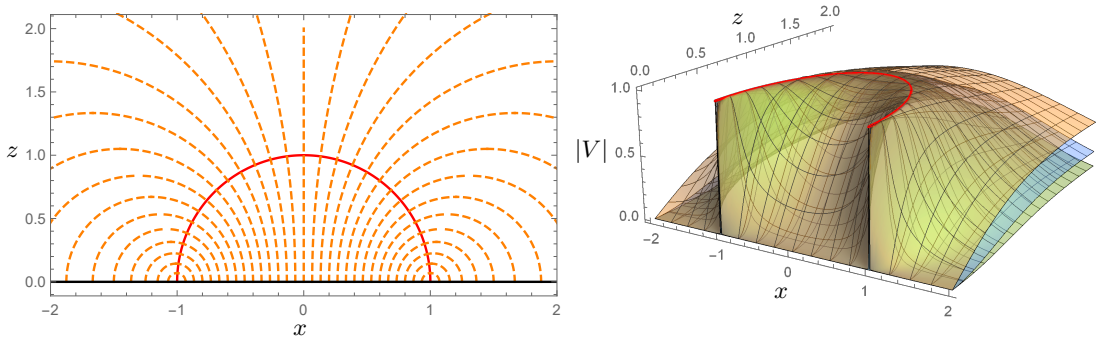

Figure 12: Vector lines and magnitude $|V|$ for a sphere in $d=1$ (orange), $d=2$ (blue) and $d=3$ (green) spatial dimensions, respectively. The vector field V exhibits spherical symmetry so, for simplicity, we have plotted only one of the spatial axis in all case. The solid red line corresponds to the minimal surface, $m(A)$. This curve also signals the location where the magnitude of the vector field attains its maximal value, $|V|=1$.

A.2 The semi-infinite plane

In CFTs, the modular hamiltonian of the semi-infinite plane is related to that of the sphere by a conformal transformation. Therefore, we expect to be able do derive an analytic flow for this case as well.

Minimal surface: Consider the minimal surface associated to a semi-infinite plane A, defined as $x_1 \equiv x \in (-\infty, 0]$, in AdS_{d+2}. In Poincare coordinates (a constant-t slice of) the metric is given by

$$ds^2 = \frac{l^2}{z^2}\left(d\vec{x}^2 + dz^2\right)\,. \tag{A.4}$$

Given the translation invariance along $\vec{x}_\perp$, these coordinates can be suppressed and the problem can be effectively reduced to two dimensions. The minimal surface $m(A)$, parametrized by (x_m, z_m), is simply a vertical surface with

$$x_m = 0\,. \tag{A.5}$$

The outward-pointing unit normal vector $\hat{n}_m$ at a point (x_m, z_m), is given by

$$\hat{n}_m^a = (z_m, 0) \,, \tag{A.6}$$

where the index a here runs over the coordinates (x, z).

Integral curves: Consider the space of geodesics that lie on the (x, z) plane that intersect $m(A)$ at (x_m, z_m) with tangent vector $\hat{\tau}$ equal to the normal $\hat{n}_m$ at that point. It is easy to check that the set of relevant geodesics is given by the one-parameter family of circumferences defined implicitly by

$$x^2 + z^2 = R_s^2 \,, \tag{A.7}$$

i.e., semi-circles centered at $x = 0$ with radii R_s. The tangent vector with unit norm at an arbitrary point along one of these geodesics is given by

$$\hat{\tau}^a = \frac{z}{lR_s} (z, -x) \,. \tag{A.8}$$

Enforcing that $\hat{\tau} = \hat{n}_m$ at a point (r_m, z_m) on the minimal surface leads to the simple condition

$$R_s = z_m \,. \tag{A.9}$$

Plugging (A.9) into (A.7) and (A.8) we obtain an implicit expression for the family of geodesics orthogonal to $m(A)$ with the correct parametrization,

$$x^2 + z^2 = z_m^2 \,, \tag{A.10}$$

and tangent vector

$$\hat{\tau}^a = \frac{z}{lz_m} (z, -x) \,. \tag{A.11}$$

It is straightforward to check that these geodesics are nested, which validates our choice as integral curves.

Vector field: We can now proceed to find the appropriate norm of the vector field $|V|$. First, we compute the orthogonal metric at different points along the minimal surface,

$$h_{ab}(z_m; x, z) = g_{ab} - \hat{\tau}_a \hat{\tau}_b \,, \tag{A.12}$$

where $\hat{\tau}$ is the unit tangent vector, given in (A.11). A brief calculation leads to

$$ds_\perp^2 \equiv h_{ab} dx^a dx^b = \frac{l^2}{z^2 z_m^2} (x dx + z dz)^2 \,. \tag{A.13}$$

Now, we can use the geodesic equation (A.10) to (i) eliminate one of the variables, and (ii) express (A.13) as a differential along the transverse coordinate, namely dz_m. By doing so, and restoring the coordinates $\vec{x}_\perp$, we find that

$$ds_\perp^2 = \frac{l^2}{z^2} \left(dz_m^2 + d\vec{x}_\perp^2 \right) \,. \tag{A.14}$$

The magnitude of the vector field reads

$$|V| = \frac{\sqrt{h(z_m; x_m, z_m)}}{\sqrt{h(z_m; x, z)}} = \left(\frac{z}{z_m} \right)^d \,. \tag{A.15}$$

Finally, we would like to express our vector field as a function of (x, z) without reference to the minimal surface. This can be achieved by solving for $z_m = z_m(x, z)$ from the geodesic (A.10) and plugging it back into the relevant equations. A short calculation leads to

$$|V| = \left(\frac{z}{\sqrt{x^2 + z^2}} \right)^d \,, \tag{A.16}$$

and

$$\hat{\tau}^a = \frac{z}{l\sqrt{x^2+z^2}}\,(z,-x)\ . \tag{A.17}$$

Putting all together, we find that the full vector field $V = |V|\hat{\tau}$ is given by

$$V^a = \frac{1}{l}\left(\frac{z}{\sqrt{x^2+z^2}}\right)^{d+1}(z,-x)\ . \tag{A.18}$$

In the above we have suppressed the components of the vector in the transverse directions $\vec{x}_\perp$, which are zero (the must vanish by translation invariance). In Figure 13 we show plots of the vector lines as well as the magnitude of V for $d = 1$, $d = 2$ and $d = 3$ spatial dimensions.

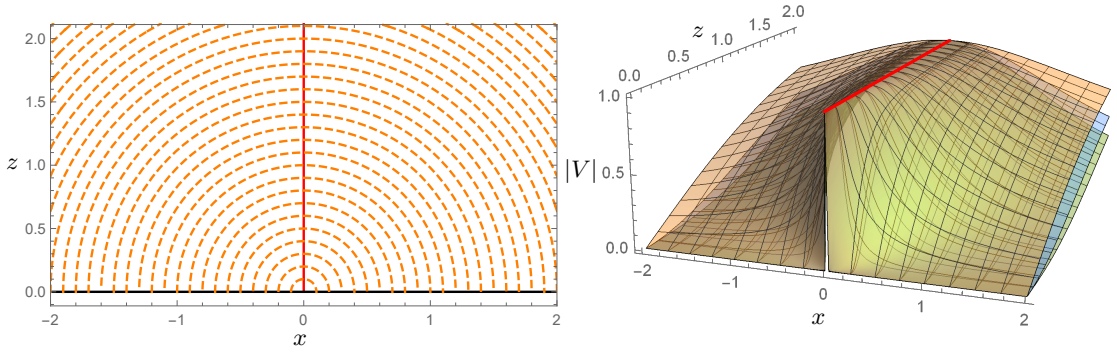

Figure 13: Vector lines and magnitude $|V|$ for a semi-infinite plane in $d = 1$ (orange), $d = 2$ (blue) and $d = 3$ (green) spatial dimensions, respectively. The vector field V exhibits translation invariance along the transverse directions $\vec{x}_\perp$, for simplicity, we have plotted only the plane (x, z). The solid red line corresponds to the minimal surface, $m(A)$. This curve also signals the location where the magnitude of the vector field attains its maximal value, $|V| = 1$.

Appendix B Integral identities

B.1 First identities

We want to solve the following integral two integrals

$$\int_0^{2\pi} \frac{\cos x \; dx}{(c-\cos x)^2} \qquad\qquad \int_0^{2\pi} \frac{dx}{(c-\cos x)^2} \tag{B.1}$$

given $c > 1$. We make a substitution to complex coordinates $e^{ix} = z$ then $\cos x = \frac{1}{2}\left(z + \frac{1}{z}\right)$, $dz = izdx$ and the domain of integration is now S^1 the unit circle in the complex plane. The first integral becomes

$$\begin{aligned}
\int_0^{2\pi} \frac{\cos x \; dx}{(c-\cos x)^2} &= \int_{S^1} \frac{1}{2iz} \frac{\left(z+\frac{1}{z}\right) dz}{\left(c - \frac{1}{2}\left(z+\frac{1}{z}\right)\right)^2} \\
&= \int_{S^1} \frac{1}{2i} \frac{(z^2+1)dz}{(cz - \frac{1}{2}(z^2+1))^2} \\
&= \frac{2}{i} \int_{S^1} \frac{(z^2+1)dz}{\left(z-c-\sqrt{c^2-1}\right)^2 \left(z-c+\sqrt{c^2-1}\right)^2}
\end{aligned}$$

and the second

$$\begin{aligned}
\int_0^{2\pi} \frac{dx}{(c-\cos x)^2} &= \int_{S^1} \frac{1}{iz} \frac{dz}{\left(c - \frac{1}{2}\left(z+\frac{1}{z}\right)\right)^2} \\
&= \int_{S^1} \frac{1}{i} \frac{zdz}{(cz - \frac{1}{2}(z^2+1))^2} \\
&= \frac{4}{i} \int_{S^1} \frac{zdz}{\left(z-c-\sqrt{c^2-1}\right)^2 \left(z-c+\sqrt{c^2-1}\right)^2}
\end{aligned}$$

where the roots of the quadratic equation in the denominator are calculated with the abc-formula. Because $c > 1$, only one of the second-degree poles is enclosed by the unit circle. Let

$$f_1(z) = \frac{2(z^2+1)}{i\left(z-c-\sqrt{c^2-1}\right)^2 \left(z-c+\sqrt{c^2-1}\right)^2} \quad f_2(z) = \frac{4z}{i\left(z-c-\sqrt{c^2-1}\right)^2 \left(z-c+\sqrt{c^2-1}\right)^2}$$

and $z_1 = c - \sqrt{c^2-1}$ so that the residues become

$$\begin{aligned}
\int_0^{2\pi} \frac{\cos x \; dx}{(c-\cos x)^2} &= 2\pi i \operatorname{Res}(f_1, z_1) = 2\pi i \lim_{z\to z_1} \frac{d}{dz}\left(\left(z-c+\sqrt{c^2-1}\right)^2 f_1(z)\right) \\
&= 4\pi \lim_{z\to z_1} \frac{d}{dz}\left(\frac{z^2+1}{\left(z-c-\sqrt{c^2-1}\right)^2}\right) \\
&= 4\pi \lim_{z\to z_1} \frac{2z\left(z-c-\sqrt{c^2-1}\right)^2 - 2(z^2+1)(z-c-\sqrt{c^2-1})}{\left(z-c-\sqrt{c^2-1}\right)^4} \\
&= -8\pi \lim_{z\to z_1} \frac{z(c+\sqrt{c^2-1})+1}{\left(z-c-\sqrt{c^2-1}\right)^3} = -8\pi \frac{2}{\left(-2\sqrt{c^2-1}\right)^3} = \frac{2\pi}{(c^2-1)^{\frac{3}{2}}}
\end{aligned} \tag{B.2}$$

and

$$\begin{aligned}
\int_0^{2\pi} \frac{dx}{(c-\cos x)^2} &= 2\pi i \operatorname{Res}(f_2, z_1) = 2\pi i \lim_{z\to z_1} \frac{d}{dz}\left(\left(z-c+\sqrt{c^2-1}\right)^2 f_2(z)\right) \\
&= 8\pi \lim_{z\to z_1} \frac{d}{dz}\left(\frac{z}{\left(z-c-\sqrt{c^2-1}\right)^2}\right) \\
&= 8\pi \lim_{z\to z_1} \frac{\left(z-c-\sqrt{c^2-1}\right)^2 - 2z(z-c-\sqrt{c^2-1})}{\left(z-c-\sqrt{c^2-1}\right)^4} \\
&= 8\pi \lim_{z\to z_1} \frac{z-c-\sqrt{c^2-1}-2z}{\left(z-c-\sqrt{c^2-1}\right)^3} = -8\pi \frac{2c}{\left(-2\sqrt{c^2-1}\right)^3} = \frac{2\pi c}{(c^2-1)^{\frac{3}{2}}}
\end{aligned} \tag{B.3}$$

B.2 Second identity

We are looking for the anti-derivative of

$$\int \frac{\tan^2 x}{\cos^2 x} dx.$$

Let $u = \tan x$ then $du = dx/\cos^2 x$ and the integral becomes

$$\int u^2 du = \frac{1}{3}u^3 + c = \frac{1}{3}\tan^3 x + c \tag{B.4}$$

B.3 Third identity

We want to solve the following integral

$$\begin{aligned} I_\alpha &\equiv \int_{-\infty}^{\infty} \frac{dx}{(x^2+c^2)^\alpha} = \frac{1}{c^2}\int_{-\infty}^{\infty} \frac{dx}{(x^2+c^2)^{\alpha-1}} - \frac{1}{c^2}\int_{-\infty}^{\infty} \frac{x^2 dx}{(x^2+c^2)^\alpha} \\ &= \frac{1}{c^2}\left(I_{\alpha-1} - \int_{-\infty}^{\infty} x \frac{x\ dx}{(x^2+c^2)^\alpha} \right) \end{aligned} \tag{B.5}$$

where we used partial fraction decomposition to rewrite the integral. We will now use partial integration for the remaining integral. Note that

$$\int \frac{x\ dx}{(x^2+c^2)^\alpha} = \frac{1}{2}\int \frac{du}{u^\alpha} = \frac{1}{2}\frac{1}{1-\alpha}u^{1-\alpha} = \frac{1}{2(1-\alpha)}\frac{1}{(x^2+c^2)^{\alpha-1}}$$

by substitution of $u = x^2 + c^2$ and that the boundary term in the partial integration will go to zero. We end up with

$$\begin{aligned} c^2 I_\alpha &= I_{\alpha-1} + \frac{1}{2(1-\alpha)}\int_{-\infty}^{\infty} \frac{dx}{(x^2+c^2)^{\alpha-1}} = I_{\alpha-1}\left(1 + \frac{1}{2(1-\alpha)}\right) \\ &= I_{\alpha-1}\frac{3-2\alpha}{2(1-\alpha)} \end{aligned}$$

and hence

$$I_\alpha = \frac{\alpha - \frac{3}{2}}{c^2(\alpha-1)} I_{\alpha-1} = \frac{\alpha-\frac{3}{2}}{c^2(\alpha-1)}\frac{\alpha-\frac{5}{2}}{c^2(\alpha-2)}\cdots\frac{\frac{1}{2}}{c^2} I_1.$$

Now since we know $\Gamma(\alpha) = (\alpha-1)\Gamma(\alpha-1)$, hence $\Gamma(n) = (n-1)!$ for integer n and $\Gamma(1/2) = \sqrt{\pi}$ we see that

$$I_\alpha = \frac{\Gamma(\alpha - \frac{1}{2})}{\Gamma(\frac{1}{2})\Gamma(\alpha)}(c^2)^{1-\alpha} I_1.$$

We also know

$$I_1 = \int_{-\infty}^{\infty} \frac{dx}{x^2+c^2} = \frac{1}{c^2}\int_{-\infty}^{\infty} \frac{dx}{\left(\frac{x}{c}\right)^2 + 1} = \frac{1}{c}\int_{-\infty}^{\infty} \frac{du}{u^2+1} = \frac{\pi}{c}$$

to finally obtain

$$I_\alpha = \int_{-\infty}^{\infty} \frac{dx}{(x^2+c^2)^\alpha} = \frac{\Gamma(\alpha-\frac{1}{2})}{\sqrt{\pi}\Gamma(\alpha)}(c^2)^{1-\alpha}\frac{\pi}{(c^2)^{\frac{1}{2}}} = \sqrt{\pi}\frac{\Gamma(\alpha-\frac{1}{2})}{\Gamma(\alpha)}(c^2)^{\frac{1}{2}-\alpha} \tag{B.6}$$

Appendix C Vector potential of an ellipse

These calculations were done just before we encountered the problem with the ellipse. They might be of use to anyone encountering a similar integral in their research. We will now try a different approach to finding the vector field generated by a current running through an ellipse. Namely, using the description for the vector potential. Once we obtain this, the divergent less field can be obtained by taking the curl of the vector potential. Also, to find the flux of the magnetic field through the surface of the ellipse, one only has to integrate the vector potential along the ellipse. This is of course due to Stokes' theorem.

We start with our modified version of the vector potential

$$\mathbf{A}(\mathbf{r}) = \frac{1}{2}\int \frac{\mathbf{J}(\mathbf{r}')dr'}{|\mathbf{r}-\mathbf{r}'|^2}$$

the factor 1/2 in front is there to make sure that when we take the curl, this agrees with the magnetic field with $\mu_0 = 4\pi$. In our case $\mathbf{r} = (x, y, z), \mathbf{r}'(\theta) = (a\cos\theta, b\sin\theta, 0)$ and we define

$$E = \left\{ (x,y) \in \mathbb{R} \,\middle|\, \left(\frac{x}{a}\right)^2 + \left(\frac{y}{b}\right)^2 = 1 \right\}.$$

We want $\mathbf{J}(\mathbf{r}')$ to flow in the direction parallel to the curve E and to be normalized. This gives

$$\mathbf{J}(\mathbf{r}') = \begin{pmatrix} -a\sin\theta \\ b\cos\theta \\ 0 \end{pmatrix} \frac{1}{\sqrt{a^2\sin^2\theta + b^2\cos^2\theta}}.$$

Now

$$dr'(\theta) = \left|\frac{d\mathbf{r}'(\theta)}{d\theta}\right| d\theta = \sqrt{a^2\sin^2\theta + b^2\cos^2\theta}\; d\theta$$

yielding the following expression for the vector potential

$$\begin{aligned}
\mathbf{A}(\mathbf{r}) &= \frac{1}{2}\int_E \frac{\mathbf{J}(\mathbf{r}')dr'}{|\mathbf{r}-\mathbf{r}'|^2} \\
&= \frac{1}{2}\int_0^{2\pi} \begin{pmatrix} -a\sin\theta \\ b\cos\theta \\ 0 \end{pmatrix} \frac{1}{\sqrt{a^2\sin^2\theta + b^2\cos^2\theta}} \frac{\sqrt{a^2\sin^2\theta + b^2\cos^2\theta}\; d\theta}{(x-a\cos\theta)^2 + (y-b\sin\theta)^2 + z^2} \\
&= \frac{1}{2}\int_0^{2\pi} \frac{d\theta}{(x-a\cos\theta)^2 + (y-b\sin\theta)^2 + z^2} \begin{pmatrix} -a\sin\theta \\ b\cos\theta \\ 0 \end{pmatrix}.
\end{aligned} \tag{C.1}$$

For a moment we want to set $z = 0$ and investigate the x- component of the field. This yields

$$-\frac{2}{a}A_x(\mathbf{r}) = \int_0^{2\pi} \frac{\sin\theta\; d\theta}{(x-a\cos\theta)^2 + (y-b\sin\theta)^2}.$$

We want to tackle this integral by complex integration. By making the substitution of $z = e^{i\theta}$, the integration will be transformed to an integral over S^1 in the complex plane. By then locating potential poles in the integrand we can apply Cauchy's residue theorem to find the integral in a closed from. We see that by making this subsitution we get that $dz = ie^{i\theta}\; d\theta = iz\; d\theta$. Also, $\cos\theta = \frac{1}{2}(z + z^{-1})$ and $\sin\theta = \frac{1}{2i}(z - z^{-1})$. Implementing this substitution to the x-component of the vector potential we obtain

$$-\frac{2}{a}A_x(\mathbf{r}) = \int_{S^1} \frac{\frac{1}{2i}(z-z^{-1})\frac{dz}{iz}}{(x - a\frac{1}{2}(z+z^{-1}))^2 + (y - b\frac{1}{2i}(z-z^{-1}))^2}. \tag{C.2}$$

Multiplying both sides with -2 and the numerator and denominator of the integrand with z we get

$$\frac{4}{a}A_x(\mathbf{r}) = \int_{S^1} \frac{(z^2-1)dz}{(xz - \frac{a}{2}(z^2+1))^2 + (yz - \frac{b}{2i}(z^2-1))^2}. \tag{C.3}$$

We recognize that the denominator is the sum of two squares and this can be factorized over $\mathbb{C}$.[21] We obtain the equation

$$\begin{aligned}\frac{4}{a}A_x(\mathbf{r}) &= \int_{S^1} \frac{(z^2-1)dz}{(xz-\frac{a}{2}(z^2+1)+yzi-\frac{b}{2}(z^2-1))(xz-\frac{a}{2}(z^2+1)-yzi+\frac{b}{2}(z^2-1))} \\ &= \int_{S^1} \frac{(z^2-1)dz}{\left(\frac{a+b}{2}z^2-(x+iy)z+\frac{a-b}{2}\right)\left(\frac{a-b}{2}z^2-(x-iy)z+\frac{a+b}{2}\right)}. \end{aligned} \tag{C.4}$$

Next we define the complex number $w = x + iy$ and using the fact that $c^2 = (a+b)(a-b)$ we calculate the roots of the quadratic equations. Let us define $P_1(z) = \frac{a+b}{2}z^2 - (x+iy)z + \frac{a-b}{2}$ the first quadratic equation and $P_2(z) = \frac{a-b}{2}z^2 - (x-iy)z + \frac{a+b}{2}$ the second. The discriminant of $P_1(z)$ is $D_1 = w^2 - c^2$ and of $P_2(z)$ is $D_2 = \bar{w}^2 - c^2$. Giving us the roots of

$$P_1(z) : z_{1\pm} = \frac{w \pm \sqrt{w^2-c^2}}{a+b}, \quad P_2(z) : z_{2\pm}\frac{\bar{w} \pm \sqrt{\bar{w}^2-c^2}}{a-b}.$$

We now take $c^2/4$ out of the denominator to make the first coefficient of each quadratic equation equal to one. Then each $P_j(z) = (z - z_{j-})(z - z_{j+})$. We end up with

$$\frac{c^2}{a}A_x(\mathbf{r}) = \int_{S^1} \frac{(z^2-1)dz}{(z-z_{1-})(z-z_{1+})(z-z_{2-})(z-z_{2+})} \tag{C.5}$$

if we assume that $w \neq c$ (the focal point). This gives us four simple poles. To determine which of the four poles lie inside the unit circle, we decided to look at the limit for a=b=R. In this limit we see that

$$z_{1-} \to 0, \; z_{1+} \to \frac{w}{R}, \; z_{2-} \to \frac{R}{\bar{w}} \text{ and } z_{2+} \to \infty.$$

considering the field within the ellipse, we see that the poles $z_{1\pm}$ would be in D^2 if we take the limit to the circle. This motivates us to look at the residues of these two poles.

Before we do so we note that the y-component of the vector potential is given by $-b/aA_x(\mathbf{r})$ except with a $\cos\theta$ in the numerator instead of a $\sin\theta$. Thus we get that

$$\frac{ic^2}{b}A_y(\mathbf{r}) = \int_{S^1} \frac{(z^2+1)dz}{(z-z_{1-})(z-z_{1+})(z-z_{2-})(z-z_{2+})} \tag{C.6}$$

which motivates us to define

$$f_\pm(z) = \frac{(z^2 \pm 1)}{(z-z_{1-})(z-z_{1+})(z-z_{2-})(z-z_{2+})}.$$

Now we can write

$$A_x(\mathbf{r}) = \frac{a2\pi i}{c^2}\sum_{\pm}\text{Res}\big(f_-(z), z_{1\pm}\big) \text{ and } A_y(\mathbf{r}) = \frac{b2\pi}{c^2}\sum_{\pm}\text{Res}\big(f_+(z), z_{1\pm}\big) \tag{C.7}$$

by the residue theorem.

C.1 The residues of $f_\pm$

We will focus now on computing the residues of $f_\pm$ and simplifying. Let us start with

$$\begin{aligned}\text{Res}\big(f_\pm, z_{1\pm}\big) &= \frac{z_{1\pm}^2 \pm 1}{(z_{1\pm}-z_{1\mp})(z_{1\pm}-z_{2-})(z_{1\pm}-z_{2+})} \\ &= \frac{\left(\frac{w\pm\sqrt{w^2-c^2}}{a+b}\right)^2 \pm 1}{\left(\frac{w\pm\sqrt{w^2-c^2}}{a+b}-\frac{w\mp\sqrt{w^2-c^2}}{a+b}\right)\left(\frac{w\pm\sqrt{w^2-c^2}}{a+b}-\frac{\bar{w}-\sqrt{\bar{w}^2-c^2}}{a-b}\right)\left(\frac{w\pm\sqrt{w^2-c^2}}{a+b}-\frac{\bar{w}+\sqrt{\bar{w}^2-c^2}}{a-b}\right)}\end{aligned}$$

[21] $z^2 + w^2 = (z + iw)(z - iw)$

where the red colored $\pm$ sign is independent from the black $\pm$. We proceed by writing the numerator as one fraction. The factor $(a+b)^{-2}$ then cancels in the denominator leaving us with

$$\mathrm{Res}\big(f_\pm, z_{1\pm}\big) = \frac{(w\pm\sqrt{w^2-c^2})^2 \pm (a+b)^2}{\pm 2\sqrt{w^2-c^2}\left(w\pm\sqrt{w^2-c^2} - \frac{a+b}{a-b}(\bar{w}-\sqrt{\bar{w}^2-c^2})\right)\left(\frac{w\pm\sqrt{w^2-c^2}}{a+b} - \frac{\bar{w}+\sqrt{\bar{w}^2-c^2}}{a-b}\right)}.$$

Let us now focus on the last two factors in the denominator. Expanding the brackets will give us

$$\begin{aligned}
&\left(w\pm\sqrt{w^2-c^2} - \frac{a+b}{a-b}(\bar{w}-\sqrt{\bar{w}^2-c^2})\right)\left(\frac{w\pm\sqrt{w^2-c^2}}{a+b} - \frac{\bar{w}+\sqrt{\bar{w}^2-c^2}}{a-b}\right)\\
&= \frac{(w\pm\sqrt{w^2-c^2})^2}{a+b} - \frac{1}{a-b}\left((w\pm\sqrt{w^2-c^2})(\bar{w}+\sqrt{\bar{w}^2-c^2}) + (w\pm\sqrt{w^2-c^2})(\bar{w}-\sqrt{\bar{w}^2-c^2})\right)\\
&+ \frac{a+b}{(a-b)^2}(\bar{w}-\sqrt{\bar{w}^2-c^2})(\bar{w}+\sqrt{\bar{w}^2-c^2})\\
&= \frac{1}{c^2}\left((a-b)(w\pm\sqrt{w^2-c^2})^2 - (a+b)(w\pm\sqrt{w^2-c^2})2\bar{w} + \frac{(a+b)^2}{a-b}(\bar{w}^2-\bar{w}^2+c^2)\right)\\
&= \frac{1}{c^2}\left((a-b)(w\pm\sqrt{w^2-c^2})^2 - 2(a+b)(w\pm\sqrt{w^2-c^2})\bar{w} + (a+b)^3\right) \qquad \text{(C.8)}
\end{aligned}$$

and we obtain

$$\mathrm{Res}\big(f_\pm, z_{1\pm}\big) = \pm\frac{c^2}{2}\frac{(w\pm\sqrt{w^2-c^2})^2 \pm (a+b)^2}{\sqrt{w^2-c^2}\left((a-b)(w\pm\sqrt{w^2-c^2})^2 - 2(a+b)(w\pm\sqrt{w^2-c^2})\bar{w} + (a+b)^3\right)}.$$

Next we want to define another complex number to simply our calculations. Let $v = \sqrt{w^2-c^2}$, than $w^2+v^2 = 2w^2-c^2$ and

$$\begin{aligned}
(a-b)2wv - 2(a+b)v\bar{w} &= 2v((a-b)w - (a+b)\bar{w})\\
&= 2v(a(w-\bar{w}) - b(w+\bar{w}))\\
&= 2v(a2iy - 2bx) = -4v(bx - iay). \qquad \text{(C.9)}
\end{aligned}$$

The residue now becomes

$$\begin{aligned}
\frac{2}{c^2}\mathrm{Res}\big(f_\pm, z_{1\pm}\big) &= \pm\frac{(w\pm v)^2 \pm (a+b)^2}{v\left((a-b)(w\pm v)^2 - 2\bar{w}(a+b)(w\pm v) + (a+b)^3\right)}\\
&= \pm\frac{1}{v}\frac{w^2+v^2\pm 2vw \pm (a+b)^2}{(a-b)(w^2+v^2\pm 2vw) - 2(a+b)|w|^2 \mp 2(a+b)v\bar{w} + (a+b)^3}\\
&= \pm\frac{1}{v}\frac{2w^2 - c^2 \pm (a+b)^2 \pm 2vw}{(a-b)(2w^2-c^2) - 2(a+b)|w|^2 + (a+b)^3 \pm 2(a-b)vw \mp 2(a+b)v\bar{w}}. \qquad \text{(C.10)}
\end{aligned}$$

Let us continue to derive some identities that will simplify the denominator. First of all we have that

$$\begin{aligned}
2(a-b)w^2 - 2(a+b)|w|^2 &= 2w((a-b)w - (a+b)\bar{w})\\
&= 2w(a(w-\bar{w}) - b(w+\bar{w}))\\
&= 2w(a2iy - b2x) = -4w(bx - iay) \qquad \text{(C.11)}
\end{aligned}$$

and

$$\begin{aligned}
-(a-b)c^2 + (a+b)^3 &= (a+b)((a+b)^2 - (a-b)^2)\\
&= (a+b)(a+b+a-b)(a+b-a+b) = 4ab(a+b). \qquad \text{(C.12)}
\end{aligned}$$

Using now (C.9), (C.11) and (C.12) we can simplify the denominator of (C.10) to obtain

$$\begin{aligned}
\frac{2}{c^2}\mathrm{Res}\big(f_\pm, z_{1\pm}\big) &= \pm\frac{1}{v}\frac{2w^2 - c^2 \pm (a+b)^2 \pm 2vw}{2(a-b)w^2 - 2(a+b)|w|^2 - (a-b)c^2 + (a+b)^3 \pm (2(a-b)vw - 2(a+b)v\bar{w})}\\
&= \pm\frac{1}{v}\frac{2w^2 - c^2 \pm (a+b)^2 \pm 2vw}{-4w(bx-iay) + 4ab(a+b) \mp 4v(bx-iay)}\\
&= \pm\frac{1}{4v}\frac{2w^2 - c^2 \pm (a+b)^2 \pm 2vw}{ab(a+b) - w(bx-iay) \mp v(bx-iay)}. \qquad \text{(C.13)}
\end{aligned}$$

Looking at (C.13) we see that it makes sense to define a third and last complex number. Namely, let $u = bx - iay$ and we get

$$\frac{2}{c^2}\sum_{\pm}\mathrm{Res}\big(f_{\pm}, z_{1\pm}\big) = \frac{1}{4v}\left(\frac{2w^2 - c^2 \pm (a+b)^2 + 2vw}{ab(a+b) - wu - vu} - \frac{2w^2 - c^2 \pm (a+b)^2 - 2vw}{ab(a+b) - wu + vu}\right). \tag{C.14}$$

Now looking at the two fractions in (C.14) we recognize the form

$$\begin{aligned}\frac{\alpha+\beta}{\gamma-\delta} - \frac{\alpha-\beta}{\gamma+\delta} &= \frac{(\alpha+\beta)(\gamma+\delta) - (\alpha-\beta)(\gamma-\delta)}{\gamma^2-\delta^2} \\ &= \frac{\alpha\gamma + \alpha\delta + \beta\gamma + \beta\delta - \alpha\gamma + \alpha\delta + \beta\gamma - \beta\delta}{\gamma^2-\delta^2} \\ &= 2\frac{\alpha\delta + \beta\gamma}{\gamma^2-\delta^2}\end{aligned} \tag{C.15}$$

with in our case

$$\begin{aligned}\alpha &= 2w^2 - c^2 \pm (a+b)^2, & \beta &= 2vw \\ \gamma &= ab(a+b) - wu, & \delta &= vu.\end{aligned} \tag{C.16}$$

With this we compute that

$$\begin{aligned}\frac{2}{c^2}\sum_{\pm}\mathrm{Res}\big(f_{\pm}, z_{1\pm}\big) &= \frac{1}{2v}\frac{(2w^2 - c^2 \pm (a+b)^2)vu + 2vw(ab(a+b) - wu)}{(ab(a+b) - wu)^2 - (vu)^2} \\ &= \frac{uw^2 - \frac{1}{2}uc^2 \pm \frac{1}{2}u(a+b)^2 + wab(a+b) - w^2u}{a^2b^2(a+b)^2 + w^2u^2 - 2ab(a+b)wu - v^2u^2} \\ &= \frac{wab(a+b) - \frac{1}{2}u(c^2 \mp (a+b)^2)}{a^2b^2(a+b)^2 - 2ab(a+b)wu + u^2c^2}\end{aligned} \tag{C.17}$$

and we start to see that the sum over the residues is starting to take on a more appealing shape. Also, we can simplify even further. Let us focus on the denominator of (C.17). This can be written as

$$\begin{aligned}&a^2b^2(a+b)^2 - 2ab(a+b)wu + u^2c^2 = \\ &(a+b)\big(a^2b^2(a+b) - 2ab(x+iy)(bx-iay) + (a-b)(bx-iay)^2\big) \\ &= (a+b)\big(a^2b^2(a+b) - 2ab(bx^2 + ay^2 + i(bxy - axy)) + (a-b)(b^2x^2 - a^2y^2 - 2iabxy)\big) \\ &= (a+b)\big(a^2b^2(a+b) - 2ab^2x^2 - 2ba^2y^2 - 2iabxy(b-a) \\ &+ ab^2x^2 - a^3y^2 - b^3x^2 + ba^2y^2 + 2iabxy(b-a)\big) \\ &= (a+b)\big(a^2b^2(a+b) - ab^2x^2 - ba^2y^2 - a^3y^2 - b^3x^2\big) \\ &= (a+b)\big(a^2b^2(a+b) - (b^2x^2(a+b) + a^2y^2(a+b)\big) \\ &= (a+b)^2\big(a^2b^2 - (b^2x^2 + a^2y^2)\big).\end{aligned} \tag{C.18}$$

Finally the sum over the residues can be written as

$$\begin{aligned}\frac{2}{c^2}\sum_{\pm}\mathrm{Res}\big(f_{\pm}, z_{1\pm}\big) &= \frac{wab(a+b) - \frac{1}{2}u(c^2 \mp (a+b)^2)}{(a+b)^2\big(a^2b^2 - (b^2x^2 + a^2y^2)\big)} \\ &= \frac{wab - \frac{1}{2}u((a-b) \mp (a+b))}{(a+b)\big(a^2b^2 - (b^2x^2 + a^2y^2)\big)}.\end{aligned} \tag{C.19}$$

In conclusion, we see that the denominator is completely real! This is the first indication that we might be on the right track. Let us see what happens to the numerator for each component of the field.

C.2 The components of the vector potential

To see if our method for finding the vector potential gives us the right expression, there are three things that need to be checked off in order for our expression to make sense. First of all, we would

need each component of the field to be real. By switching to complex numbers to perform the integral, the residue has introduced various complex numbers in our expressions. In order for our calculations to make sense, the imaginary parts of our expressions have to cancel. This way we are left with a real field.

Second of all, we expect our expressions to reduce to the vector potential of the circle if we take $a = b = R$. If this is not the case our method is not the right one. Finally, we want the components of our field to diverge on the ellipse. Since the vector potential is ill-defined there.

Looking back at (C.7) for the x-component of the field and combining it with (C.19) we see that

$$\begin{aligned} A_x(\mathbf{r}) &= \frac{a2\pi i}{c^2}\sum_{\pm}\mathrm{Res}\big(f_-(z), z_{1\pm}\big) = a\pi i\frac{wab - \frac{1}{2}u((a-b)+(a+b))}{(a+b)\big(a^2b^2 - (b^2x^2+a^2y^2)\big)} \\ &= a\pi i\frac{abx + iaby - (abx - ia^2y)}{(a+b)\big(a^2b^2 - (b^2x^2+a^2y^2)\big)} \\ &= \frac{-\pi a^2 y(a+b)}{(a+b)\big(a^2b^2 - (b^2x^2+a^2y^2)\big)} \\ &= \frac{\pi a^2 y}{b^2x^2 + a^2y^2 - a^2b^2}. \end{aligned} \tag{C.20}$$

In a similar way, we compute the y-component. This is given by

$$\begin{aligned} A_y(\mathbf{r}) &= \frac{b2\pi}{c^2}\sum_{\pm}\mathrm{Res}\big(f_+(z), z_{1\pm}\big) = b\pi\frac{wab - \frac{1}{2}u((a-b)-(a+b))}{(a+b)\big(a^2b^2 - (b^2x^2+a^2y^2)\big)} \\ &= b\pi\frac{abx + iaby + b^2x - iaby}{(a+b)\big(a^2b^2 - (b^2x^2+a^2y^2)\big)} \\ &= \frac{\pi b^2 x(a+b)}{(a+b)\big(a^2b^2 - (b^2x^2+a^2y^2)\big)} \\ &= -\frac{\pi b^2 x}{b^2x^2 + a^2y^2 - a^2b^2}. \end{aligned} \tag{C.21}$$

Finally, we can combine the two to conclude that

$$\mathbf{A}(\mathbf{r}) = \frac{\pi}{b^2x^2 + a^2y^2 - a^2b^2}\begin{pmatrix} a^2y \\ -b^2x \\ 0 \end{pmatrix}. \tag{C.22}$$

In conclusion, we see that the field is indeed real. The denominator is zero only when $b^2x^2 + a^2y^2 = a^2b^2$. This is the equation of the ellipse, so the field is divergent on the ellipse. Finally, if we take the limit to $a = b = R$ we end up with

$$\mathbf{A}(\mathbf{r}) = \frac{\pi}{x^2 + y^2 - R^2}\begin{pmatrix} y \\ -x \\ 0 \end{pmatrix} \tag{C.23}$$

and this is the correct vector potential for the circle.

References

[1] S. W. Hawking. Particle creation by black holes. *Communications in Mathematical Physics*, 43(3), 1975.

[2] Gerard 't Hooft. Dimensional reduction in quantum gravity. *Conf. Proc. C*, 930308:284–296, 1993.

[3] Gerard 't Hooft. The holographic principle. *Basics and Highlights in Fundamental Physics*, Apr 2001.

[4] Jacob D. Bekenstein. Black holes and entropy. *Phys. Rev. D*, 7:2333–2346, Apr 1973.

[5] Juan Maldacena. *International Journal of Theoretical Physics*, 38(4):1113–1133, 1999.

[6] G. Vidal. Class of quantum many-body states that can be efficiently simulated. *Phys. Rev. Lett.*, 101:110501, Sep 2008.

[7] G. Vidal. Entanglement renormalization. *Physical Review Letters*, 99(22), Nov 2007.

[8] Fernando Pastawski, Beni Yoshida, Daniel Harlow, and John Preskill. Holographic quantum error-correcting codes: toy models for the bulk/boundary correspondence. *Journal of High Energy Physics*, 2015(6), Jun 2015.

[9] Patrick Hayden, Sepehr Nezami, Xiao-Liang Qi, Nathaniel Thomas, Michael Walter, and Zhao Yang. Holographic duality from random tensor networks. *Journal of High Energy Physics*, 2016(11), Nov 2016.

[10] Ning Bao, Geoffrey Penington, Jonathan Sorce, and Aron C. Wall. Holographic tensor networks in full ads/cft, 2019.

[11] Mark Van Raamsdonk. Building up spacetime with quantum entanglement. *Gen. Rel. Grav.*, 42:2323–2329, 2010.

[12] Brian Swingle. Constructing holographic spacetimes using entanglement renormalization. 9 2012.

[13] Eugenio Bianchi and Robert C. Myers. On the Architecture of Spacetime Geometry. *Class. Quant. Grav.*, 31:214002, 2014.

[14] Thomas Faulkner, Felix M. Haehl, Eliot Hijano, Onkar Parrikar, Charles Rabideau, and Mark Van Raamsdonk. Nonlinear gravity from entanglement in conformal field theories. *Journal of High Energy Physics*, 2017(8), Aug 2017.

[15] Thomas Faulkner, Monica Guica, Thomas Hartman, Robert C. Myers, and Mark Van Raamsdonk. Gravitation from entanglement in holographic cfts. *Journal of High Energy Physics*, 2014(3), Mar 2014.

[16] Nima Lashkari, Michael B. McDermott, and Mark Van Raamsdonk. Gravitational dynamics from entanglement "thermodynamics". *Journal of High Energy Physics*, 2014(4), Apr 2014.

[17] Matthew Headrick and Tadashi Takayanagi. A Holographic proof of the strong subadditivity of entanglement entropy. *Phys. Rev. D*, 76:106013, 2007.

[18] Patrick Hayden, Matthew Headrick, and Alexander Maloney. Holographic Mutual Information is Monogamous. *Phys. Rev. D*, 87(4):046003, 2013.

[19] Ning Bao, Sepehr Nezami, Hirosi Ooguri, Bogdan Stoica, James Sully, and Michael Walter. The Holographic Entropy Cone. *JHEP*, 09:130, 2015.

[20] David Tong. Lectures on string theory, 2012.

[21] Steven Weinberg. *Gravitation and Cosmology: Principles and Applications of the General Theory of Relativity*. Wiley, New York, NY, 1972.

[22] Alexander Jahn and Jens Eisert. Holographic tensor network models and quantum error correction: a topical review. *Quantum Science and Technology*, 6(3):033002, Jun 2021.

[23] Edward Witten. Anti-de Sitter space and holography. *Adv. Theor. Math. Phys.*, 2:253–291, 1998.

[24] Alex Hamilton, Daniel N. Kabat, Gilad Lifschytz, and David A. Lowe. Holographic representation of local bulk operators. *Phys. Rev. D*, 74:066009, 2006.

[25] Xi Dong, Daniel Harlow, and Aron C. Wall. Reconstruction of Bulk Operators within the Entanglement Wedge in Gauge-Gravity Duality. *Phys. Rev. Lett.*, 117(2):021601, 2016.

[26] Andrew Strominger. The ds/cft correspondence. *Journal of High Energy Physics*, 2001(10):034–034, Oct 2001.

[27] Michael A. Nielsen and Isaac L. Chuang. *Quantum Computation and Quantum Information: 10th Anniversary Edition*. Cambridge University Press, USA, 10th edition, 2011.

[28] Pasquale Calabrese and John Cardy. Entanglement entropy and quantum field theory. *Journal of Statistical Mechanics: Theory and Experiment*, 2004(06):P06002, Jun 2004.

[29] Shinsei Ryu and Tadashi Takayanagi. Holographic derivation of entanglement entropy from the anti–de sitter space/conformal field theory correspondence. *Physical Review Letters*, 96(18), May 2006.

[30] Shinsei Ryu and Tadashi Takayanagi. Aspects of holographic entanglement entropy. *Journal of High Energy Physics*, 2006(08):045–045, Aug 2006.

[31] Tatsuma Nishioka, Shinsei Ryu, and Tadashi Takayanagi. Holographic entanglement entropy: an overview. *Journal of Physics A: Mathematical and Theoretical*, 42(50):504008, Dec 2009.

[32] Mukund Rangamani and Tadashi Takayanagi. Holographic entanglement entropy. *Lecture Notes in Physics*, 2017.

[33] Veronika E Hubeny, Mukund Rangamani, and Tadashi Takayanagi. A covariant holographic entanglement entropy proposal. *Journal of High Energy Physics*, 2007(07):062–062, Jul 2007.

[34] Aitor Lewkowycz and Juan Maldacena. Generalized gravitational entropy. *JHEP*, 08:090, 2013.

[35] Xi Dong, Aitor Lewkowycz, and Mukund Rangamani. Deriving covariant holographic entanglement. *JHEP*, 11:028, 2016.

[36] Xi Dong. Holographic Entanglement Entropy for General Higher Derivative Gravity. *JHEP*, 01:044, 2014.

[37] Joan Camps. Generalized entropy and higher derivative Gravity. *JHEP*, 03:070, 2014.

[38] Thomas Faulkner, Aitor Lewkowycz, and Juan Maldacena. Quantum corrections to holographic entanglement entropy. *JHEP*, 11:074, 2013.

[39] Netta Engelhardt and Aron C. Wall. Quantum Extremal Surfaces: Holographic Entanglement Entropy beyond the Classical Regime. *JHEP*, 01:073, 2015.

[40] Michael Freedman and Matthew Headrick. Bit threads and holographic entanglement. *Communications in Mathematical Physics*, 352(1):407–438, Nov 2016.

[41] Matthew Headrick and Veronika E Hubeny. Riemannian and lorentzian flow-cut theorems. *Classical and Quantum Gravity*, 35(10):105012, Apr 2018.

[42] Jonathan Harper, Matthew Headrick, and Andrew Rolph. Bit Threads in Higher Curvature Gravity. *JHEP*, 11:168, 2018.

[43] Andrew Rolph. Quantum bit threads. 5 2021.

[44] Cesar A. Agón and Juan F. Pedraza. Quantum bit threads and holographic entanglement. 5 2021.

[45] Cesar A. Agón, Elena Cáceres, and Juan F. Pedraza. Bit threads, Einstein's equations and bulk locality. *JHEP*, 01:193, 2021.

[46] Shawn X. Cui, Patrick Hayden, Temple He, Matthew Headrick, Bogdan Stoica, and Michael Walter. Bit Threads and Holographic Monogamy. *Commun. Math. Phys.*, 376(1):609–648, 2019.

[47] Juan F. Pedraza, Andrea Russo, Andrew Svesko, and Zachary Weller-Davies. Lorentzian Threads as Gatelines and Holographic Complexity. *Phys. Rev. Lett.*, 127(27):271602, 2021.

[48] Juan F. Pedraza, Andrea Russo, Andrew Svesko, and Zachary Weller-Davies. Sewing spacetime with Lorentzian threads: complexity and the emergence of time in quantum gravity. 6 2021.

[49] Chong-Bin Chen, Fu-Wen Shu, and Meng-He Wu. Quantum bit threads of mera tensor network in large c limit *. *Chinese Physics C*, 44(7):075102, Jul 2020.

[50] Cesar A. Agón, Jan de Boer, and Juan F. Pedraza. Geometric aspects of holographic bit threads. *Journal of High Energy Physics*, 2019(5), May 2019.

[51] Michele Caraglio and Ferdinando Gliozzi. Entanglement entropy and twist fields. *Journal of High Energy Physics*, 2008(11):076–076, Nov 2008.

[52] Piermarco Fonda, Luca Giomi, Alberto Salvio, and Erik Tonni. On shape dependence of holographic mutual information in ads4. *Journal of High Energy Physics*, 2015(2), Feb 2015.

Acknowledgements

This thesis has been a collaborative project between Dr. Umut Gürsoy, Dr. Juan Pedraza, myself, and later also Guim Planella. I want to thank all three of them for the time and effort they put into this project. Apart from them, I would like to thank my fellow students Sacha de Wind and Thomas Bakx, they offered different techniques and angles to tackling some difficult integrals in the appendix. Which eventually helped me solve them. Also, I would like to say a special word of gratitude to my fellow students and roommates Maarten Rottier and Ima Meijer for proofreading this thesis and giving me comment on readability for the desired target audience. Apart from them, Oscar Eastman and Margot Stakenborg proofread my thesis and gave me notes on content and spelling/formalities. Finally, I would like to thank my dad, Prof. Dr. Yigal Pinto for proofreading as well as correcting on spelling and style of writing.